JCMM
Available online at
www.jcmm.ro
www.jcmm.org

J. Cell. Mol. Med. Vol 9, No 2, 2005 pp. 479-523

Special Article

Novel type of interstitial cell (Cajal-like) in human fallopian tube

L.M. Popescu [a,c] *, Sanda M. Ciontea [a], D. Cretoiu [a,c], M.E. Hinescu [a,c], E. Radu [a,c], N. Ionescu [a], M. Ceausu [c], Mihaela Gherghiceanu [c], R.I. Braga [b], Florina Vasilescu [c], L. Zagrean [b], Carmen Ardeleanu [c]

[a] *Department of Cellular and Molecular Medicine,*
[b] *Department of Physiology,*
"Carol Davila" University of Medicine and Pharmacy, Bucharest, Romania
[c] *"Victor Babes" National Institute of Pathology, Bucharest, Romania*

Received: March 21, 2005; Accepted: May 6, 2005

Abstract

We describe here – presumably for the first time – a Cajal-like type of tubal interstitial cells (t-ICC), resembling the archetypal enteric ICC. t-ICC were demonstrated *in situ* and *in vitro* on *fresh preparations* (tissue *cryosections* and primary *cell cultures*) using methylene-blue, crystal-violet, Janus-Green B or MitoTracker-Green FM Probe *vital stainings*. Also, t-ICC were identified in *fixed specimens* by *light microscopy* (methylene-blue, Giemsa, trichrome stainings, Gomori silver-impregnation) or transmission *electron microscopy* (TEM). The positive diagnosis of t-ICC was strengthened by immunohistochemistry (IHC; CD117/c-kit+ and other 14 antigens) and immunofluorescence (IF; CD117/c-kit+ and other 7 antigens). The spatial density of t-ICC (ampullar-segment cryosections) was 100–150 cells/mm^2. Non-conventional light microscopy (NCLM) of Epon semithin-sections revealed a network-like distribution of t-ICC in lamina propria and smooth muscle meshwork. t-ICC appeared located beneath of epithelium, in a 10–15µm thick 'belt', where 18±2% of cells were t-ICC. In the whole lamina propria, t-ICC were about 9%, and in muscularis ~7%. *In toto*, t-ICC represent ~8% of subepithelial cells, as counted by NCLM. *In vitro*, t-ICC were 9.9±0.9% of total cell population.

TEM showed that the diagnostic '*gold standard*' (Huizinga *et al.,* 1997) is fulfilled by 'our' t-ICC. However, we suggest a '*platinum standard*', adding a new defining criterion – *characteristic cytoplasmic processes* (number: 1–5; length: tens of µm; thickness: ≤0.5µm; aspect: moniliform; branching: dichotomous; organization: network, labyrinthic-system). Quantitatively, the ultrastructural architecture of t-ICC is: *nucleus*, 23.6±3.2% of cell volume, with heterochromatin 49.1±3.8%; *mitochondria*, 4.8±1.7%; *rough and smooth endoplasmic-reticulum* (1.1±0.6%, 1.0±0.2%, respectively); *caveolae*, 3.4±0.5%. We found more caveolae on the surface of cell processes versus cell body, as confirmed by IF for caveolins. Occasionally, the so-called 'Ca^{2+}-release units' (subplasmalemmal close associations of caveolae+endoplasmic reticulum±mitochondria) were detected in the dilations of cell processes. Electrophysiological single unit recordings of t-ICC in primary cultures indicated sustained spontaneous electrical activity (amplitude of field potentials: 57.26±6.56mV).

Besides the CD117/c-kit marker, t-ICC expressed variously CD34, caveolins 1&2, α-SMA, S-100, vimentin, nestin, desmin, NK-1. t-ICC were negative for: CD68, CD1a, CD62P, NSE, GFAP, chromogranin-A, PGP9.5, but IHC showed the possible existence of (neuro)endocrine cells in tubal interstitium. We call them 'JF cells'.

In conclusion, the identification of t-ICC might open the door for understanding some tubal functions, *e.g.* pace-making/peristaltism, secretion (auto-, juxta- and/or paracrine), regulation of neurotransmission (nitrergic/purinergic) and intercellular signaling, *via* the very long processes. Furthermore, t-ICC might even be *uncommitted bipotential progenitor cells*.

Keywords: interstitial cells of Cajal • uncommitted progenitor cells • CD117/c-kit • intercellular signaling • caveolae/caveolins • vimentin • calcium release units • uterine tube • oviduct • tubal endocrine cells

* Correspondence to: L.M. POPESCU, M.D., Ph.D.
Department of Cellular and Molecular Medicine,
"Carol Davila" University of Medicine and Pharmacy,
P.O. Box 35-29, Bucharest 35, Romania.
Tel: +40(0)744 535 298; Fax: +40(0)21-312 4885
E-mail: LMP@univermed-cdgm.ro

Motto:

'As long as there is a hunger for knowledge and a deep desire to uncover the truth, microscopy will continue to unveil Mother Nature's deepest and most beautiful secrets.'

L. Orci & M.S. Pepper, Microscopy: an art ?, 2002 (ref. [1]***)***

Reprinted from:
Journal of Cellular and Molecular Medicine

Published by:
the CMM Foundation

Introduction

Santiago Ramon y Cajal reported at the end of the nineteenth century a special type of cell ('nervous interstitial cell') in the gastrointestinal tract and in other mammalian tissues, using methylene-blue vital staining and/or Golgi impregnation method [2, 3]. Although Cajal could not discern an axon among the cytoplasmic processes of these cells, he considered them possible accessory neurons (a short review in ref. [4]). Nowadays, habitually, such cells are called interstitial cells of Cajal (ICC) [5].

ICC were described along the digestive tube [6–12] and several TEM ground rules for *in situ* ICC identification were formulated [13–15], even an 8-criteria 'gold standard' was proposed by Huizinga *et al.* [15]. ICC are now considered to play a key role in pacemaking and neurotransmission in gastrointestinal tract [16–20]. Moreover, CD117/c-kit became a widely accepted, reliable marker for ICC at the microscopic level [21–24].

In a series of recent papers, ICC-like cells have been claimed to occur in other organs: vas deferens [25], urethra [26–28], bladder [29–33], ureter [34, 35], uterus [36, 37], blood vessels [38–40], lymphatics [41], prostate [42, 43], penis [44], mammary gland [45] and pancreas [46].

Apparently, the fallopian tube was unexplored for the occurrence of interstitial (Cajal-like) cells, in spite of the fact that this hollow organ is a *tube* (like the digestive *tube*) and exibits peristaltic waves (like the digestive tube, again !). We were unable to find out any reference in the international biomedical literature concerning the possible existence of ICC or Cajal-like cells in human fallopian tube.

From a microscopical point of view, the fallopian tube appears disappointingly simple: an epithelium + lamina propria (stroma) and two interwined smooth muscle layers covered by serosa. Moreover, histologic findings in fallopian tubes have been only sporadically described [47, 48], although fallopian tubes have a vital (subtle) role in promoting human fertility [49]. Albeit in mammals fertilization and early embryo development take place in the fallopian tube [50], a mystery remains: how this organ manages to orchestrate the transfer [47] so that spermatozoa moving towards the ovary and the egg moving away from the ovary meet in the right place, at the right time, for fertilization. A presumptive t-ICC network might hence be the microscopic missing-link (conductor ?) of the tubal players: the epithelial 'conveyer', multidirectional smooth-muscle bundles, nerve endings, and small blood vessels.

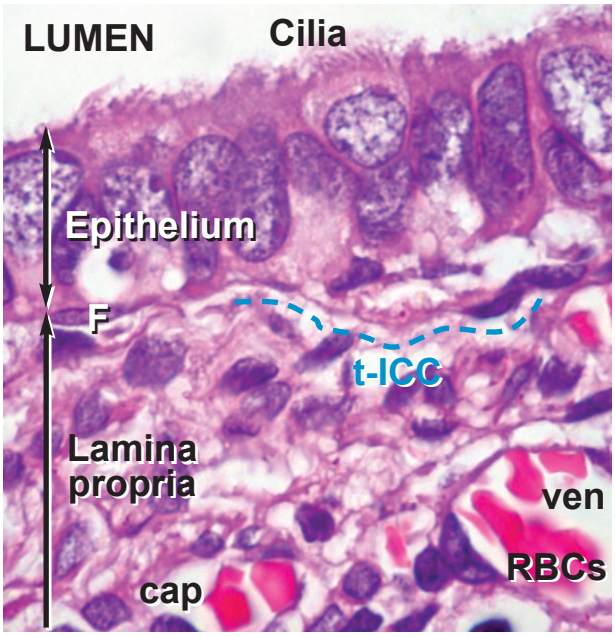

Fig. 1 Human fallopian tube; mucosal layer; 100x, oil immersion. Routine light microscopy, *hematoxylin & eosin* staining. Note the possible t-ICC, with a *very long* (over 25 μm), *moniliform* (uneven caliber) *cytoplasmic prolongation*. 'F' marks the euchromatic nucleus of a fibroblast-like cell; cap = capillary; ven = venule; RBCs = red blood cells.

We present here morphological, immunochemical and electrophysiological evidence for the occurence of Cajal-like interstitial cells in the human fallopian tube, in the non-epithelial space.

Material and methods

Human tissue specimens

Histologically normal portions of fallopian tube ampullar region were obtained from 11 healthy women of non-reproductive age, after surgical procedures for leiomyoma (total abdominal hysterectomy with bilateral salpingo-oophorectomy). Samples were taken after informed consent, using a protocol approved by the local Bioethics Committee, in accordance to generally accepted international practice. Tissue samples have been divided into appropriate-sized slices for cell culture, conventional histology and TEM. For immunohistochemistry, tissue samples were obtained from 14 archived paraffin-embedded specimens of patients that had undergone surgical procedures (total abdominal hysterectomy with bilateral anexectomy) for a non-neoplastic disease, as well as after salpingectomy or tubal ligation.

Cell culture

Human fallopian tube fragments were collected into sterile tubes containing Dulbecco's Modified Eagle's Medium (DMEM), supplemented with 100 UI/ml penicillin, 0.1 mg/ml streptomycin, and 0.25 µg/ml amphotericin (Sigma Chemical, St. Louis, MO, USA), placed on ice, and transported to the cell culture laboratory. Samples were processed within 30 min from surgery, rinsing them with sterile DMEM. Then fragments were dissected in Petri dishes along the longitudinal axis, exposing the epithelium, and the mucosal layer was gently peeled off. The experimental protocol was an adaptation of recently described methods [51, 52]. The remaining muscular tissue was minced in fragments of about 1 mm^3 and incubated on an orbital shaker for 4 h, at 37°C, with 10 mg/ml collagenase type Ia and 2000 U/ml deoxyribonuclease I (Sigma Chemical, St. Louis, MO, USA) in PBS, without Ca^{2+} and Mg^{2+}. Dispersed cells were separated from non-digested tissue by filtration through a 40 µm diameter cell strainer (BD Labware, San Jose, CA, USA), collected by centrifugation at 300g, and resuspended in a 1:1 DMEM: Ham's Nutrient F-12 mixture, supplemented with 10% fetal calf serum, 1.5 mM HEPES, 100 UI/ml penicillin, 0.1 mg/ml streptomycin and 0.25 µg/ml amphotericin (Sigma Chemical, St. Louis, MO, USA). Cell density was counted in a haemocytometer and viability was assessed using the Trypan blue dye exclusion test.

Cells were distributed in 25 cm^2 plastic culture flasks, or on glass coverslips into 24-well plates (BD Labware, San Jose, CA, USA) at a density of 50,000 cells/cm^2, and maintained at 37°C, in a humidified atmosphere (5% CO_2 in air) until becoming semi-confluent (usually 4 days after plating). Culture medium was changed every 48 h. Cell cultures were examined by phase contrast microscopy, under an inverted Nikon TE200 microscope.

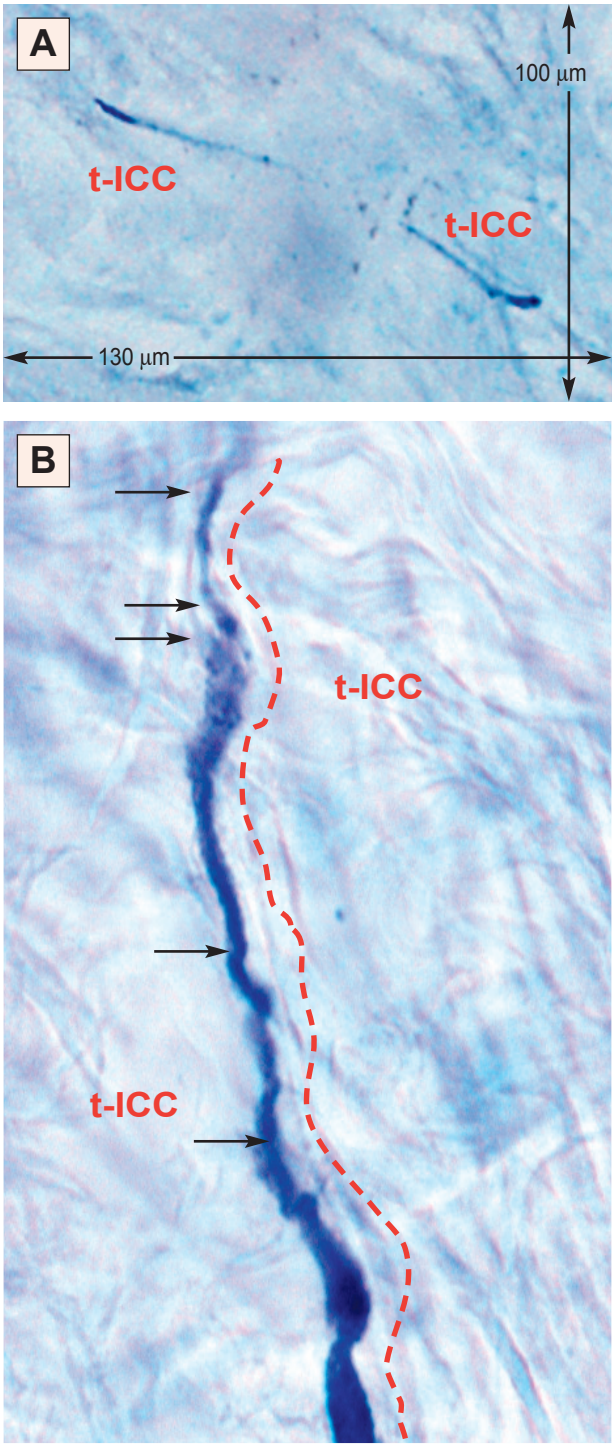

Fig. 2 A–C Human fallopian tube; muscularis; light microscopy. *Vital methylene-blue* staining, *before fixation* (cryosections). **A.** Original magnification, 10x. Note the very selective staining of only two t-ICC in a field of 13,000 $µm^2$, which normally would display tens of cells, when routine methodology is used (see Fig. 1 for comparison). **B**, **C**. Higher magnification (100x, oil immersion), photographic reconstructions. Note the very long (over 100 µm), moniliform cytoplasmic processes (arrows) emerging from t-ICC body.

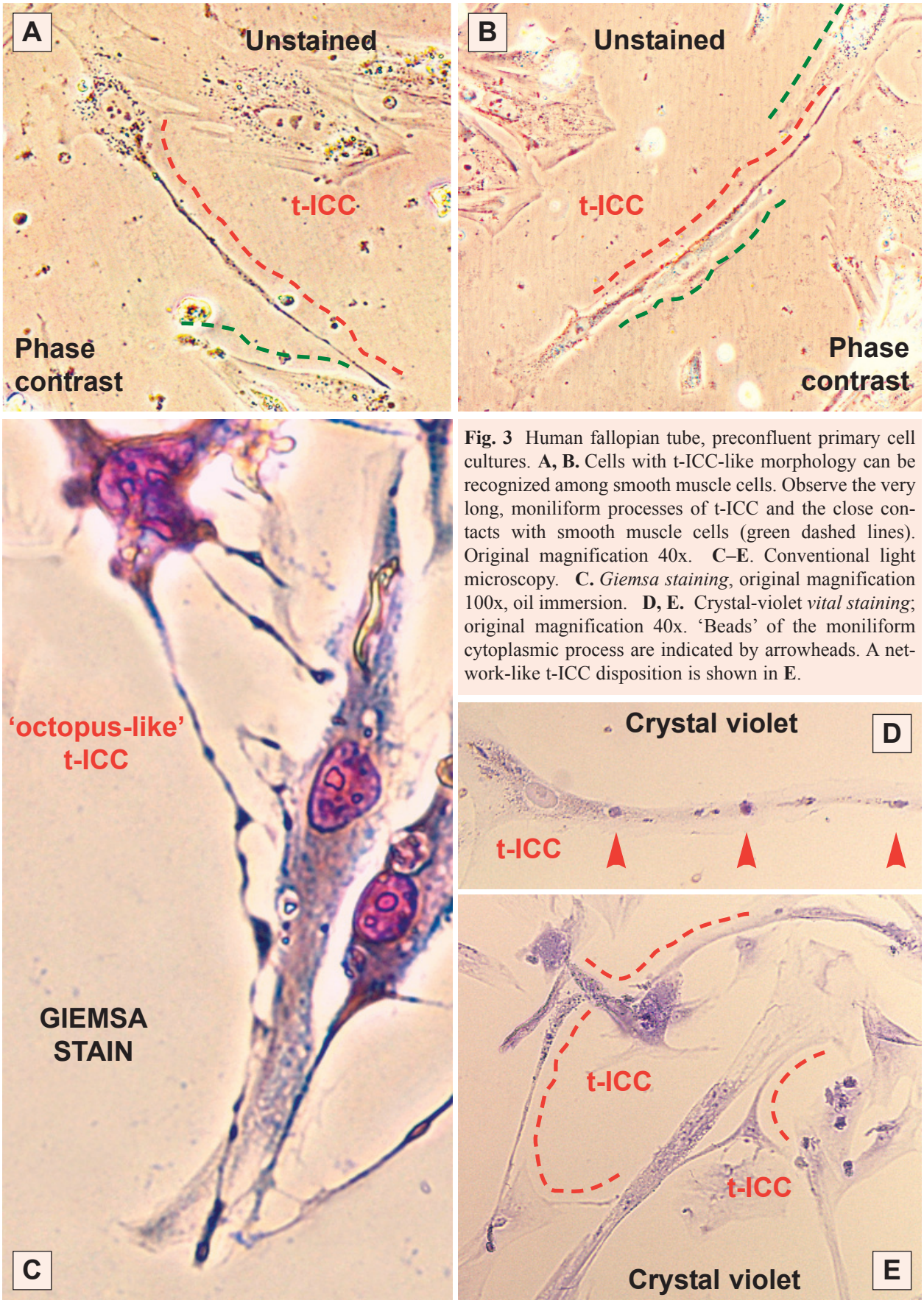

Fig. 3 Human fallopian tube, preconfluent primary cell cultures. **A, B.** Cells with t-ICC-like morphology can be recognized among smooth muscle cells. Observe the very long, moniliform processes of t-ICC and the close contacts with smooth muscle cells (green dashed lines). Original magnification 40x. **C–E.** Conventional light microscopy. **C.** *Giemsa staining*, original magnification 100x, oil immersion. **D, E.** Crystal-violet *vital staining*; original magnification 40x. 'Beads' of the moniliform cytoplasmic process are indicated by arrowheads. A network-like t-ICC disposition is shown in **E**.

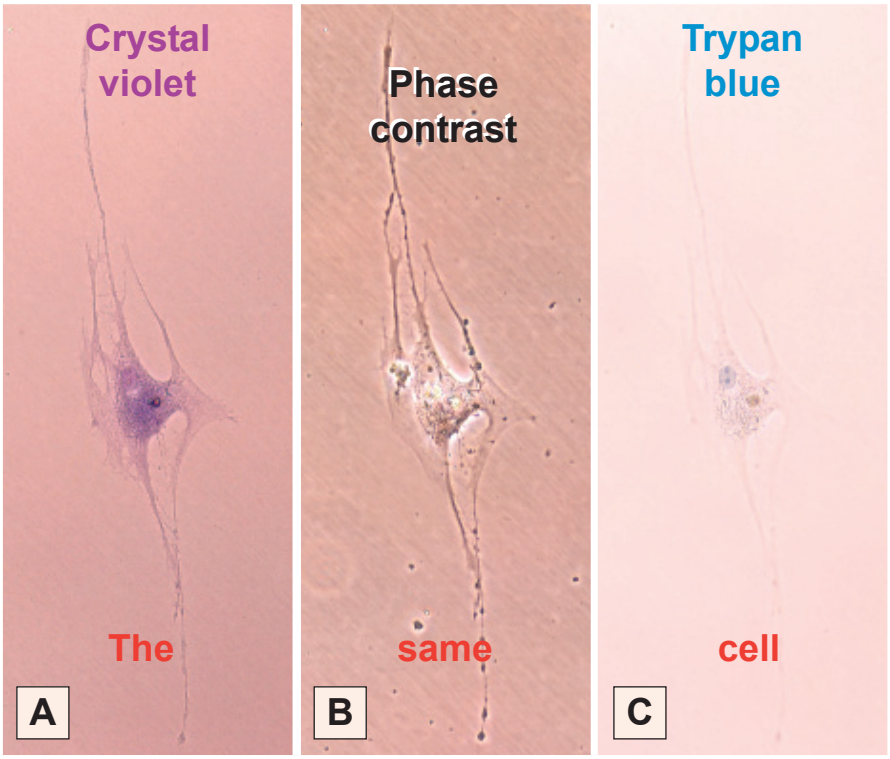

Fig. 4 t-ICC in primary culture, original magnification 40x. **A.** Crystal-violet *vital staining* makes the t-ICC visible, using conventional light microscopy; **B.** The same cell after the dye was washed-out (30 min with DMEM); the t-ICC was visible only in phase contrast. **C.** The same cell after Trypan blue staining; (this *viability test* shows that the cell is still alive, since the dye was excluded). 'Invisible' prolongations may be only presumed using conventional light microscopy.

Cytogenetic analysis was performed in order to evaluate the cell genome status. The cells were grown until 70–80% confluency at which point colchicines was added to a final concentration of 2µg/ml for 3 h. Cells were then trypsinized, pelleted by centrifugation, resuspended in 0.075 M KCl solution and incubated at 37°C, for 30 min. Cells were fixed in a 3:1 methanol:acetic acid fixative solution for 30 min, at 4°C, pelleted by centrifugation, supernatant was removed and fresh fixative was added. Karyotyping was assessed on GTG-banded slides. 50 metaphases were counted with a Nikon Microphot SA microscope and karyotyping was performed using a Lucia Cytogenetics 1.2.9 system. *A normal 46,XX karyotype was revealed*.

Vital stainings

Fresh tissue samples. For the *vital methylene blue staining* we used Shabadash's method, modified by Niculescu [53] in 1958. In brief, fallopian tube samples were immersed in a bath of warm (37°C) methylene blue dye (0.025%) and incubated for 30 min in the presence of resorcine (0.015%), glucose (0.02%), magnesium chloride (0.15%) and sodium chloride (0.85%). Staining procedure was stopped, under light microscope control, by fixation with 8% ammonium molibdate solution. After extensive washing, tissue samples were frozen (minus 25°C) and cut with a cryomicrotome (Leica; Bensheim, Germany). Sections (4–5 µm thickness) were dehydrated in absolute ethanol, cleared in toluene and mounted on slides, in synthetic resin. Slides were examined under Nikon 600E microscope.

Primary cell cultures. *Methylene blue vital staining:* cells were washed in pre-warmed phenol red-free DMEM (Sigma Chemical, St. Louis, MO, USA), and incubated for 20 min in a 0.02% methylene blue solution, 37°C (Merck KGaA, Darmstadt, Germany). After a rapid wash with phenol red-free DMEM medium, pictures were taken within 10 min to avoid the spontaneous color loss. A Nikon inverted TE200 microscope equipped with a Nikon DN-5 digital camera was used to examine the samples.

Crystal-violet vital staining. Cells grown on coverslips in 2 cm round wells (the 4th day of culture), in DMEM with 10% fetal bovine serum (FBS), HEPES 1.5 mM, were washed three times in pre-warmed (37°C) culture medium. The cells were immersed in 0.01% crystal-violet (E. Letz Zweiggeschäft, Berlin NW, Germany) in culture medium for 2–5 min, at 37°C (in a humidified atmosphere, 5% CO_2 in air), and afterwards rapidly washed with phenol red-free DMEM, and examined. Cells were then incubated at 37°C in DMEM, and gently agitated periodically to remove the dye. After 30 min, cells viability was tested with Trypan blue 0.2%, 5 min, at 37°C, washed three times with DMEM, and examined under microscope.

Janus green B vital staining. Cultured cells were immersed for 30 min in 0.02% Janus green B (Schering Kahlbaum AG, Berlin, Germany) [54] in DMEM and kept at 37°C, in a humidified atmosphere, 5% CO_2 in air. After repeated washes in DMEM, cells were examined under inverted Nikon TE200 microscope with heated object-stage, and photographed.

Mitochondria labeling with MitoTracker Green FM. Cultures were labeled with MitoTracker Green FM (Molecular Probes, Eugene, OR, USA), the lipophylic, selective

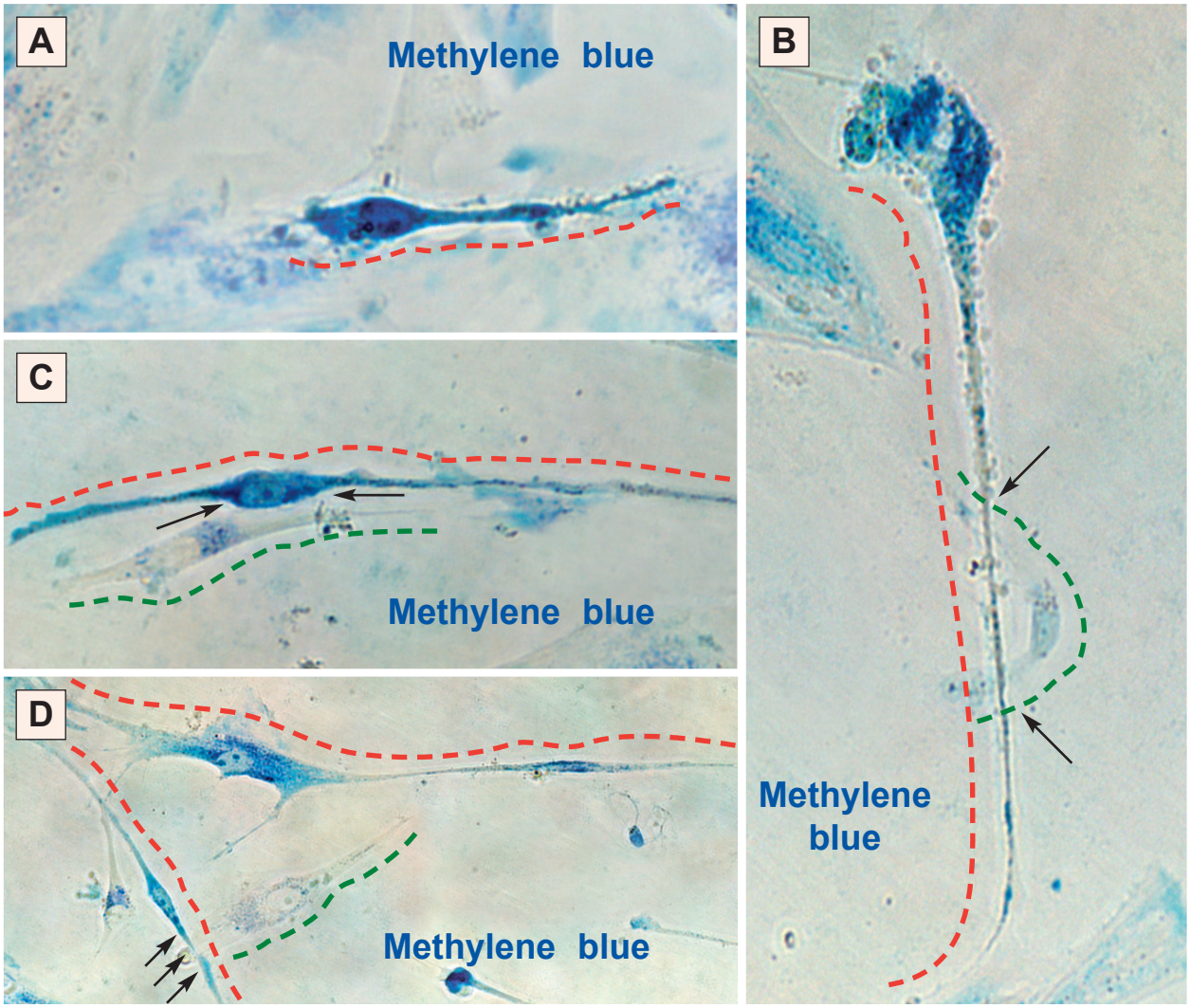

Fig. 5 A–D Human fallopian tube. Methylene-blue *vital staining* of cells having t-ICC morphology. Note *selectively* stained cells with long, moniliform, prolongations (red dashed lines). Day 4 of primary culture. Arrows indicate close contacts between t-ICC and smooth muscle cells (green dashed lines). Original magnification 40x, Nikon TE 300.

dye, which is concentrated by active mitochondria [55, 56]. Cells grown on coverslips were removed from culture and incubated in phenol red-free DMEM completed with 10% fetal calf serum and antibiotic-antimycotic solution (Sigma Chemical, St. Louis, MO, USA) in the presence of 80nM MitoTracker Green FM. Cells were incubated for 30 min, at 37°C, in a humidified atmosphere (5% CO_2 in air), subsequently washed, and examined by fluorescence microscopy (450-490 nm excitation light, 520 nm barrier filter; Nikon TE200 microscope).

Giemsa staining. This procedure is *not* a real vital staining, since the dye and the fixation agent (methanol) are acting concomitantly *on* live cells. Giemsa stain was performed after removing the medium from culture wells and adding a 1/1 (v/v) mixture of 0.4% Giemsa solution in methanol and distilled water (pH 6.9) and incubating, for 30 min, at room temperature. Coverslips were then washed three times in distilled water and examined.

Conventional light microscopy

Classic techniques. Paraffin embedded sections (4 µm thickness) of formalin-fixed material were examined after usual staining (hematoxylin&eosin, HE), trichrome stainings (hematoxylin&eosin/methylene-blue, van Gieson) and silver impregnations, according to generally accepted procedures [57], adapted to our laboratory.

Gomori silver impregnation. After de-waxing, sections were treated with 1% potassium permanganate for 3 min, rinsed in tap water and then bleached in 1% oxalic acid. After

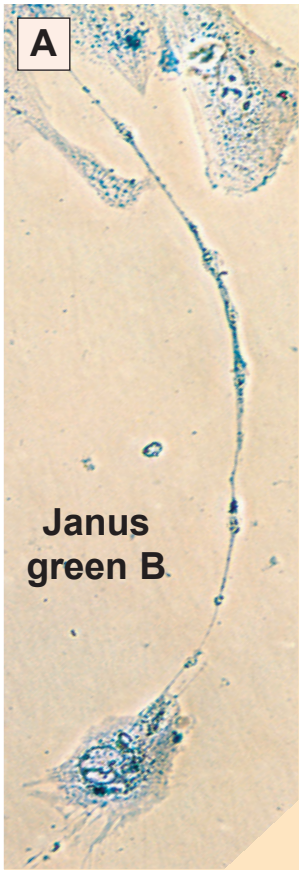

another series of rinsing, the sections were treated with 2% iron alumn for 15 min. Following repeated washes in deionised water, sections were immersed in ammoniacal silver nitrate, for 1 min, rinsed again, dehydrated, cleared in xylene and counterstained with eosin.

Giemsa stain was applied on fallopian tube paraffin-embedded sections, after deparaffination and rehydration through graded alcohols to water. Working Giemsa solution (Giemsa stock diluted with distilled water) was maintained on sections for about 10 min, under microscopic control. Slides were then washed in distilled water, followed by dehydration in alcohol 96% and two changes of isopropilic alcohol, cleared in benzene, and mounted in Entellan (Merck KGaA, Darmstadt, Germany).

Vital dyes on fixed and paraffin-embedded tissue

Janus green B stain. Sections were flooded with freshly prepared Janus green B (aqueous solution 0.1%) under microscopic control, and then rinsed in acidulated (acetic acid) distilled water. Samples were then dehydrated through alcohols, cleared in xylen and mounted in a synthetic resin.

Crystal violet stain. Hydrated sections were maintained in crystal violet solution (1%) under microscopic control. After dehydration in 96% and absolute alcohols, samples were differentiated. Differentiation was stopped in water and repeated until good contrast was obtained and mounted in a synthetic resin.

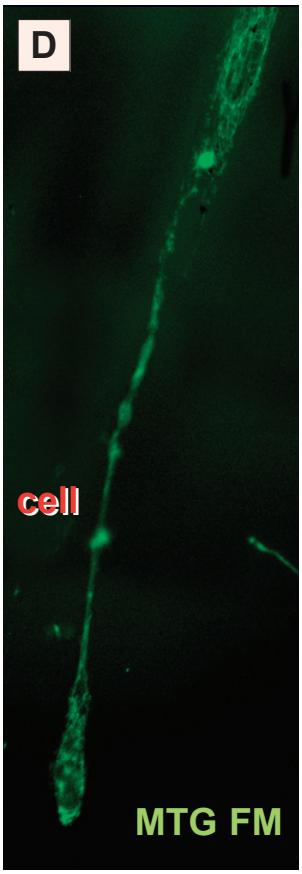

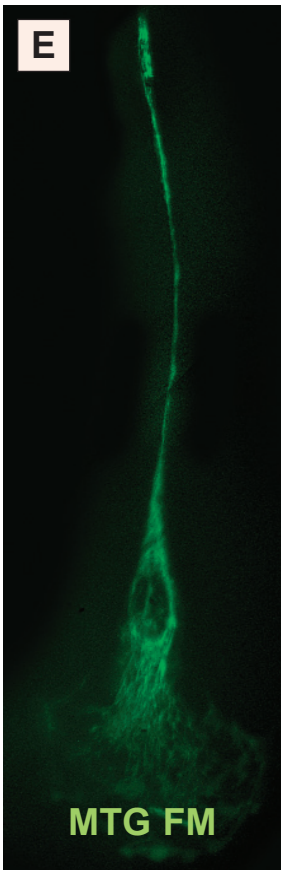

Fig. 6 A–E Human t-ICC in primary culture.
A, B. *Vital staining* with Janus green B, a marker for mitochondria in living cells. Note the location of mitochondria at the cell-body level, as well as along the long, moniliform processes. In fact, the dilations of processes are filled with Janus green B positive mitochondria. Original magnification, 40x.
C. Phase contrast microscopy of a living t-ICC. The same t-ICC after loading (**D**) with MitoTracker Green FM.
D, E. Fluorescence images of mitochondria with MitoTracker Green FM. Green fluorescent mitochondria can be seen around the cell nuclei and within expansions located either along or at the endings of long, moniliform, cell processes (original magnification: 40x objective).

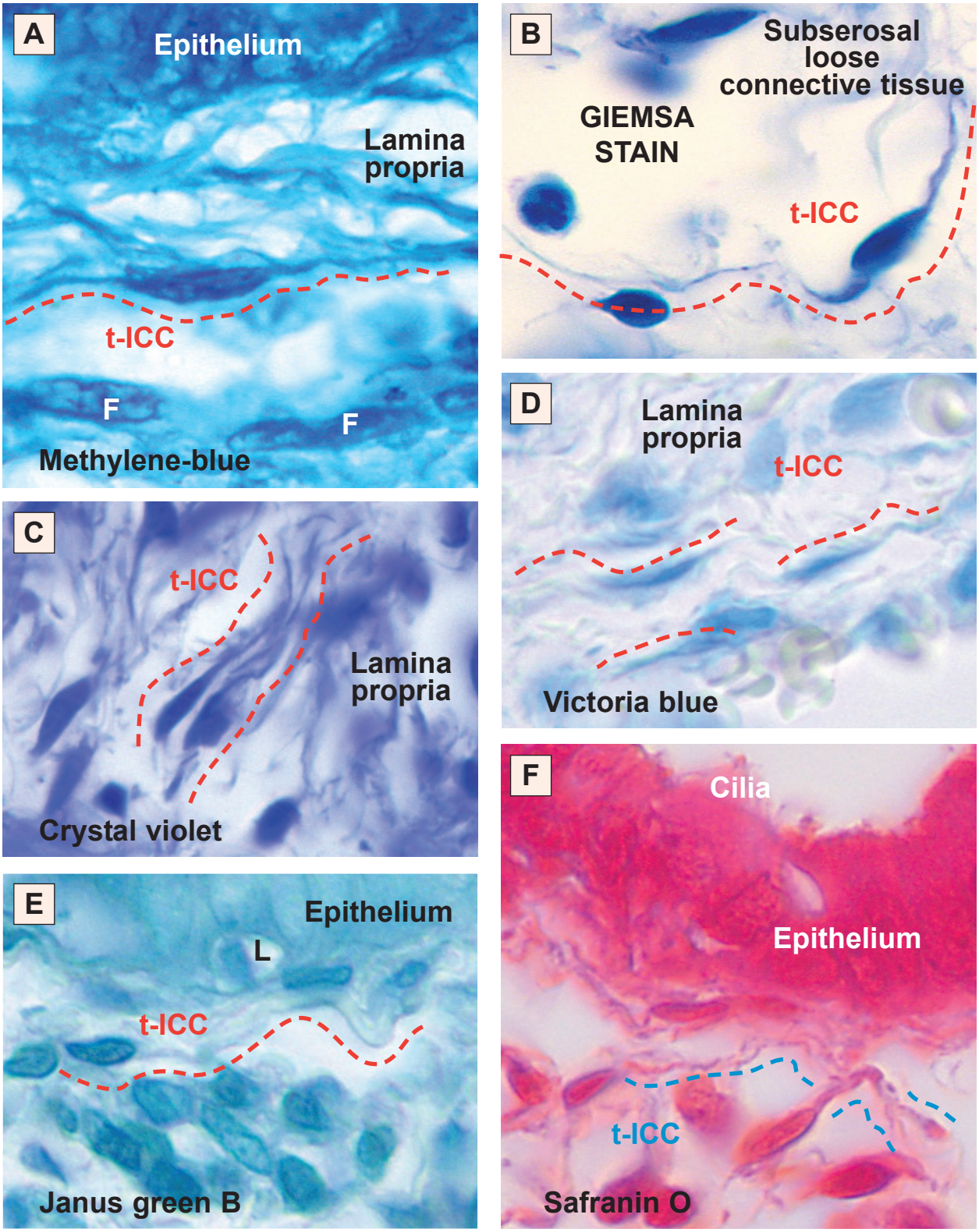

Fig. 7 Human fallopian tube; 100x, oil immersion. *Routine light microscopy*; different staining methods, *after fixation*, paraffin embedding and sectioning. Note the spindle-shaped t-ICC (dashed lines), with *very long, moniliform, cytoplasmic processes*. F = nuclei of fibroblast-like cells; L = lymphocyte.

Safranin O (Basic Red 2). Paraffin-embedded sections were de-waxed, hydrated and stained with safranin O (Dr. Grübler & Co., Leipzig, Germany) aqueous solution (1%), under microscopic control. After a brief wash and dehydration in absolute alcohol, sections were cleared in xylene and mounted in a synthetic resin.

Victoria blue (Basic Blue 26). Sections mounted onto slides were stained with Victoria-blue (Dr. Grübler & Co., Leipzig, Germany) alcoholic solution (1%), and processed as above.

Transmission electron microscopy (TEM)

Small fragments (about 1 mm^3) were fixed in 4% glutaraldehyde (in 0.1 M cacodylate buffer), pH 7.3, for 4 h, at 4°C. After a brief wash in 0.1 M cacodylate buffer (CB), tissue samples were post-fixed with 1% osmium tetroxide in 0.1 M cacodylate buffer, pH 7.3, at 4°C, followed by dehydration in a graded series of ethanols. After impregnation in propylene oxide, the samples were immersed overnight in a mixture of propylene oxide and Epon resin, and embedded in Epon 812, as usually. Ultrathin sections were cut using an MT-7000 ultramicrotome (Research Manufacturing Company Inc., Tucson, AZ, USA). These sections (50 nm) were collected on Formvar-coated copper grids, stained with uranyl acetate and lead citrate, and observed in a CM 12 Philips electron microscope, at an acceleration voltage of 60 kV.

The quantitative evaluation of t-ICC ultrastructural characteristics, (*e.g.* relative volumes occupied by nucleus, mitochondria etc.) was performed using the classical test-system described by Weibel [58].

Non-conventional light microscopy (NCLM)

Control semi-thin sections (less than 1 μm) were stained with 0.25% Toluidine blue and examined by light microscopy (Nikon Eclipse E600). Representative photomicrographs were taken using Nikon Plan 40x and Nikon Plan Fluor 100x/1.30 oil.

Because semi-thin sections are about 100 times thinner, the spatial resolving power in NCLM is much better than using paraffin-embedded sections. Therefore, NCLM was preferentially used for quantitative and morphometric analysis of t-ICC (*e.g.* total and relative number of cells, number and length of processes etc.).

Immunohistochemistry (IHC)

The human fallopian-tube specimens were tested using the following **antibodies**: **CD117/c-kit**, polyclonal, 1:100 (DAKO, Glostrup, Denmark), **CD34**, monoclonal, 1:100, clone QBEND10 (Biogenex, San Ramon, CA, USA), **S-100**, poly-

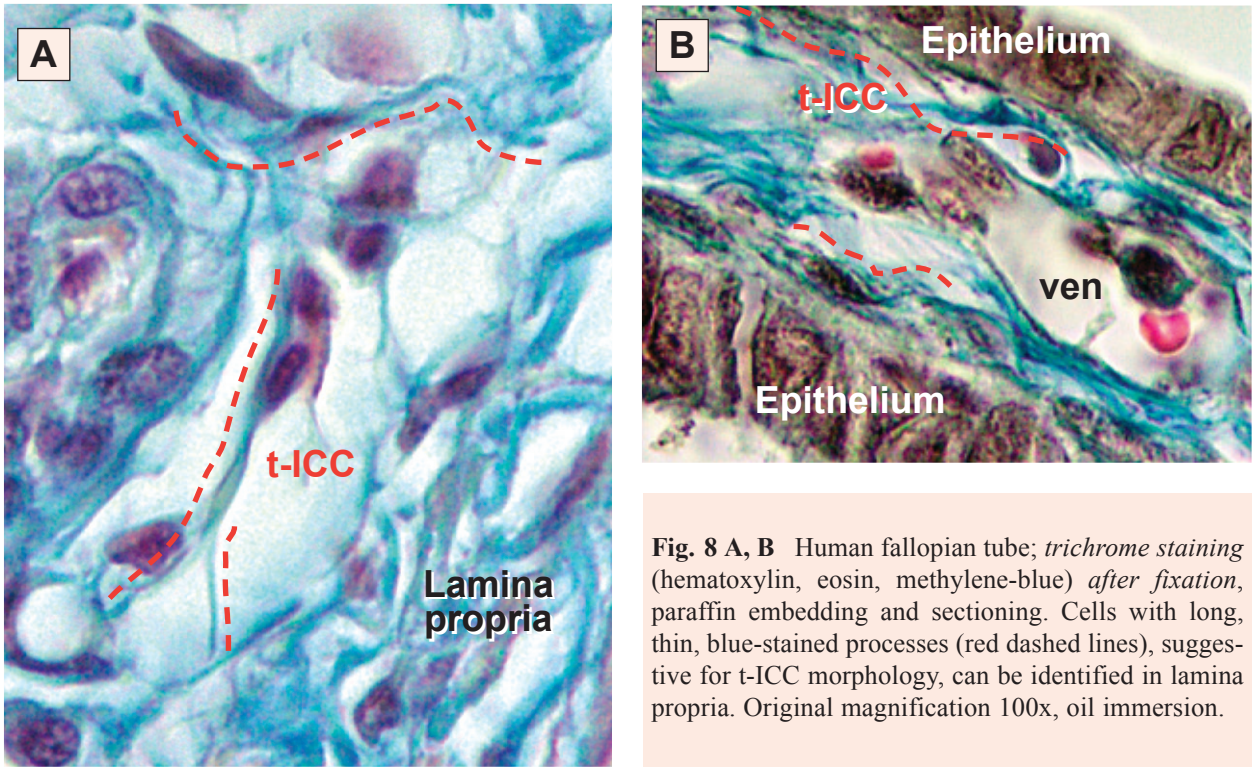

Fig. 8 A, B Human fallopian tube; *trichrome staining* (hematoxylin, eosin, methylene-blue) *after fixation*, paraffin embedding and sectioning. Cells with long, thin, blue-stained processes (red dashed lines), suggestive for t-ICC morphology, can be identified in lamina propria. Original magnification 100x, oil immersion.

clonal, 1:500 (DAKO, Glostrup, Denmark), **α-smooth muscle actin** (α-SMA), monoclonal, 1:1500, clone 1A4 (Sigma Chemical, St. Louis, MO), **CD57**, monoclonal, 1:50, clone **NK1**, (DAKO, Glostrup, Denmark), **nestin**, monoclonal, 1:100, clone 5326 (Santa Cruz, CA, USA), **desmin**, monoclonal, 1:50, clone D33, (DAKO, Glostrup, Denmark), **vimentin**, monoclonal, 1:50, clone V9, (DAKO, Glostrup, Denmark), **NSE**, monoclonal, 1:50, clone BBS/NC/VI-H14, (DAKO, Glostrup, Denmark), **GFAP**, monoclonal, 1:50, clone 6F2, (DAKO, Glostrup, Denmark), **CD68**, monoclonal, 1:50, clone PG-M1, (DAKO, Glostrup, Denmark), **CD62P** (**selectin**), monoclonal, 1:25, clone 1E3, (DAKO, Glostrup, Denmark), **CD1a**, monoclonal, 1:30, clone CD1a-235, (Novocastra, Newcastle upon Tyne, UK), **chromogranin A**, monoclonal, 1:50, clone LK2H10 (Novocastra, Newcastle upon Tyne, UK), **PGP 9.5**, monoclonal, 1:40, clone 10A1, (Novocastra, Newcastle upon Tyne, UK). All specimens were counterstained with Mayer's hematoxylin, examined and photographed on a Nikon Eclipse 600 microscope.

Immunohistochemistry was performed on 3 μm thick sections from formalin-fixed paraffin-embedded specimens, according to the Avidin-Biotin-Complex method of Hsu [59], modified by Bussolati and Gugliotta [60]. Briefly, the procedure comprised: deparaffination in xylene and alcohol series, rehydration, washing in phosphate buffer saline (PBS), blocking with normal serum, for 20 min, incubation with primary antibody overnight then with standard labeled streptavidin-antibody biotin (LSAB kit, DAKO, Glostrup, Denmark), washing in carbonate buffer and developing in 3,3'-DAB hydrochloride/H_2O_2. Microwave antigen retrieval (in 10 mM citrate buffer, pH 6.0) was performed for CD117/c-kit, chromogranin A, S-100 and CD68.

For CD117 and CD34 *double immunostaining* in human fallopian tube an ABC indirect tristadial method was used:

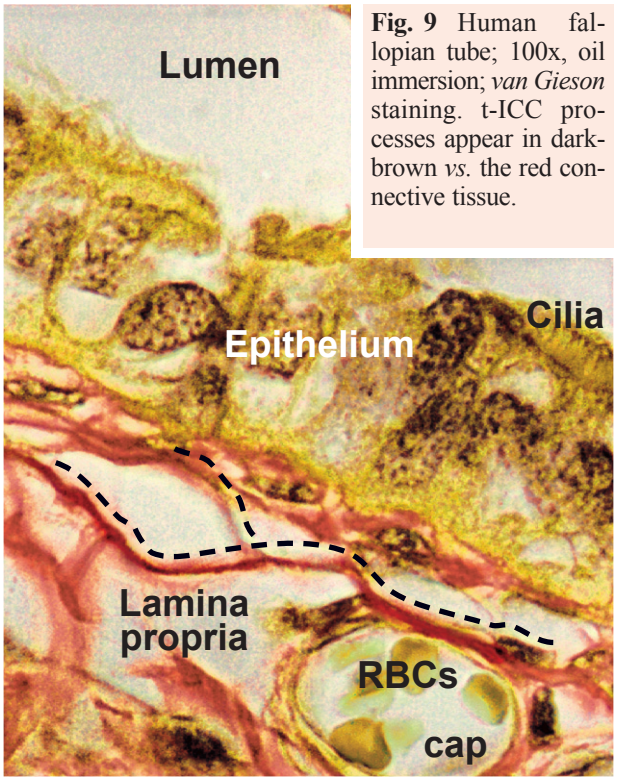

Fig. 9 Human fallopian tube; 100x, oil immersion; *van Gieson* staining. t-ICC processes appear in dark-brown *vs.* the red connective tissue.

DAB (diaminobenzidine), HRP (horse radish peroxidase) chromogenic substrate developing for CD117 polyclonal antibody (brown stain) and fast red alpha naphtol AP (alkaline phosphatase) chromogenic substrate in 0.2M Tris buffer, pH 10, for CD34 monoclonal antibody (red stain).

Negative controls were done using an irrelevant primary antibody or replacing the secondary antibody with phos-

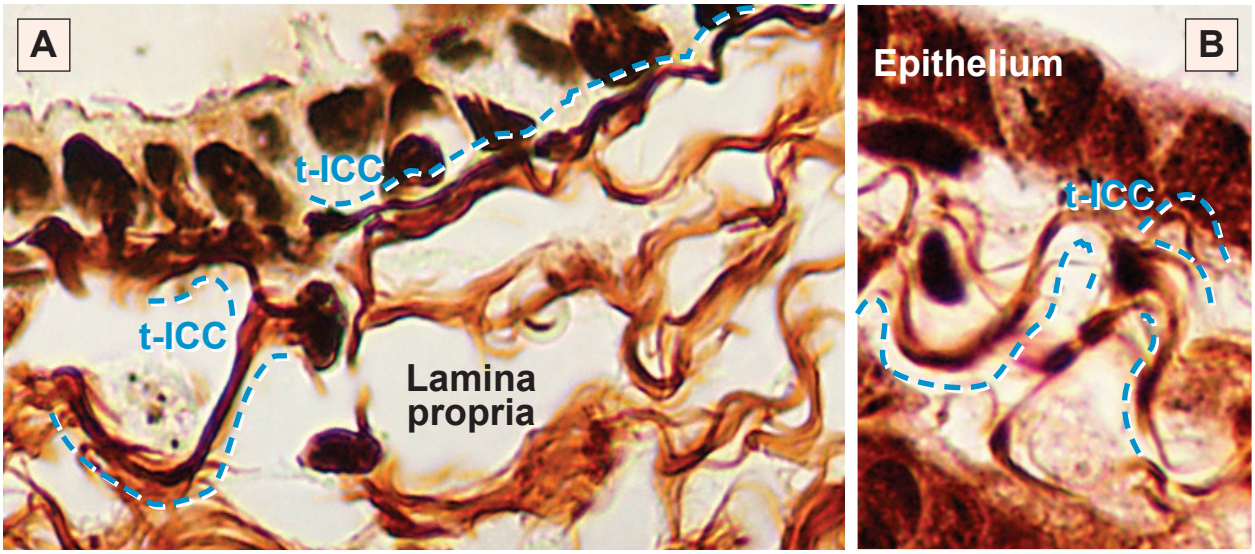

Fig. 10 A, B *Gomori silver impregnation* of human fallopian fimbriae (**A**) and additional eosin counterstaining of the same (**B**). t-ICC with one, two and four processes can be seen underlying the epithelium. Original magnification 100x.

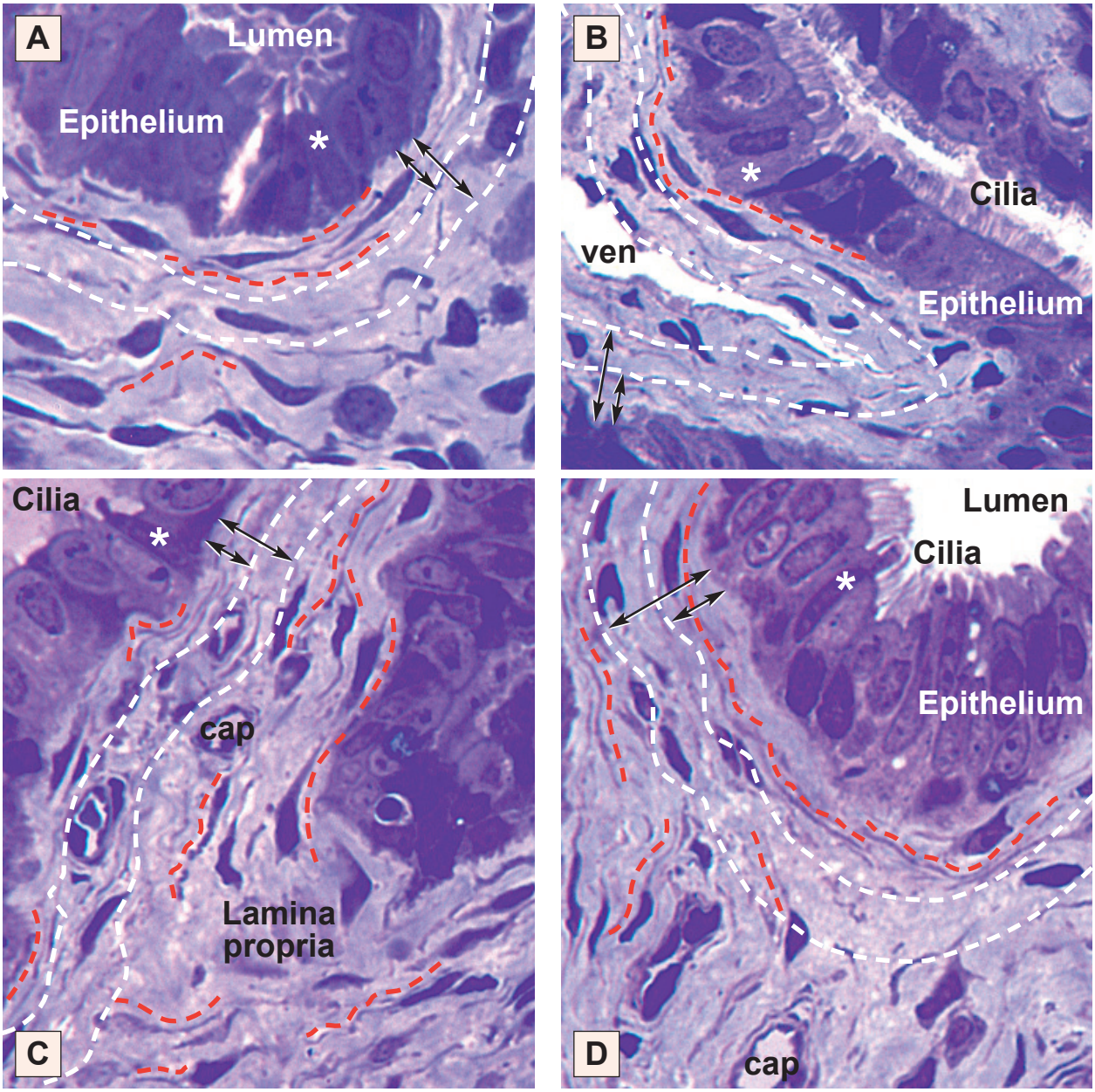

Fig. 11 A–D Non-conventional light microscopy (NCLM). Semi-thin sections (0.5–1 μm thick) of fallopian-tube wall; Epon-block cross sections were stained with toluidine blue, and photographed under a light microscope. The absolute and relative numbers of t-ICC were counted. White dashed lines mark areas where counts were done: superficial and, subepithelial regions of lamina propria, equivalent to 50% and 100% of epithelium height, respectively (arrows). At least 20 t-ICC are shown by red dashed lines in lamina propria. * = epithelial peg cells. Original magnification, 40x.

phate buffered saline. A positive control (a tissue known to express the marker in question) was used for every specific immunocytochemical stain. To ensure the reliability of experimental study, internal quality control of immunocytochemical techniques was performed as a part of an implemented and certified quality assurance system (ISO 9001/2001).

Immunofluorescence (IF)

Primary cultured cells grown on coverslips were fixed in 2% paraformaldehyde for 10 min, then washed in PBS and permeabilized in PBS containing 0.5% bovine serum albumin (BSA) and 0.075% saponin (PBSSA) for 15 min (all from Sigma Chemical, St. Louis, MO, USA). Cells were

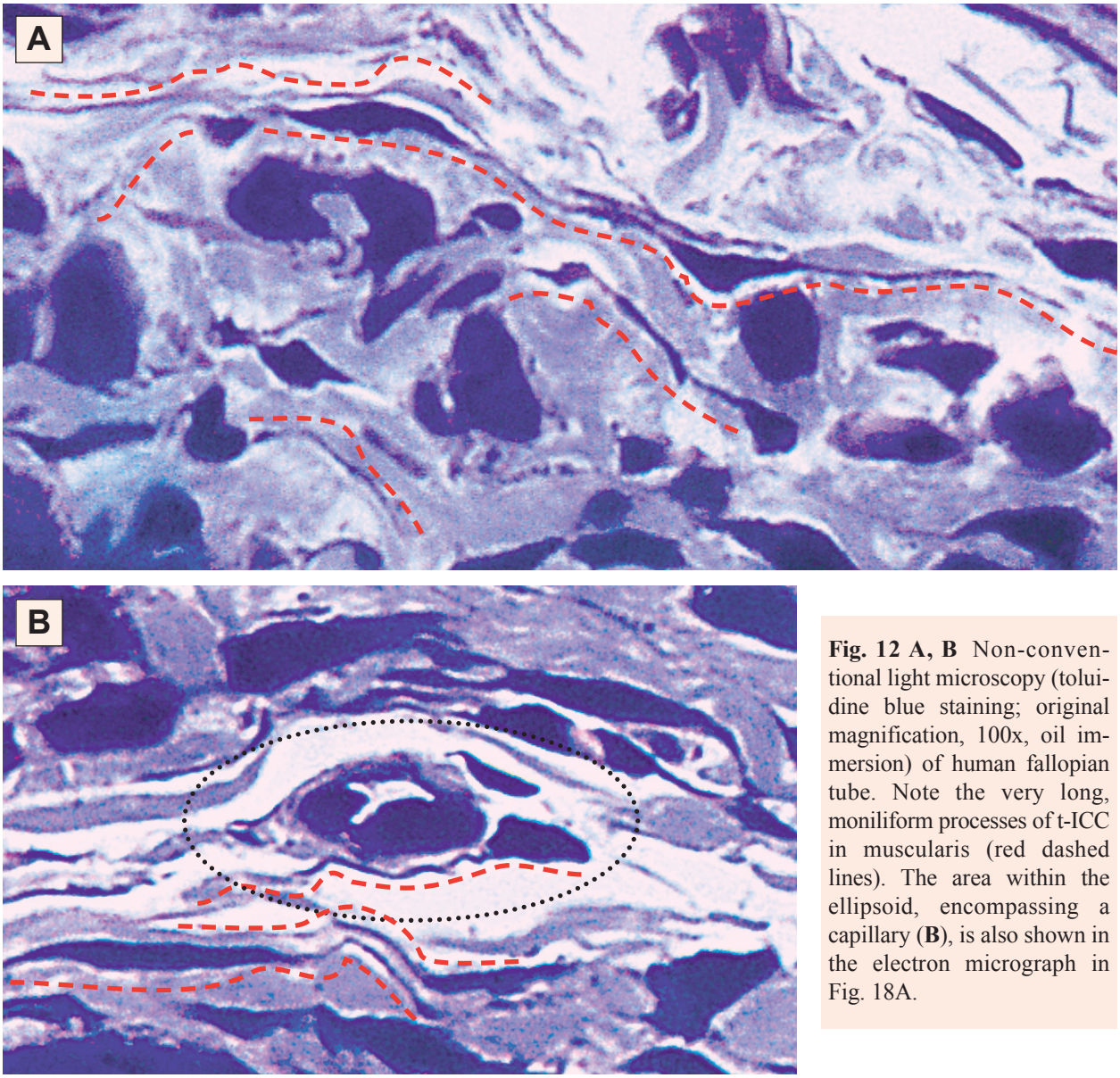

Fig. 12 A, B Non-conventional light microscopy (toluidine blue staining; original magnification, 100x, oil immersion) of human fallopian tube. Note the very long, moniliform processes of t-ICC in muscularis (red dashed lines). The area within the ellipsoid, encompassing a capillary (**B**), is also shown in the electron micrograph in Fig. 18A.

incubated with primary antibodies, diluted in PBSSA, for 4 h at room temperature on an orbital shaker. After three serial rinses, primary antibodies were detected using secondary monoclonal rat anti-mouse biotinylated antibodies, clone A85-1, 1:200 (BD Pharmingen, San Jose, CA, USA) and streptavidin - Alexa Fluor 546 (Invitrogen Molecular Probes, Eugene, OR, USA). A second primary antibody was then applied and, subsequently, a secondary FITC-conjugated polyclonal antibody. Finally, nuclei were counterstained with 1 μg/ml Hoechst 33342 (Sigma Chemical, St. Louis, MO, USA). Cultured cells were tested using the following primary **antibodies**: mouse anti-human **CD117/c-kit**, monoclonal, clone Ab 81, 1:100 (Santa Cruz Biotech); mouse anti-human **CD34-FITC**, monoclonal, clone 8G12, 1:10 (BD Immunocytometry systems San Jose, CA, USA); mouse anti-**vimentin**, monoclonal, clone V9, 1:100 (DakoCytomation, Glostrup, Denmark); mouse anti-**α-smooth muscle actin**, FITC-conjugated, monoclonal, clone 1A4, 1:200 (Sigma Chemical, St. Louis, MO, USA); mouse anti-**desmin**, monoclonal, clone RD30, 1:50 (BD Pharmingen, San Jose, CA, USA); mouse anti-**caveolin 1**, monoclonal, clone 2297, 1:100 (BD Pharmingen, San Jose, CA, USA); mouse anti-**caveolin 2**, monoclonal, clone 65, 1:100 (BD Pharmingen, San Jose, CA, USA). Negative controls used the same technique, without primary antibodies. Pictures

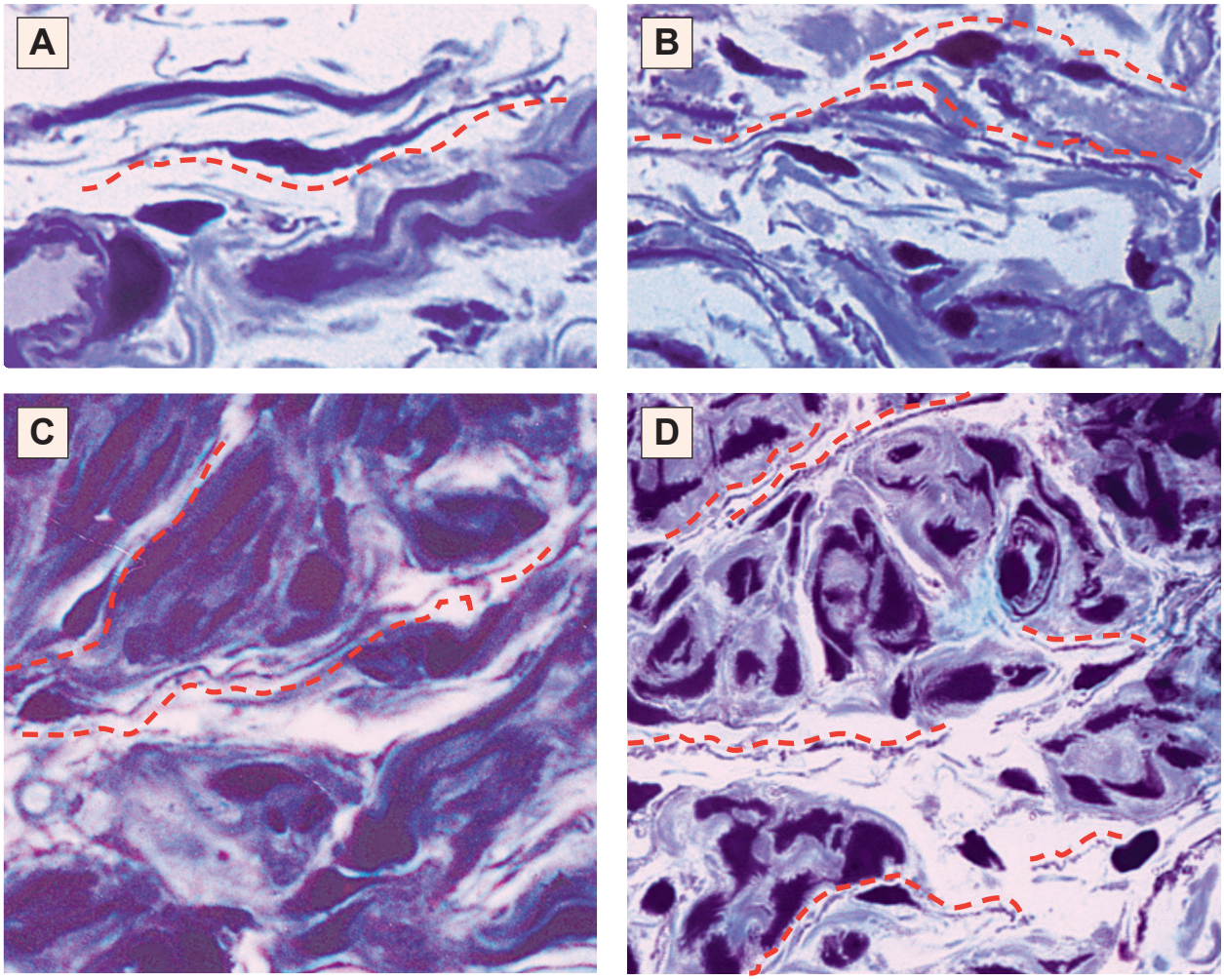

Fig. 13 A–D Non-conventional light microscopy. Toluidine blue stained semi-thin sections: longitudinal (**A**), oblique (**B&C**) or cross-sections (**D**). The red dashed lines indicate at least 10 t-ICC (cell bodies and the emergent long, moniliform processes) amongst the smooth muscle fascicles. Original magnification, 100x, oil immersion.

were taken using a Nikon DX1 camera mounted on a Nikon TE300 microscope and Nikon PlanApo 40x and 60x objectives.

Paraffin-embedded formalin-fixed sections of human oviducts were also used to study CD1a expression using IF. Standard dewaxed sections were rinsed in PBS, blocked using PBS supplemented with 0.5% bovine serumalbumin (BSA), and incubated overnight at room temperature with a FITC-conjugated monoclonal CD1a antibody (clone HI149, working dilution 1:10 in PBS supplemented with 0.5% BSA and 2mM sodium azide, BD Pharmingen, San Jose, CA, USA). The slides were subsequently rinsed in PBS, coverslipped using a fluorescence mounting medium (DakoCytomation, Glostrup, Denmark) and examined. Non-specific fluorescence was evaluated using an irrelevant isotype-matched FITC conjugated antibody as negative control.

Electrophysiology

Extracellular single unit recordings were performed on t-ICC in primary cultures (the 3rd day of culture), grown on coverslips in 2 cm round wells, in DMEM supplemented with 10% fetal bovine serum (FBS), HEPES 1.5mM. A Nikon inverted TE200 microscope equipped with a Nikon DN-5 digital camera and an Eppendorf (Eppendorf AG, Hamburg, Germany) NK I micromanipulator were used to position the microelectrodes. On-site made glass microelectrodes (WPI 1B150F-4) were filled with 3 mol/L potassium acetate and had resistances between 4 and 8 MOhms. The field potential variation was measured using a WPI Duo 773 electrometer (World Precision Instruments, Sarasota, FL, USA), and outputs were displayed on an oscilloscope. Electrical signals were digitized using a Digidata 1322A data processor (Axon Instruments, Union City, CA, USA) and digitally stored. The Clampex 8.2 software was used for data acquisition and analysis.

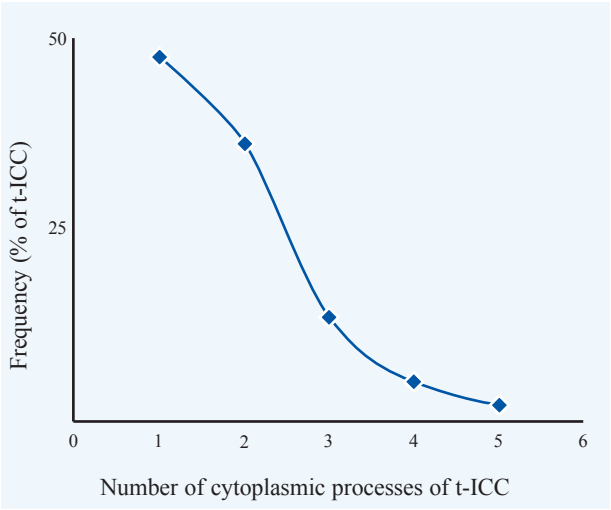

Fig. 14 The number of cytoplasmic processes (expanding from t-ICC body) plotted against the frequency in the whole population of t-ICC (lamina propria + muscularis); NCLM: 232 t-ICC were counted, on 52 photographs. The curve looks like the right 'portion of a typical Gaussian curve'.

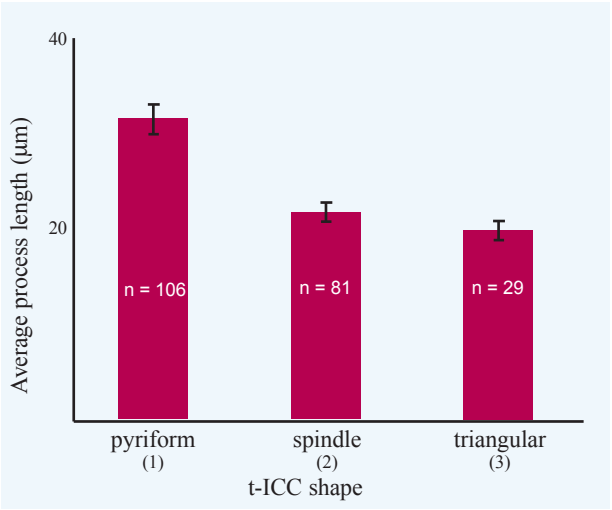

Fig. 15 Histogram showing the average length (µm) of t-ICC processes as a function of cell-body shape; number of processes in brackets; NCLM: 216 cells, on 50 photographs were counted ($p < 0.001$).

Results

Interstitial cells resembling the archetypal enteric ICC, if present in human fallopian tube (t-ICC), might be found in:

- **mucosa**: in the 'unremarkable' *lamina propria* - the interstitium containing fibroblasts, mast cells, lymphoid cells, collagen and reticular fibers, etc.;
- **muscularis**, in the loose connective tissue which fills interstitial spaces between the bundles of circular and longitudinal smooth muscle fibers, or in
- **subserosa**, the loose connective tissue between serosa and the muscularis.

The traditional, routine staining with hematoxylin and eosin (Fig. 1) cannot be succesfully used for identification of t-ICC. The main bias remains the difficulty to differentiate between the cell processes and collagen fibres.

Supravital staining of fallopian tube fragments with methylene-blue resulted in the visualization of Cajal-like interstitial cells (Fig. 2). Interpreting in visual terms, Fig. 2 seems the first (strong) indication that t-ICC do exist. Additional proof was provided by growing t-ICC *in vitro*.

We estimated the *spatial density* of t-ICC in the ampullary region of the fallopian tube since this is the location of fertilization and early embryo cleavage. Using the methylene-blue vital staining followed by cryosectioning, we found a value of 100-150 cells/mm^2 (Fig. 2). This density is of the same order of magnitude as that reported by Alberti *et al.* [61], who estimated the distribution of c-kit positive ICC in rat colon.

t-ICC in primary culture

t-ICC were successfully maintained in primary culture and can easily be identified (distinguished from the smooth muscle cells) before reaching confluence (Fig. 3A, B). *Starting with the 3rd day in culture, t-ICC appear with long, moniliform processes extending from the cell body* (Figs. 3–6). Concomitantly, some cells begin to contact each other or establish 'connections' with smooth muscle cells, creating a *network* appearance. A rough quantitative estimation of *in vitro* cell population (n = 324) reveals 9.9±0.9% t-ICC and 69±2.5% smooth muscle cells. The remaining were fibroblasts (17.8±1.8%) or cells of other (difficult to establish) phenotypes.

We used **Giemsa stain** to recognize cultured t-ICC, since this stain is a mixture containing methylene-blue eosinate and methylene-blue chloride, dissolved in methyl alcohol, with glycerol as a

stabiliser. Fig. 2C displays a spectacular octopus-like t-ICC. Since Giemsa stain is acting concomitantly as dye and fixative, we searched for the characteristic moniliform aspect of t-ICC processes using *vital stains*: crystal violet (Fig. 3D, E; Fig. 4A–C), methylene blue (Fig. 5A–D), Janus green B (Fig. 6A, B), MitoTracker Green FM (Fig. 6D, E).

Vital stainings with **crystal violet** and **methylene blue** revealed that in *living cells*, the t-ICC processes are very long (several tens of μm), have an uneven caliber, with dilated portions, resembling 'beads on a string'.

Previous TEM studies on pancreatic Cajal-like cells in our laboratory showed that the dilated portions of the long processes, frequently accomodate mitochondria [46]. **Janus green B**, a well-known *vital stain, with high affinity for mitochondria* [62] was used to assess t-ICC viability and localize mitochondria. The initial dark green-blue color, due to mitochondria stained with Janus green B, became a brownish gray one, and finally decolorized (leuco-compound). Fig. 6A, B illustrate the staining of t-ICC body and dilations of the processes. Color changes are obvious. To double-check these results, we used a *fluorescent probe for mitochondria*, **MitoTracker Green FM** [55, 56]. Figs. 6C & E indicate that fluorescent mitochondria are located in both cell body and dilations of long, moniliform cell processes.

Other tested vital dyes (orange G, methyl green and safranin O) failed to stain t-ICC in primary culture, under our experimental conditions.

Usual light microscopy

Since t-ICC were successfully identified in primary cell cultures with various staining procedures, we further tried to figure out, whether is possible to stain 'selectively' Cajal-type cells in fixed, paraffin-embedded sections, using vital dyes.

Vital stains (methylene blue, crystal violet, Victoria blue, Janus green B and safranin O), as well as Giemsa stain are effective in pointing out the t-ICC processes (Fig. 7A–F). Similar results (Figs. 8, 9) were obtained using trichrome stainings methods (hematoxylin/eosin/methylene-blue, and van Gieson). Taking into account that Ramon y Cajal discovered the 'interstitial neurons' using Golgi silver impregnation, besides methylene-blue vital staining, it appeared attractive to test silver impregnation too. Modified Gomori silver impregnation (Fig. 10) particularly reveals more and longer cell processes than the other mentioned techniques. For instance, 'octopus'-like t-ICC depicted in Fig. 10B seems similar to those found in cell culture (compare with Figs. 3C, 24D and 41).

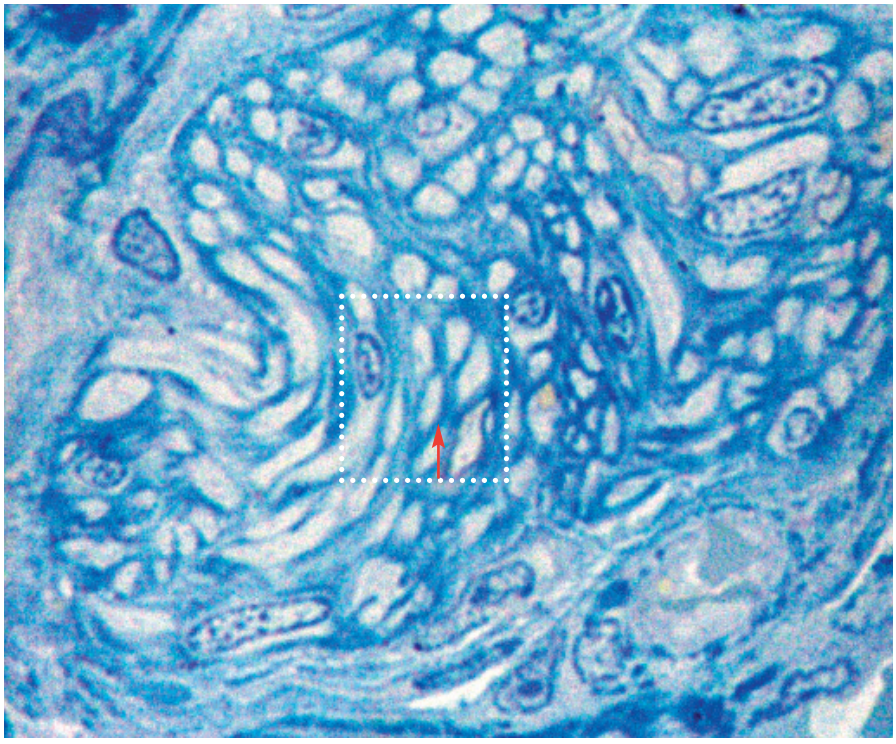

Fig. 16 *Bundles of unmyelinated nerve fibres* in the muscular layer of a human fallopian tube. Photographic reconstruction of a semi-thin (less than 1 μm) section stained with toluidine blue. Higher magnification image (TEM) of the squared dotted area is presented in Fig. 18B. Red arrow indicates the possible location of a t-ICC-process in the connective tissue surrounding nerve fibres fascicles.

Non-conventional light microscopy (NCLM):

Topography, relative density and distinctive processes of t-ICC

NCLM consists essentially in processing tissue specimens as for TEM, *but* (semi)thin sections, less than 1 μm thickness, were stained with toluidine blue, and finally examined under a light microscope. This approach enables a better structural discrimination of t-ICC; compare Figs. 1 and 7–10 with Figs. 11–13. NCLM seems the election methodology to easily establish the location and the number of t-ICC. However, the limitations of NCLM versus TEM are obvious (compare Fig. 12B with Fig. 18A, and Fig. 16 with Fig. 18B).

Localization: t-ICC are residents in the *non-epithelial interstitial domains*, mainly in the connective tissue of mucosal *lamina propria* and in *muscularis*, among the smooth muscle cells (Figs. 11–13, 49). In our opinion, the absolute **number** of t-ICC seems irrelevant for the present time, since t-ICC functions are still subjects of speculations. However, we thought that it could be useful to identify some microscopic areas where t-ICC might be located preferentially. Therefore, we chose five zones of interest across the tubal wall (from lumen to serosa) for estimating separately the *relative numeric density* (RND) of t-ICC (percentage of t-ICC out of all cells found in that area). The results were:

1. the *border epithelium/lamina propria*, a 'belt' 10 μm thick underneath the basement membrane of the endosalpinx epithelium (RND = 18 ± 2%, the *highest local density* across the tubal wall);
2. the *subepithelial portion of lamina propria* (~ 20μm thick) (RND = 11.7 ± 0.9%);
3. the whole territory of *lamina propria* (RND = ~ 8%);
4. the *muscularis* (RND = 7.8 ± 1.2%), and, apparently the less important,
5. submesothelial space (RND = not assessed).

These data, also illustrated in Fig. 49, show clearly a *decreasing* **gradient** *from epithelium to serosa*. It might not be incidental that t-ICC represent 9.9 ± 0.9% of cell population in primary culture (p. 492) and the average numeric density of t-ICC in lamina propria is about 8% or in muscularis 7.8 ± 1.2%.

Cytoplasmic processes of t-ICC: Fig. 14 shows that ~50% of t-ICC observable by NCLM exhibit only **one** long process, ~30% and ~15% have **two** and **three** processes, respectively. Therefore, cell-body shape frequency in the case of t-ICC is: pyriform, fusiform, triangular, tetragonal or pentagonal. When a t-ICC exhibits only one process, this prolongation is about 30μm (or more) long. However, when two or three processes emerge from the t-ICC body, their length is quite equal, around 20μm (Fig. 15).

Close relationships of t-ICC processes with various tissue components: 13% of lamina propria t-ICC processes 'look for' the covering *epithelium*, while, as expected, none of the muscularis t-ICC processes reaches it. Small *blood vessels* (capillaries and postcapillary venules) within the mucosal and muscular layers were contacted by 6% of all t-ICC processes, with almost equal contribution from t-ICC in both histological locations. Close relationships are also established with *nerve fibers* (Fig. 16) and between *t-ICC themselves*.

Like in other organs, *cytoplasmic processes*, which *define Cajal-like cells*, are *long* (tens of μm), *thin* (≤0.5μm) and *moniliform*. A characteristic t-ICC process *network*-like layout is noteworthy.

TEM:

Ultrastructural characterization of t-ICC

There is no question that TEM is essential to establish that a given extradigestive interstitial cell-type becomes (or not) a member of the Cajal-like cells' selective club.

During the last ten years, several authors made efforts to systematize the ultrastructural features in order to facilitate the electron microscope diagnosis of ICC [13–15, 63] or interstitial Cajal-like cells [64]. In our opinion, the most ellaborate set of criteria is the so-called '*gold standard*' proposed by Huizinga, Thuneberg, Vanderwinden, Rumessen, 1997 [15] and composed of eight criteria. Actually, this standard includes the six criteria suggested by Faussone-Pellegrini and Thuneberg, 1999 [14] and the three criteria formulated by Komuro *et al.,* 1999 [13]. We emphasize that *all the eight criteria* required by the 'gold standard'

Table 1 Semiquantitative data [a] concerning the ultrastructure (TEM) of **t-ICC** (this study) in comparison with the pancreatic [12] and archetypal enteric ICC (Auerbach's plexus from **small intestine** and **colon**), as summarized in ref. [10, 14].

ICC in	ULTRASTRUCTURAL COMPONENT [b] of ICC or ICC-like								Intercellular contacts [c]		
	Cav.	BL	sER	rER	Mi	IF	mT	A	CC	GJ	
									nerve	SMC	IC
Fallopian tube	+ +	±	+	+	+ [i]	+	+	+	+	+	+
Pancreas (exocrine)	+	±	+	+	+ + [ii]	+	+	+	+	± *	+
Small intestine	+	0	+ +	±	+ + +	+ +	+	+	+	+	+
Colon	+	0	+	+	+	+	+	±	+	+	+

[a] *Symbols*: 0 = absent; ± = occasionally present; + = present; the relative richness is marked by + + or + + +; Mitochondria as percent of cytoplasmic volume: [i] = 4.8±1.7%; [ii] = 8.7±0.8%

[b] Cav. = caveolae; BL = basal lamina; sER = smooth endoplasmic reticulum; rER = rough endoplasmic reticulum; Mi = mitochondria; IF = intermediate filaments; mT = microtubules; A = thin (actin) filaments.

[c] CC = close contacts; GJ = gap junction; SMC = smooth muscle cells; IC = ICC or interstitial Cajal-like cells.

* contacts with *ductal* smooth muscle cells.

[15] are easily recognized in our TEM images (Figs. 17–23):

1. numerous, large *mitochondria* (Figs. 17, 23; Table 1 - above & Table 2, p. 503);
2. bundles of *intermediate filaments* (Figs. 19; Table 1);
3. *absence of thick filaments* (Figs. 17–23);
4. presence of surface *caveolae* (Figs. 19–21, 23; Tables 1&2);
5. variable developed *basal lamina* (Fig. 17; Table 1);
6. *contacts between ICC and nerve bundles* (Figs. 18A, 20; Table 1);
7. presence of a *well-developed smooth and rough endoplasmic* reticulum (Figs. 17–21, 23B,C; Tables 1&2);
8. *close apposition or gap-junction* contact *with smooth muscle cells* (Fig. 22B; Table 1) or *with each other* (Figs. 19, 21; Table 1).

Table 1 shows that tubal interstitial cells are indeed Cajal-like cells, according to the 'gold standard' criteria. In our opinion, the 'gold standard' [15] is instrumental for the morphological identification of ICC and can serve to recognize interstitial Cajal-like cells outside the musculature of the gastrointestinal tract. However, we suggest that two other criteria can be added, thus obtaining a decalogue (8+2), a '**platinum standard**'. The *9th criterion*: which of the following microscopic (ultra)structures – epithelium, capillaries, smooth muscle cells or nerve fibers – is (are) the target(s) in a given organ (*e.g.* for fallopian tube, all four). The rationale for the *10th criterion* is, in our opinion, imposed by a syllogism: (1) to be Cajal-like, a cell has to have cytoplasmic processes; (2) **not** any branching interstitial cell is a Cajal(-like) cell; (3) only cells with certain **characteristic processes** could be considered Cajal-like:

- ***number*** (1–5, but 2–3 in most cases);
- ***length*** (usualy several tens of μm [45], up to 100 μm [14, 46], or even more [39]);
- ***thickness*** (around or less than 0.5 μm; frequently < 0.2 μm);
- ***aspect*** (moniliform, with dilations accomodating usually mitochondria);
- ***branching*** (dichotomous pattern);
- ***organization in network – labyrinthic system*** (processes overlapping with processes of other similar cells).

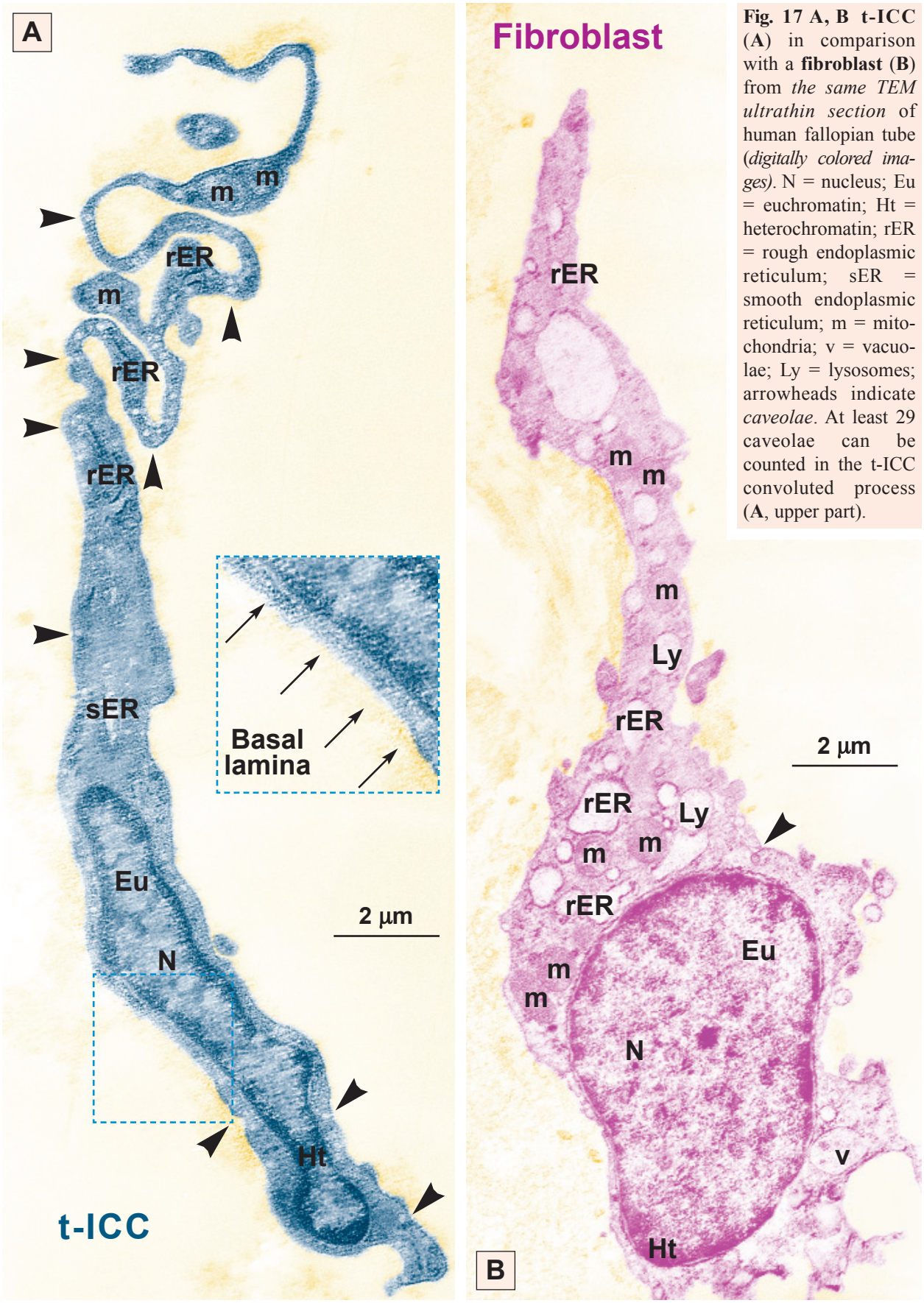

Fig. 17 A, B t-ICC (**A**) in comparison with a **fibroblast** (**B**) from *the same TEM ultrathin section* of human fallopian tube (*digitally colored images)*. N = nucleus; Eu = euchromatin; Ht = heterochromatin; rER = rough endoplasmic reticulum; sER = smooth endoplasmic reticulum; m = mitochondria; v = vacuolae; Ly = lysosomes; arrowheads indicate *caveolae*. At least 29 caveolae can be counted in the t-ICC convoluted process (**A**, upper part).

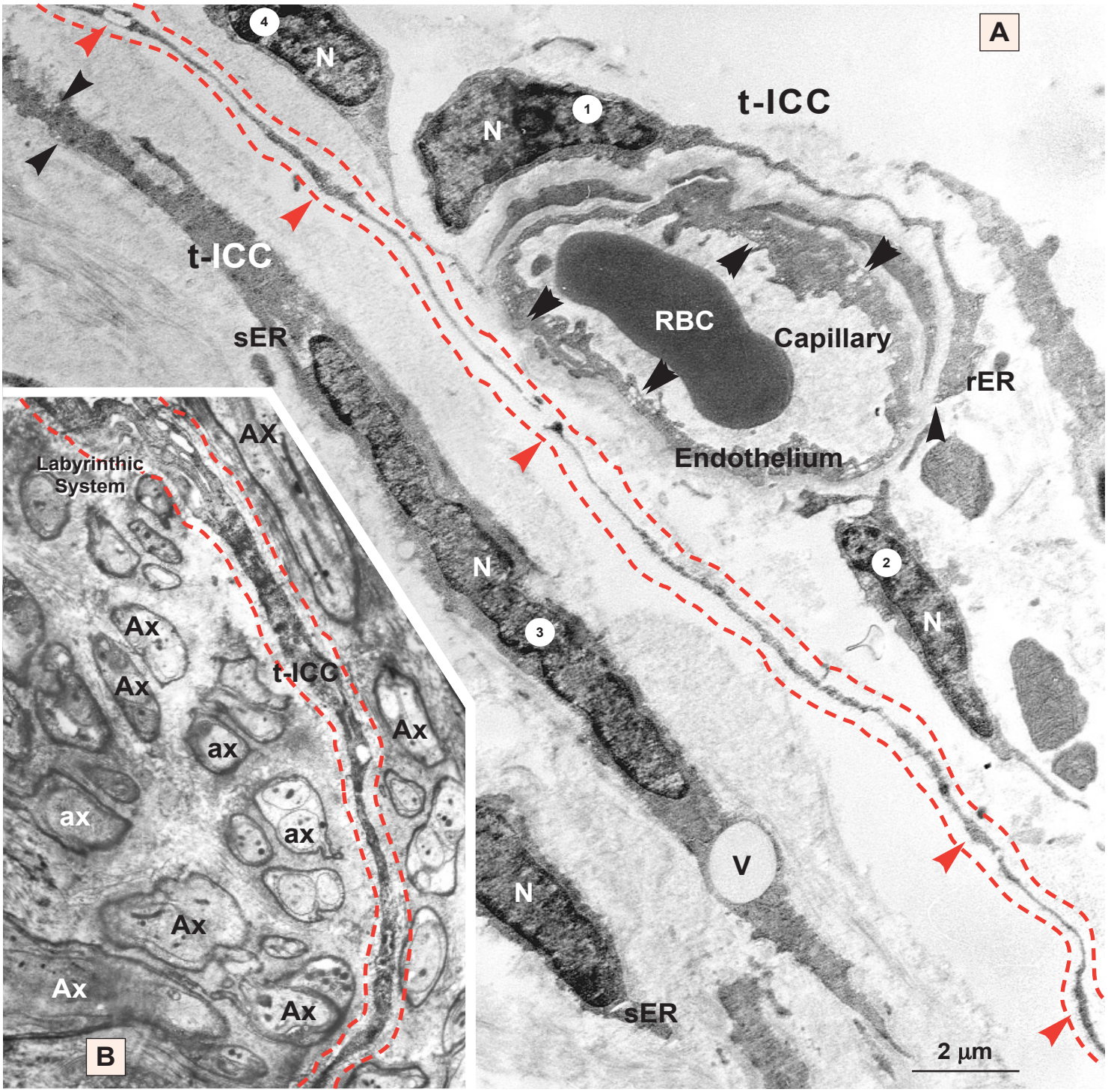

Fig. 18 A. Human fallopian tube; TEM; relationships of t-ICC with a blood capillary. Note at least two t-ICC (marked 1 & 2), but, probably, there are other two similar cells (marked 3 & 4), and a very long and thin cytoplasmic process (in between dashed lines). All these cells and processes surround a blood capillary (*RBC* = red blood cell; *double arrowheads* indicate transcytotic vesicles or endothelial caveolae). The distance between t-ICC processes and the abluminal face of the endothelium is frequently around or less than 1 µm. Red arrowheads show dilations of the cytoplasmic process, giving the moniliform aspect. The length of the process in between the dashed lines is at least 40 µm, having very thin portions, less than 0.2 µm, and, therefore, not visible in light microscopy. **B.** TEM of unmielinated nerve fibers. The axons sectioned longitudinally (AX), obliqually (Ax) or transversally (ax) are engulfed by the cytoplasm of Schwann cells. Note the long moniliform process of a t-ICC in between dashed lines which develops a labyrinthic system (upper part). N = nucleus; V = vesicle; rER = rough endoplasmic reticulum, sER = smooth endoplasmic reticulum.

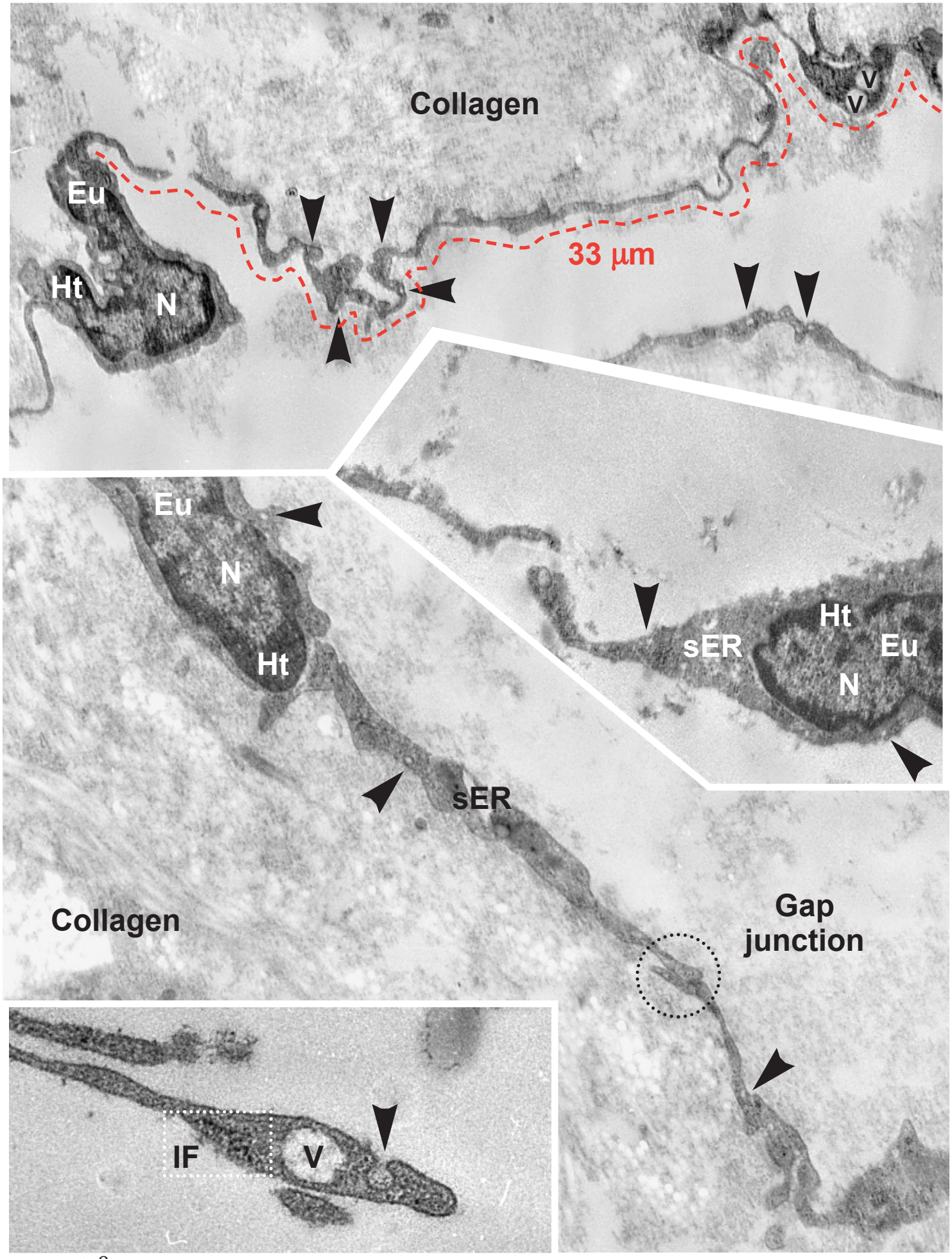
Collagen
V
V
Eu
33 μm
Ht
N
Eu
N
Ht
sER
Ht
Eu
N
sER
Collagen
Gap
junction
IF
V

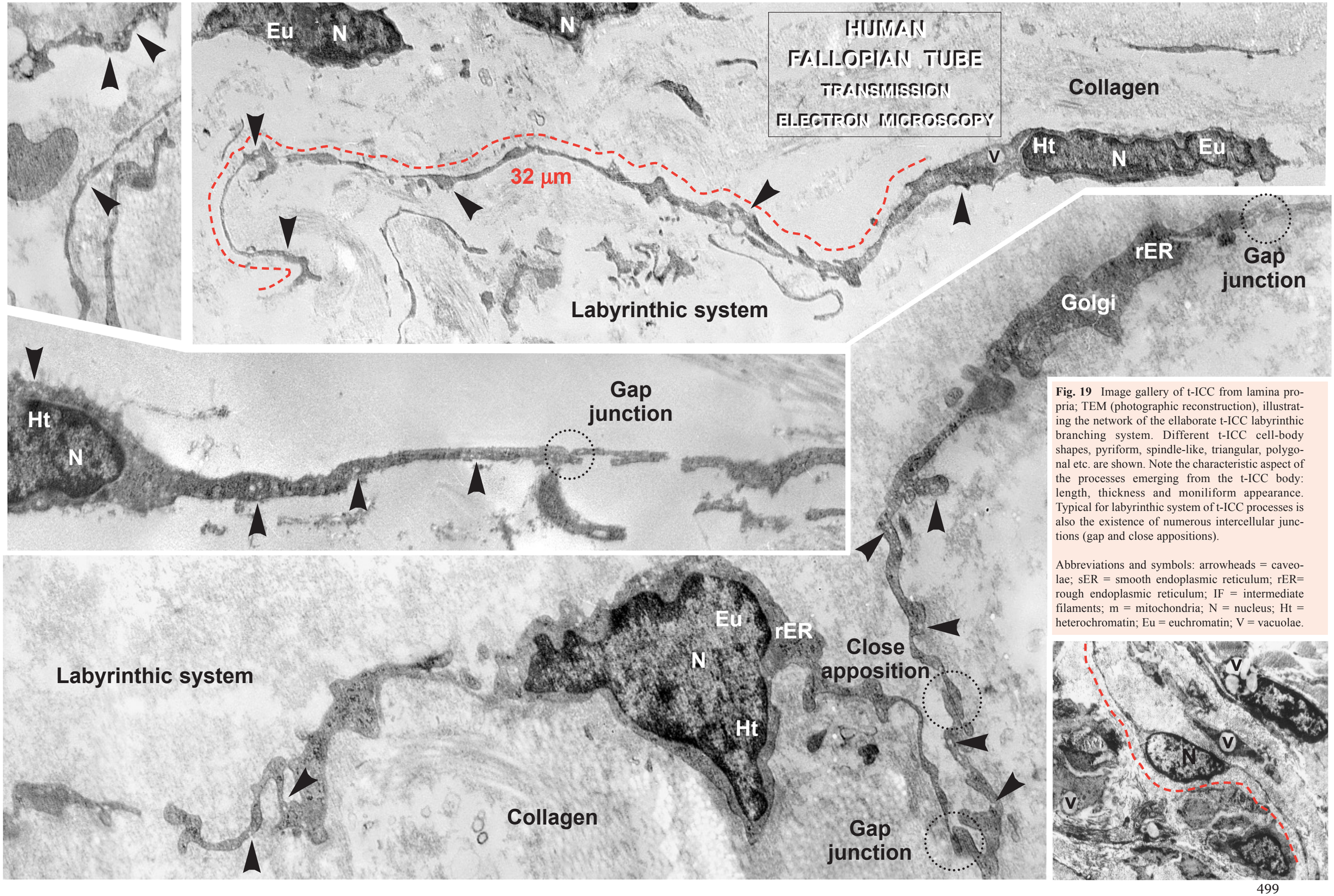

Fig. 19 Image gallery of t-ICC from lamina propria; TEM (photographic reconstruction), illustrating the network of the ellaborate t-ICC labyrinthic branching system. Different t-ICC cell-body shapes, pyriform, spindle-like, triangular, polygonal etc. are shown. Note the characteristic aspect of the processes emerging from the t-ICC body: length, thickness and moniliform appearance. Typical for labyrinthic system of t-ICC processes is also the existence of numerous intercellular junctions (gap and close appositions).

Abbreviations and symbols: arrowheads = caveolae; sER = smooth endoplasmic reticulum; rER= rough endoplasmic reticulum; IF = intermediate filaments; m = mitochondria; N = nucleus; Ht = heterochromatin; Eu = euchromatin; V = vacuolae.

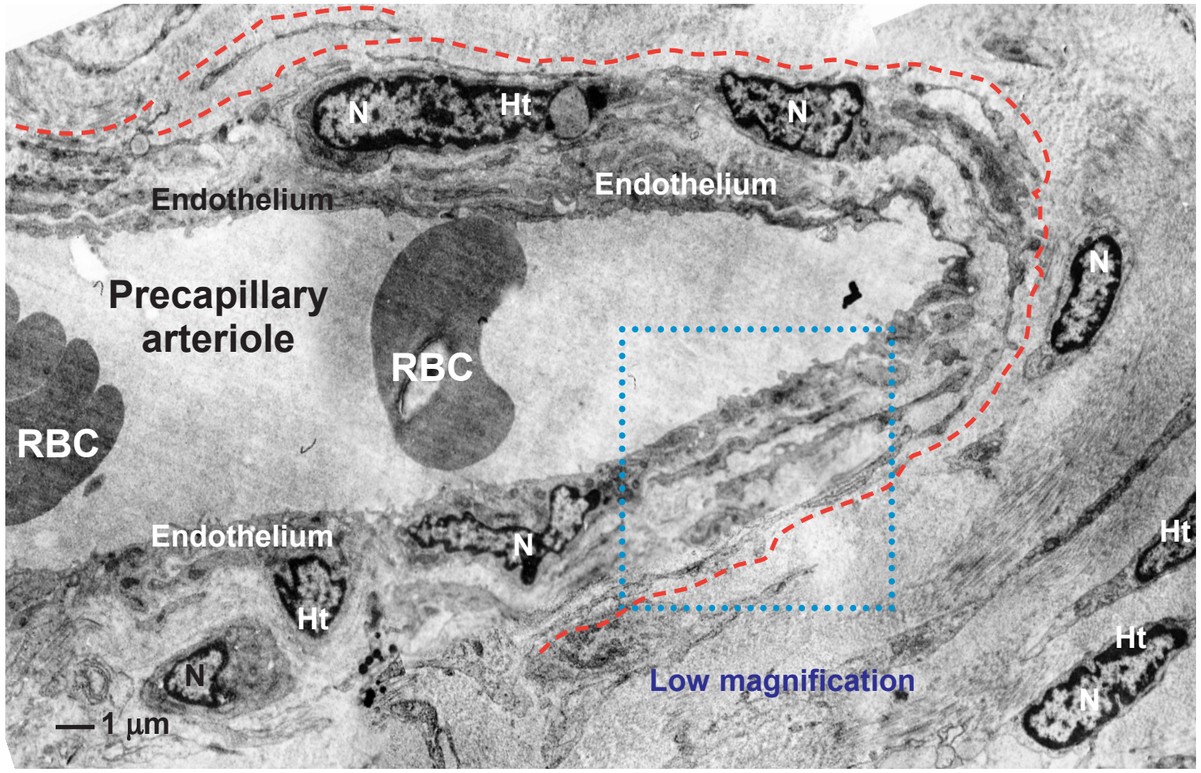

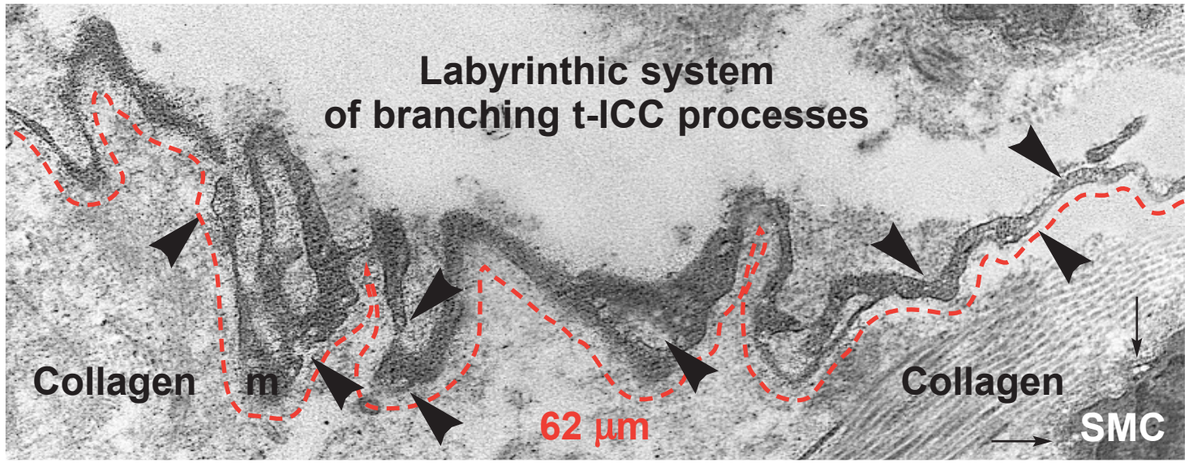

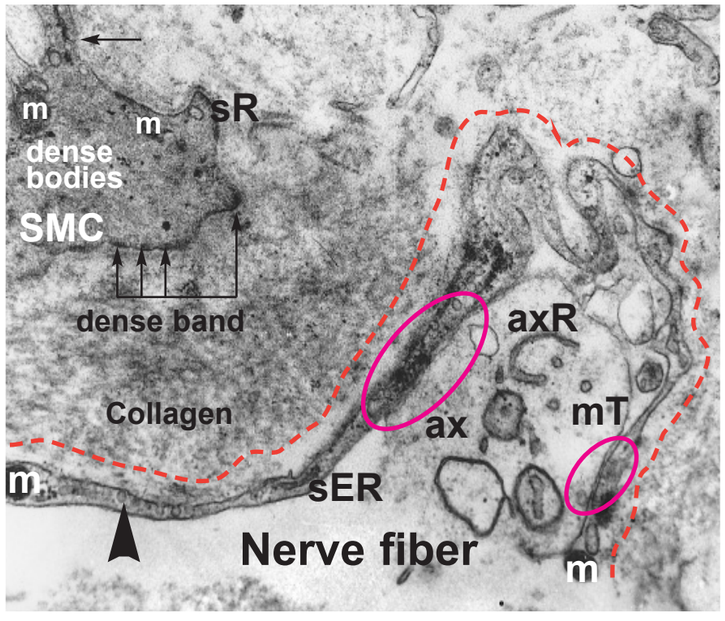

Fig. 20 TEM images showing t-ICC associated with blood vessels, nerve fibers and smooth muscle cells (SMC) from the muscular layer of human fallopian tube. SMC appear as "dark cells", with many protrusions, containing caveolae (arrows), typically for the isotonic contraction, presumably induced by the fixative. Note the basal lamina (double arrowheads), which is thick and surrounds completely each SMC.

Encircled areas (magenta) represent close apposition between the axolemma and plasmalemma of t-ICC process (red dashed line).

Abbreviations and symbols: N = nucleus; Ht = heterochromatin; Eu = euchromatin; n = nucleolus; sER = smooth endoplasmic reticulum; rER= rough endoplasmic reticulum; IF = intermediate filaments; m = mitochondria; V = vacuolae; arrowheads = caveolae; ax = axon; axR = axoplasmic reticulum; mT = microtubules; sR = sarcoplasmic reticulum; RBC = red blood cell.

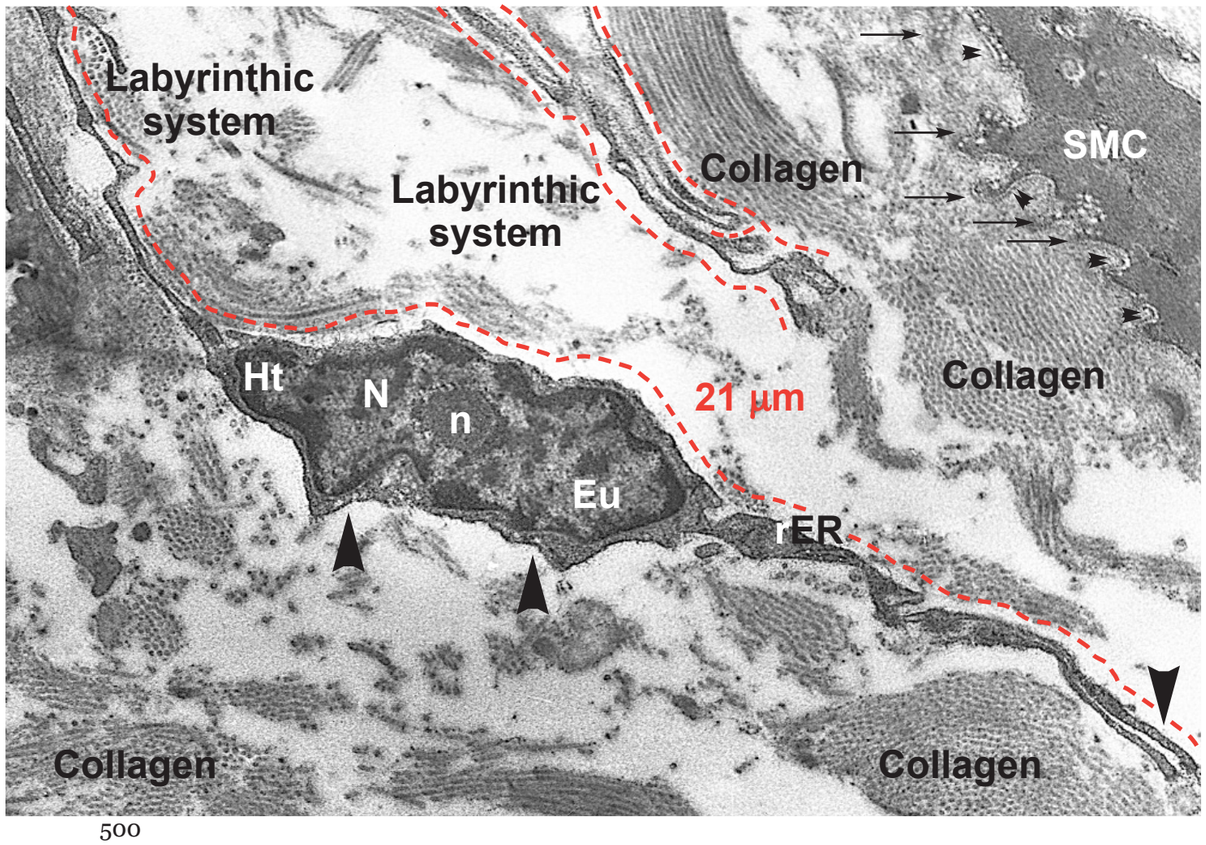

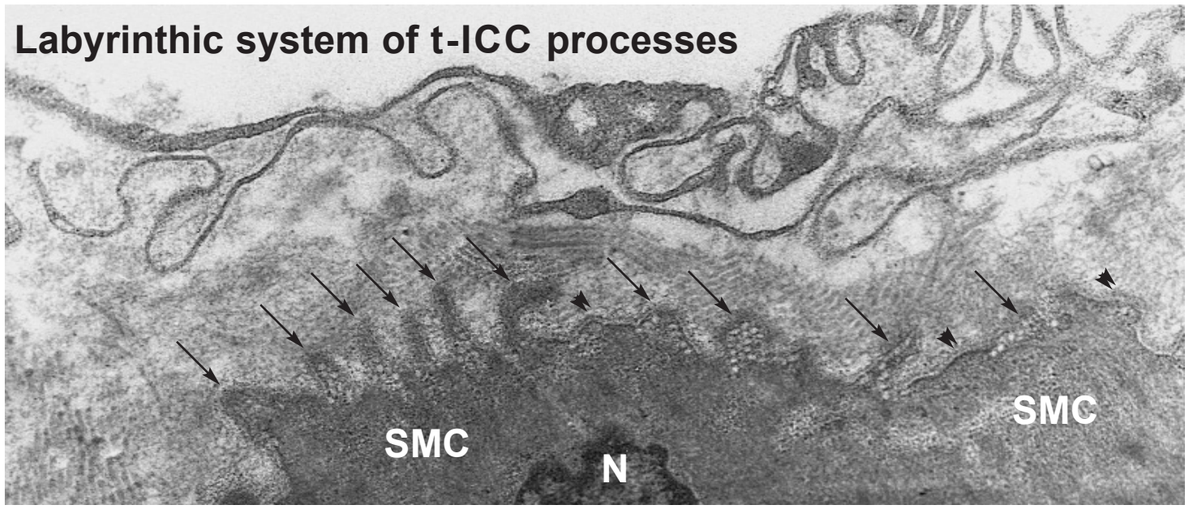

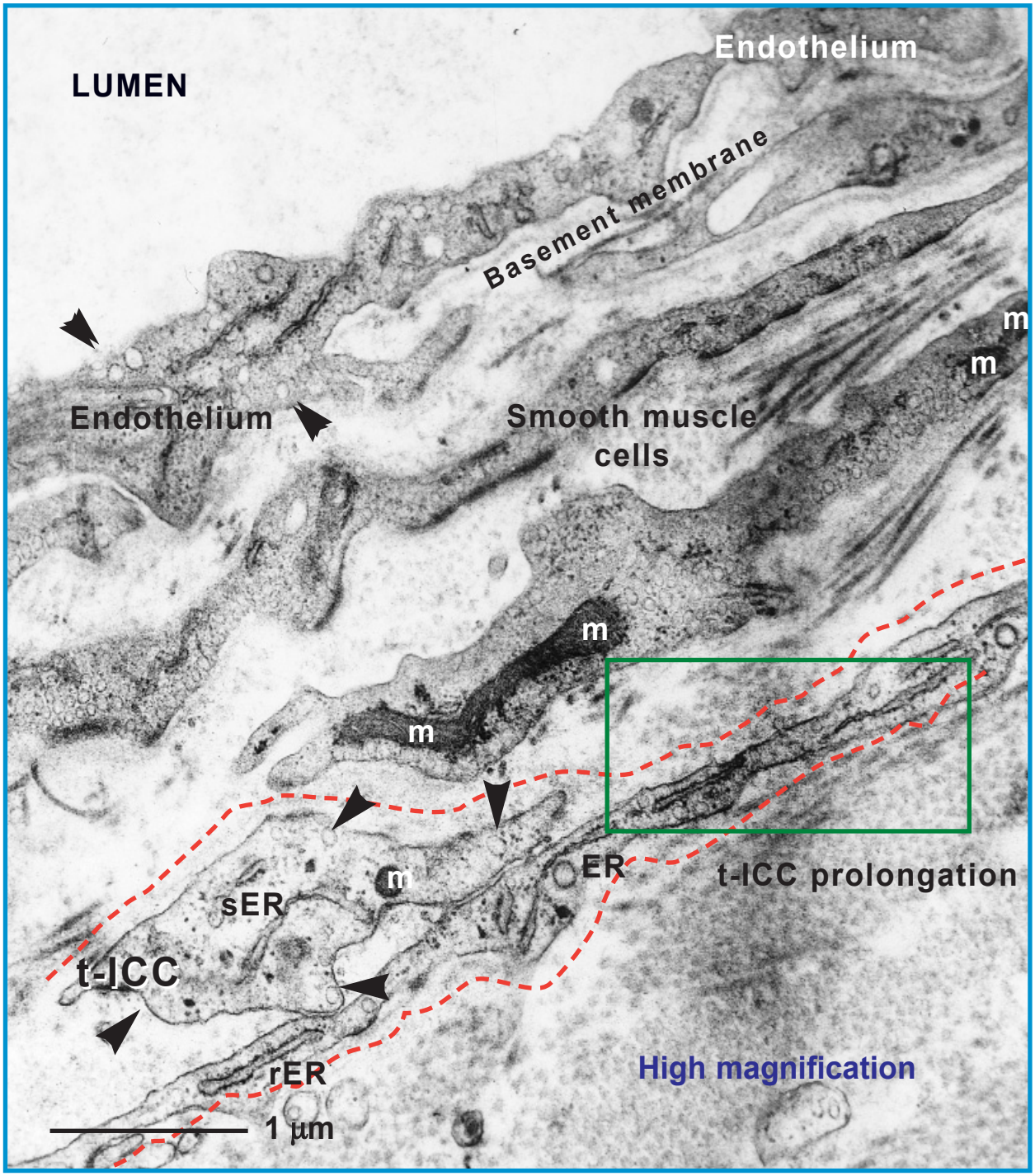

Fig. 21 Cross section (higher magnification) showing a small sector in the wall of an arteriole, corresponding to the *blue inset* from Fig. 20, p. 500. Note the endothelial cells which lie on a basement membrane and have numerous caveolae (transcytotic vesicles) on both sides (luminal and abluminal; double arrowheads). Beyond the intima, two typical smooth muscle cells with caveolae, dense plaques, dense bodies and myofilaments, can be seen. t-ICC processes (red dashed lines) are present in the peri-arteriolar space. m = mitochondria; sER = smooth endoplasmic reticulum; rER = rough endoplasmic reticulum; arrowheads = caveolae.
A striking ultrastructural finding, observable in the green inset, is shown in Fig. 23C, at higher magnification.

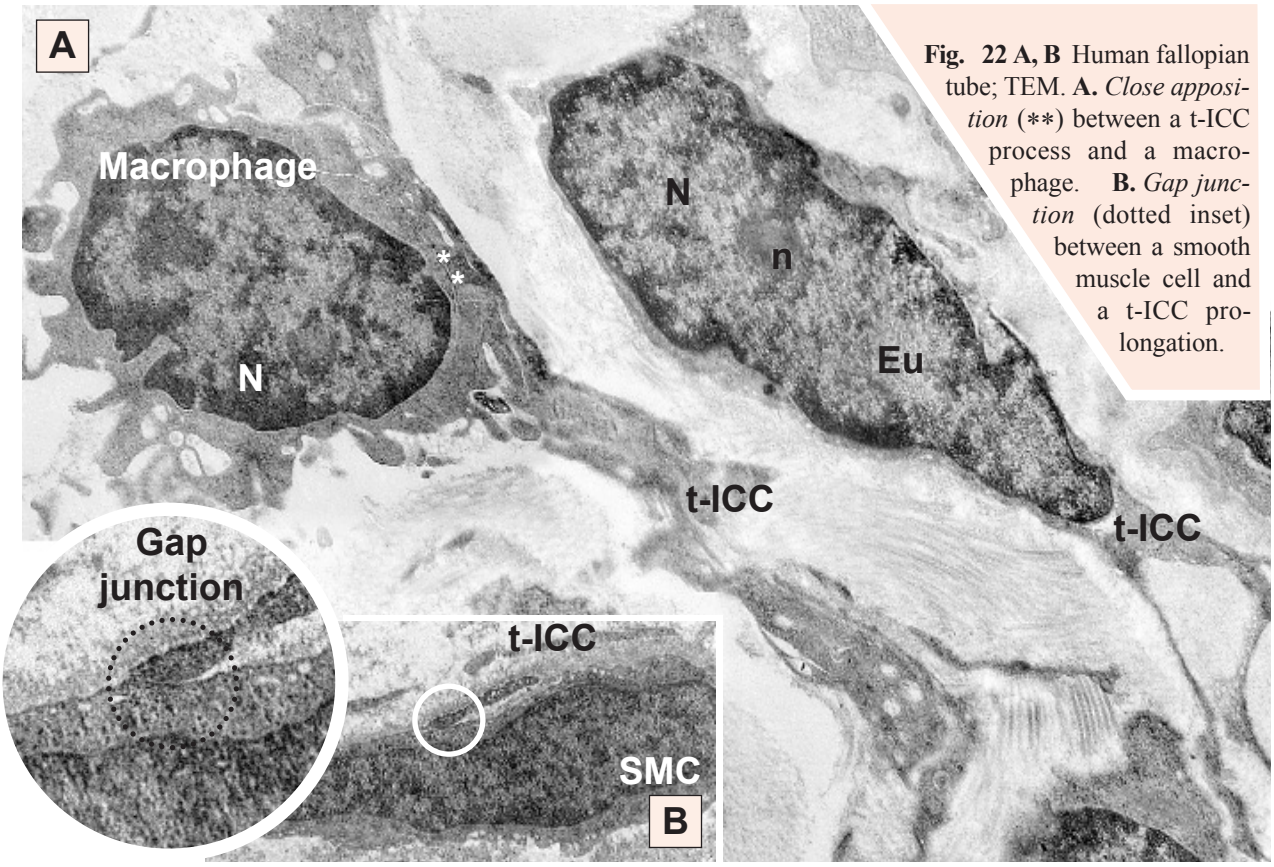

Fig. 22 A, B Human fallopian tube; TEM. **A.** *Close apposition* (**) between a t-ICC process and a macrophage. **B.** *Gap junction* (dotted inset) between a smooth muscle cell and a t-ICC prolongation.

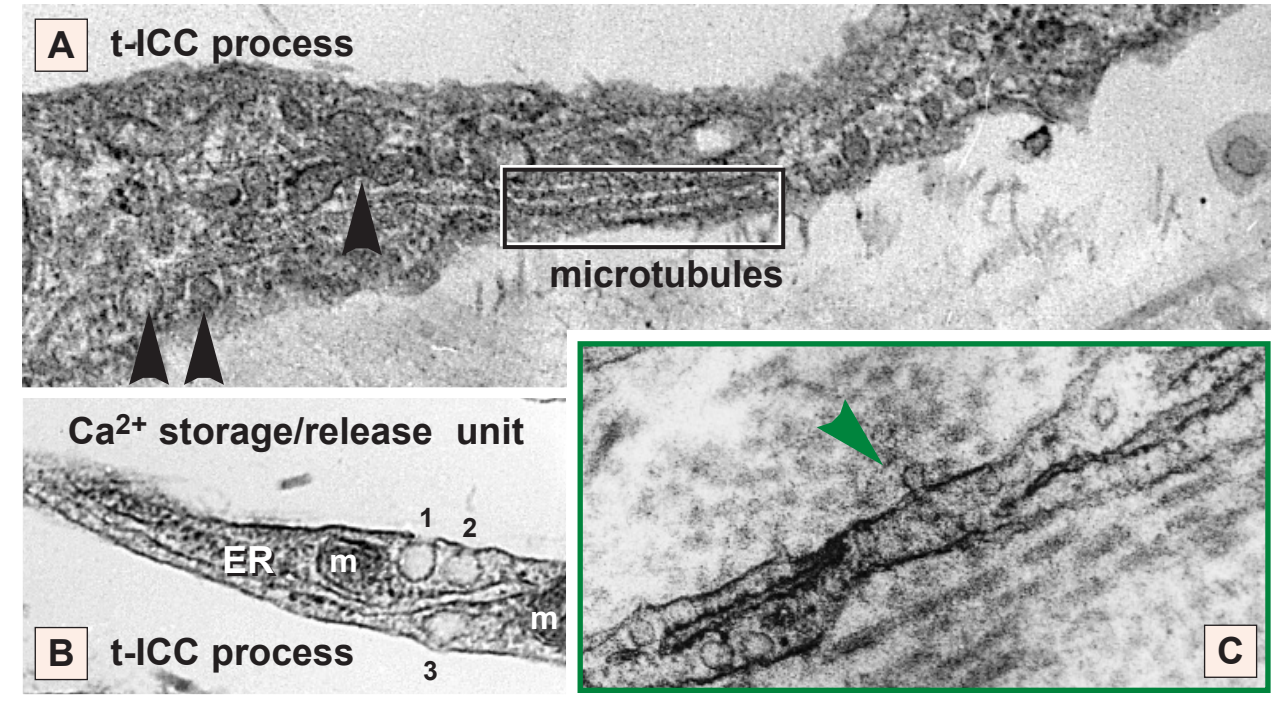

Fig. 23A–C **A.** Note the presence of numerous microtubules and caveolae (arrowheads) in the t-ICC process. **B.** A typical so called 'Ca^{2+} storage/release unit' is shown in the t-ICC process. Such units were described in the periphery of smooth muscle cells: caveolae associated with endo(sarco)plasmic reticulum (ER) and mitochondria (m). Caveola marked 1 shows clearly a *diaphragm* at the neck level. **C.** The inset presents an unexpected caveolar conformation: 'reversed caveola' (green arrowhead). To the best of our knowledge, no such image has ever been published before.

Table 2 Comparison of the *relative volumes (%)* occupied by various *subcellular components* of human tubal Cajal-like interstitial cells (t-ICC) and tubal fibroblasts (of the same specimens).

Subcellular component	%	
	t-ICC	Fibroblasts
Nucleus *	23.6 ± 3.2 (n = 15)	56.4 ± 4.2 (n = 7)
Heterochromatin **	49.1 ± 3.8 (n = 12)	28.2 ± 3.1 (n = 7)
Cytoplasm		
Mitochondria ***	4.8 ± 1.7 (n = 12)	4.9 ± 1.5 (n = 10)
Rough endoplasmic reticulum ***	1.1 ± 0.6 (n = 8)	11.2 ± 1.8 (n = 7)
Smooth endoplasmic reticulum ***	1.0 ± 0.2 (n = 8)	0.7 ± 0.2 (n = 7)
Caveolae (surface vesicles) ***	3.4 ± 0.5 (n = 12)	virtually absent ****

* % of cell volume;
** % of nuclear volume;
*** % of cytoplasmic volume;
**** less than 0.1%. NB.: *In vitro*, human cultured fibroblasts may present caveolae.

Organelles considered as characteristic features for ICC or Cajal-like cells were not ordinarily described in quantitative terms. In our opinion, elusive descriptions (*e.g.* '*numerous*' mitochondria, '*well-developed*' smooth and rough endoplasmic reticulum or '*a large number*' of caveolae etc.) [13–15, 63, 64] should be replaced by precise *numerical information*. Table 2 shows that the relative volume of mitochondria is ~5% in t-ICC. This is similar to intestinal smooth muscle cells [65], tubal fibroblasts (Table 2) or sheep endometrial stromal cells [66]. However, ~5% is only a half of the mitochondrial content in pancreatic Cajal-like cells [45] and much less than in other cell types (20–35%): cardiac myocytes, parietal gastric cells, nephrocytes, hepatocytes etc. Finally, what does 'numerous' mean ?!

The relative caveolar volume (~3.5%; Table 2) is comparable to values in intestinal smooth muscle (2–3%; [67]) or bladder smooth muscle (3.66%; M. Gherghiceanu & L.M. Popescu, to be published). In addition, we found in t-ICC, more caveolae along cytoplasmic processes (1 caveola / 1.73 μm of membrane length) *versus* cell body (1 caveola / 2.66 μm), further confirmed by IF results (*vide infra*, Fig. 24A,B).

Noteworthy, we found at the level of t-ICC processes (Fig. 21B) ultrastructural complexes called '*Ca^{2+}-release units*', composed of endoplasmic reticulum + caveolae ± mitochondria, adjacent to plasmalemma. Such units were recently described in smooth muscle [68]. To the best of our knowledge, no such '*Ca^{2+}-release units*' were previously described in ICC or ICC-like processes.

Differential diagnosis. Fig. 17A,B and Table 2 show unequivocally that the cells that we describe by TEM as interstitial (Cajal-like) cells in human fallopian tube are **not** (morphologically) **fibroblasts**. *In situ*, fibroblasts of adult humans have an euchromatic nucleus and a rough endoplasmic reticulum, with dilated cisternae, about 10 times more developed than t-ICC. Moreover, basal lamina, caveolae and intercellular junctions are absent in human fibroblasts in tissue [69]. Caveolae could be found in human [70] or mouse [71] fibroblasts, but only *in vitro,* in cultured cells.

The original definition of the **myofibroblast** was based on electron microscopy [69], and nowadays myofibroblasts are still definable essentially by ultrastructure as highly differentiated cells, having features in common with smooth muscle cells and fibroblasts [72, 73]. The three essential morphological elements of myofibroblasts are: (i) *stress fibers*, (ii) cell-to-stroma attachment sites (*fibronexuses*), and (iii) intercellular *intermediate* (adherens) and *gap* junctions. But, in the t-ICC, there are **no** *stress fibers, fibronexuses* or *adherens junctions in situ*, by TEM, despite some cells in pri-

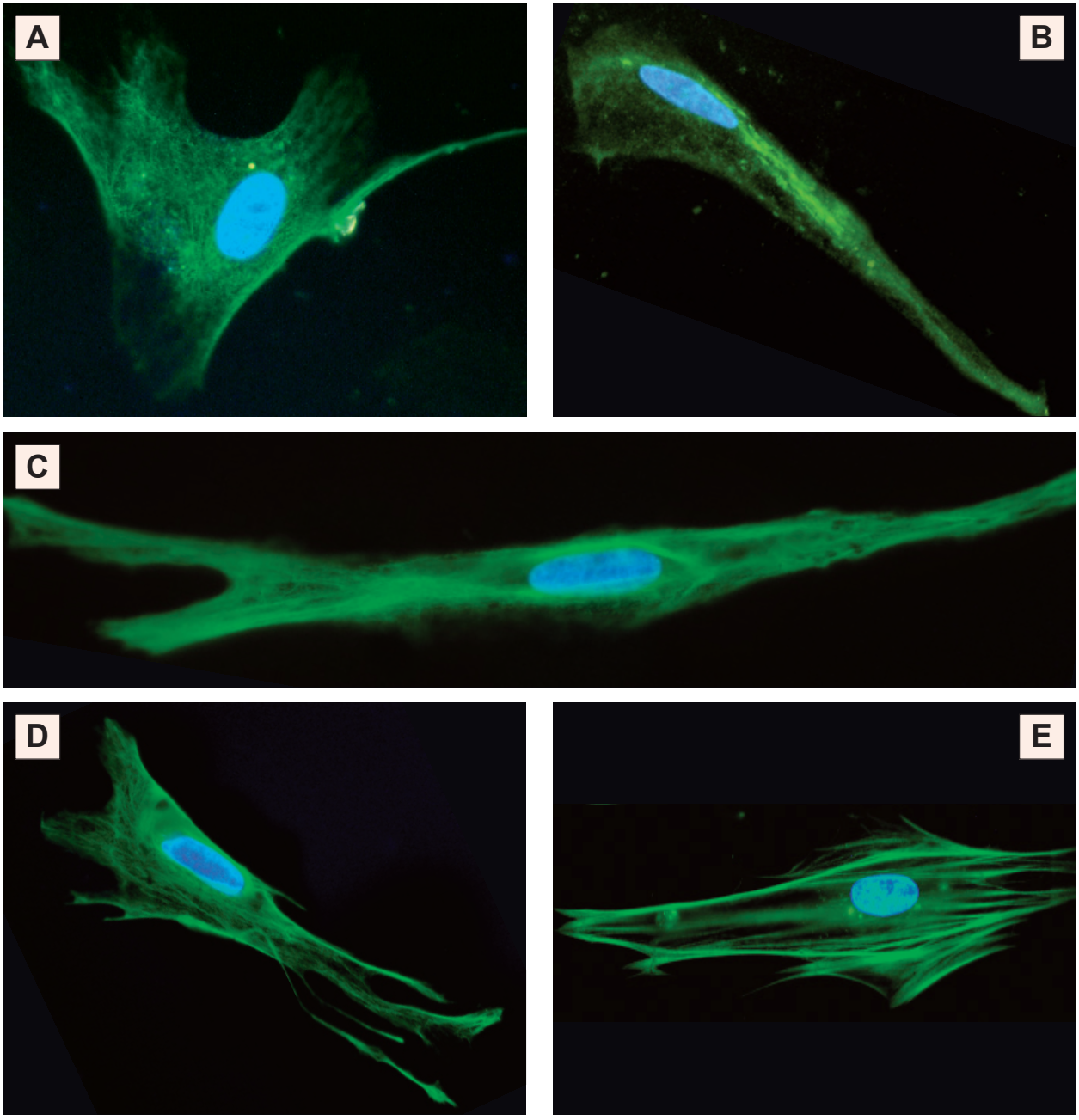

Fig. 24 A–E Human fallopian tube. t-ICC, primary culture (day 4). Immunofluorescence labeling for caveolin-1 (**A**), caveolin-2 (**B**), desmin (**C**), vimentin (**D**) and smooth muscle actin (**E**). FITC-conjugated secondary antibodies (green) were used to visualise the reactions; Hoechst 33342 (blue) for nuclear counterstaining. Antibodies against caveolin-1 (**A**) and caveolin-2 (**B**) stain preferentially t-ICC processes, similar to intermediate filaments (desmin - **C** and vimentin - **D**). Original magnification, 60x. All the cells shown above coexpressed CD117/c-kit, as seen in Figs. 26, 35, 39 and 41.

mary cultures (Figs. 24E and 35). Against myofibroblast morphological phenotype of t-ICC stand also: *absence of dense bodies and attachment plaques*, as well as a poor developed rough endoplasmic reticulum (Table 2), and Golgi area. The differential diagnosis seems obligatory, since some authors [74] considered gastric and intestinal ICC to be myofibroblasts. Although, Walter [75] suggested the presence of myofibroblasts in the mucosal layer of uterine tube of eight mammalian species, this assumption was based **only** on IHC, not by TEM, as required [69, 72, 73].

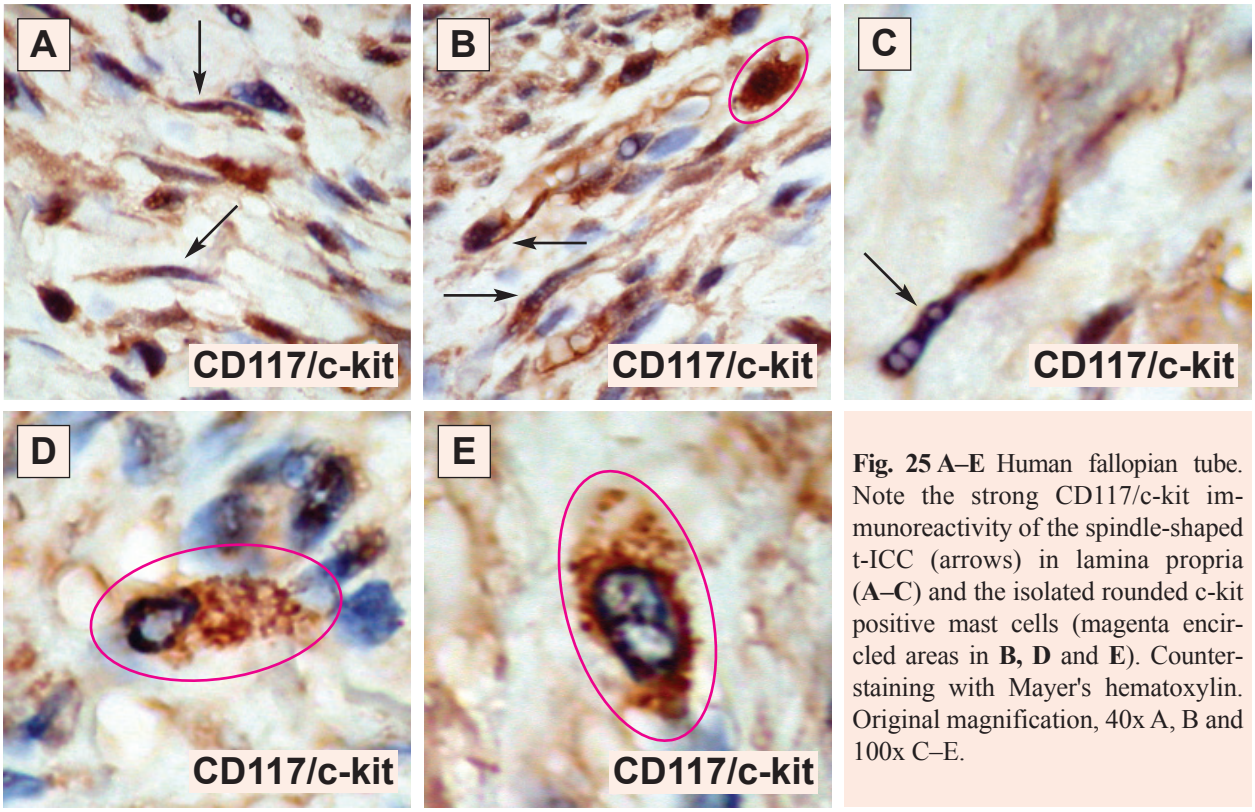

Fig. 25 A–E Human fallopian tube. Note the strong CD117/c-kit immunoreactivity of the spindle-shaped t-ICC (arrows) in lamina propria (**A–C**) and the isolated rounded c-kit positive mast cells (magenta encircled areas in **B, D** and **E**). Counterstaining with Mayer's hematoxylin. Original magnification, 40x A, B and 100x C–E.

Immunophenotyping

t-ICC were further characterized by correlations between the cell morphology and the cell immunophenotype: fifteen different antibodies were used for single- or double-immunolabeling. Staining intensities were considered, according to a score from (–) to (+ + + +) (see Table 3; [76]).

CD117/c-kit is a transmembrane receptor for stem cell factor, usually considered as a quite specific immunochemical marker for ICC or Cajal-like cells [4, 21]. However, Torihashi *et al.* [77] reported that even some typical ICC in human gut do not appear to express c-kit. Moreover, Rumessen and Vanderwinden [63] proposed the classification of mesenchimal cells: either

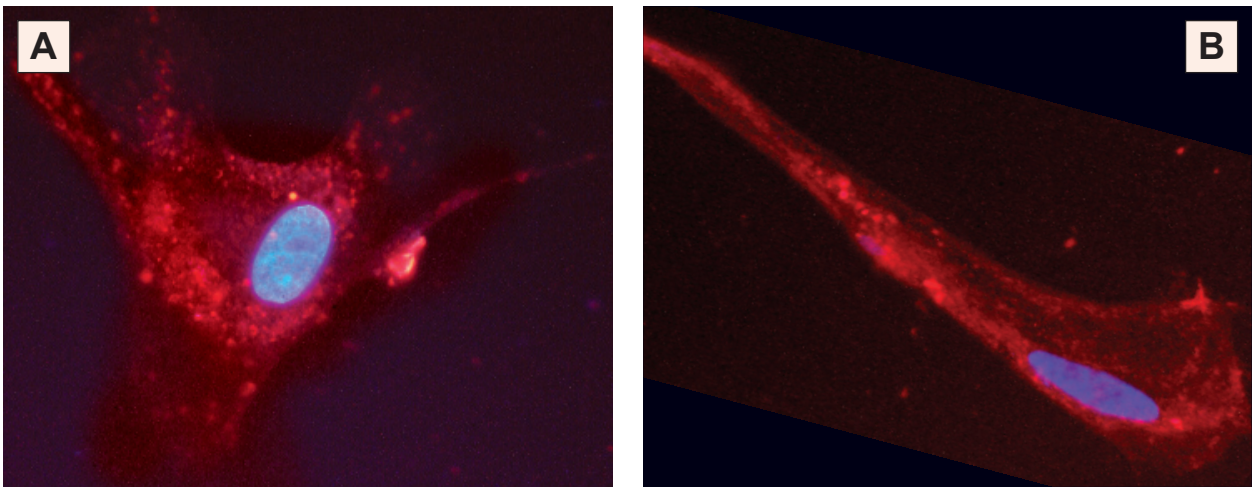

Fig. 26 A, B Human fallopian tube primary cultures. t-ICC assessed by IF for CD117/c-kit (red); nuclei counterstained with Hoechst 33342 (blue). Original magnification, 60x.

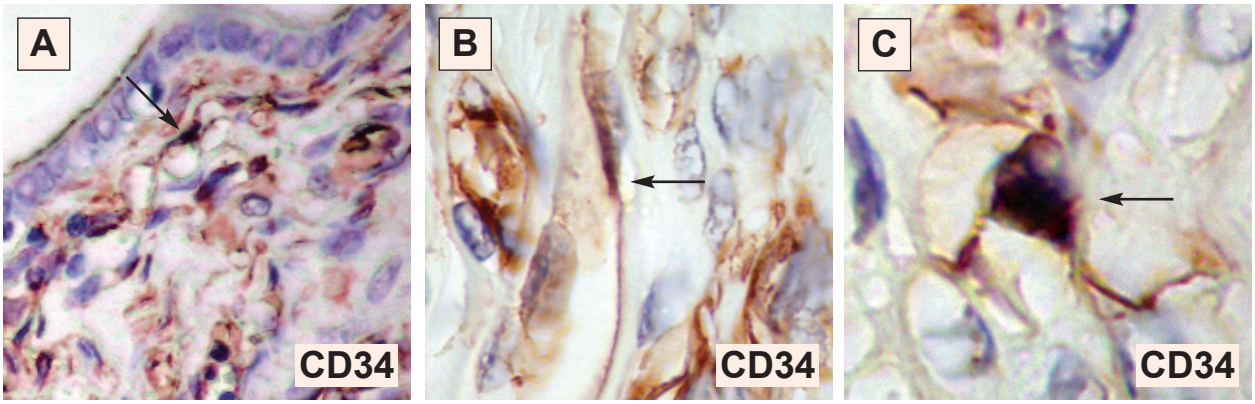

Fig. 27 A–C Human fallopian tube. The immunohistochemical staining for CD34 shows immunoreactive t-ICC in the lamina propria (arrows). Original magnifications 40x (**A**) and 100x (**B, C**).

KIT-positive (the 'ICC') or KIT-negative ('non-Cajal').

In our study, antibodies against CD117/c-kit revealed a high density of t-ICC mainly in lamina propria. CD117/c-kit was detected in cells with characteristic morphology (one or more very long, thin processes, sometimes with 'beads-on-string' appearance, that arise from pyriform, stellate or spindle-shaped cell bodies - Figs. 25A–C, 26, 29, 30, 41). CD117/c-kit was noted in discrete areas on the cell bodies or processes, in accordance to *in situ* findings reported by others [33, 78]. Since mast cells are present in ~20% of all surgically removed fallopian tubes [48] and are well-known as c-kit expressing cells [79], it was not surprising to find c-kit positive mast cells (Fig. 25B,D,E).

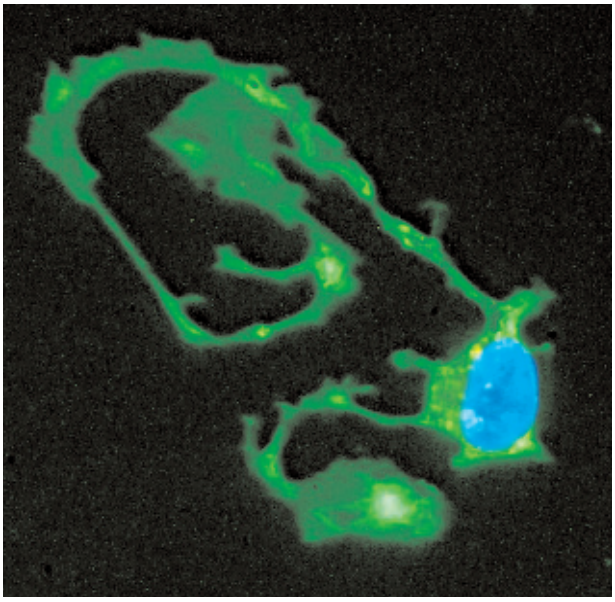

Fig. 28 Human fallopian tube; t-ICC primary culture (day 4). Immunofluorescent staining for CD34 (green). Hoechst 33342 (blue) stains the nucleus. Original magnification, 60x. Compare this cell with a similar one found by electron microscopy in Fig. 17A.

CD34 expression on Cajal-cells has been reported by Hirota *et al.* [24], while Vanderwinden *et al.* [80] described this antigen associated to fibroblasts distinct from ICC. Besides fibroblasts, CD34 is also expressed on endothelial cells (mostly in capillaries) [81], potentially leading to an overassessment of ICC. In human fallopian tube lamina propria, t-ICC constantly expressed CD34 at high levels (Figs. 27, and 28).

CD117/CD34 double IHC reaction was clearly positive for both antigens (Fig. 29). CD117 stained mainly the cell body, while CD34 stained preferentially the cell processes. IF double-staining of t-ICC *in vitro* revealed coexpression of c-kit and CD34 on the majority of t-ICC (Fig. 30). Thus, IHC and IF results were convergent (compare Figs. 29 and 30).

Human fallopian tube serial sections were also used to statistically test the correlation between CD34 and CD117 expression. A significant, positive correlation ($r = 0.87$, $p = 0.001$) was found between the two antigens (Fig. 31).

S-100 is a calcium binding protein, widely expressed on a variety of cell lineages such as Schwann cells, melanocytes, neural cells, but also Cajal-like cells in human pancreas [46] etc. Some t-ICC in lamina propria expressed S-100 (Fig. 32).

Most t-ICC from lamina propria and muscularis were non-reactive for **SMA** (Fig. 33). Double IHC

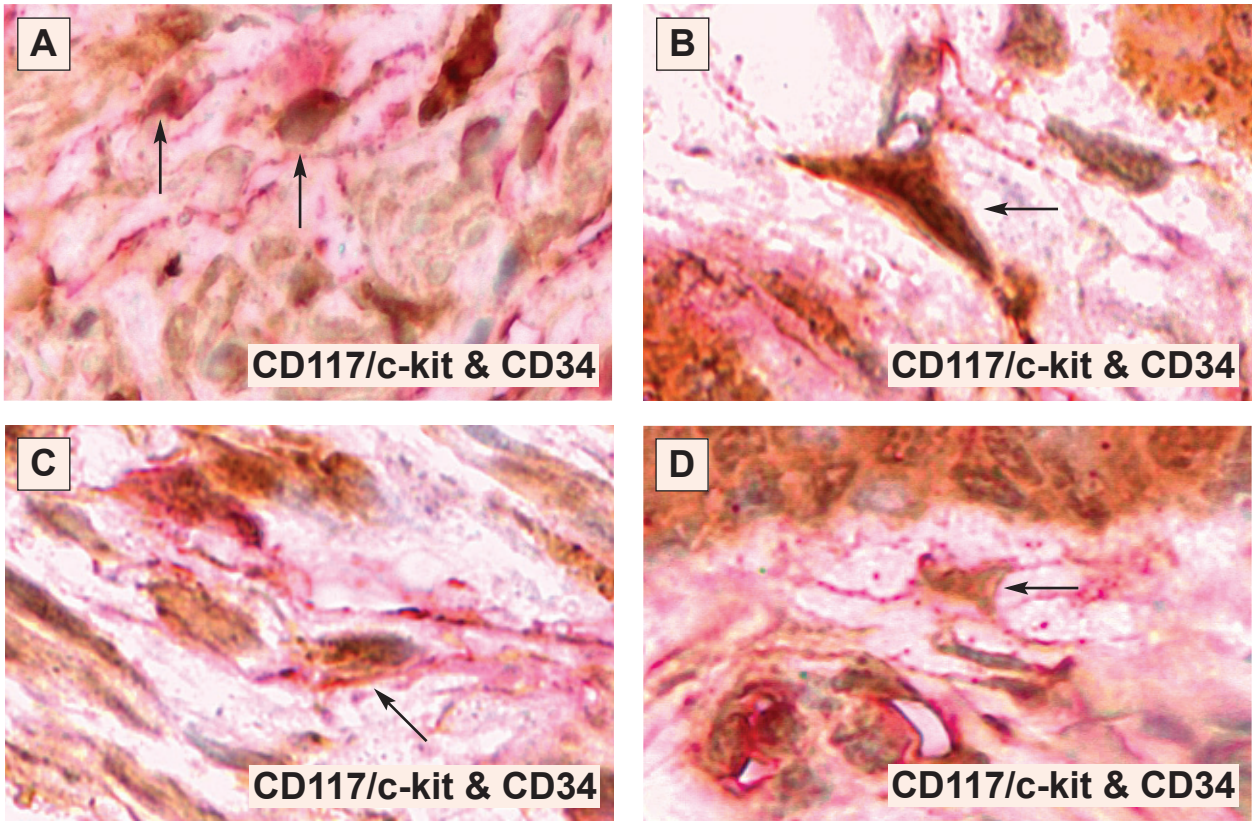

Fig. 29 A–D Human fallopian tube; lamina propria of mucosal layer. Double IHC staining. Brown staining (DAB) indicates CD117/c-kit immunoreactivity and red staining (Fast red) shows CD34 positive t-ICC (arrows). Moniliform cell processes have a stronger reactivity for CD34 than for CD117/c-kit, the second marker being preferentially distributed on cell bodies (**B**, **D**). Original magnification 100x.

for S-100 and SMA displayed two different immunoreactive patterns of t-ICC: cells expressing both S-100 & SMA in lamina propria, or expressing either S-100 or SMA in muscularis (Fig. 34). In primary cultured cells we found t-ICC expressing both c-kit and SMA (Fig. 35).

NK-1 is a monoclonal antibody directed against CD57 also present in neural cells. Fig. 36 shows scattered immunoreactive cells weakly stained for **NK1** in lamina propria.

Nestin is a component of the intermediate filament network, expressed in gastrointestinal stromal

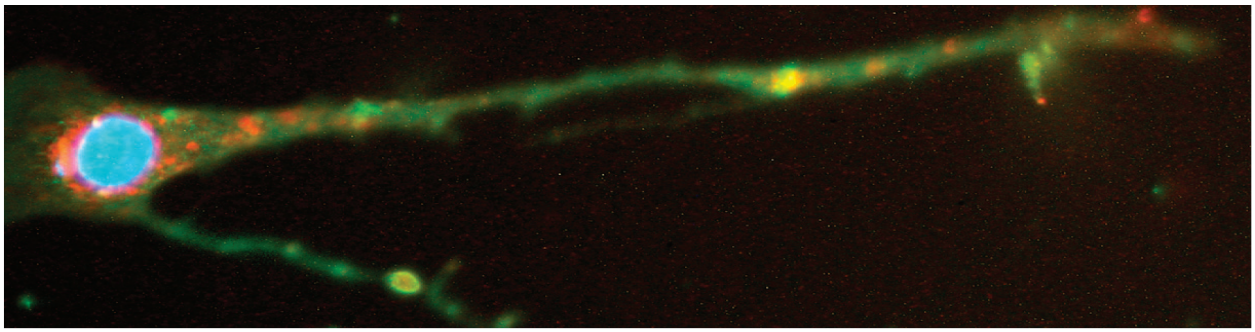

Fig. 30 Human fallopian tube; t-ICC primary culture (day 5). Double immunofluorescent labeling for CD117/c-kit (red) and CD34 (green). This cell is positive for both markers, and co-localisation appears as yellow areas. Hoechst 33342 nuclear counterstaining (blue). Original magnification, 60x.

Antibody	Clone	Dilution	Source	IHC positivity
CD117/c-kit	polyclonal	1:100	DAKO	+ + + +
CD34	QBEnd10	1:100	Biogenex	+ + +
S-100	polyclonal	1:500	DAKO	+ +
α-SMA	1A4	1:1500	Sigma	+
CD57	NK1	1:50	DAKO	+
nestin	5326	1:100	Santa Cruz	+
desmin	D33	1:50	DAKO	–
vimentin	V9	1:50	DAKO	+
NSE	BBS/NC/VI-H14	1:50	DAKO	+
GFAP	6F2	1:50	DAKO	–
CD68	PG-M1	1:50	DAKO	±
CD62P	1E3	1:25	DAKO	–
CD1a	CD1a-235	1:30	Novocastra	–
Chromo A	LK2H10	1:50	Novocastra	–
PGP9.5	10A1	1:40	Novocastra	–

Table 3 Summary of immunohistochemical results for t-ICC from human fallopian tube. The intensity of t-ICC reactivity was assessed semiquantitatively using an adaptation of Quick score method [76]. Intensity:

- **Negative** (no staining of any cellular part at high magnification): –
- **Occasionally weak positive**: ±
- **Low** (only visible at high magnification): +
- **Medium** (readily visible at low magnification): + +
- **High** (strikingly positive at high magnification): + + +
- **Strong** (strikingly positive even at low magnification): + + + +

tumors and intestinal cells of Cajal [82]. Some of t-ICC in our experiment expressed nestin (Fig. 37).

IHC for **desmin** showed the lack of expression at the level of t-ICC in lamina propria (Fig. 38A), concomitantly with immunopositive reactions in smooth muscle cells of either the circular layer (Fig. 38B) or longitudinal layer (Fig. 38C). Conversely, *in vitro*, in primary culture, t-ICC (identified by c-kit positivity) expressed desmin (Fig. 39).

IHC for **vimentin** labeled t-ICC (Fig. 40A). Double immunostaining vimentin + CD117/c-kit (Fig. 40B) demonstrates that, indeed, t-ICC express vimentin. IF images like in Fig. 41 strongly support such findings. Torihashi *et al.* [83] and Duquette *et al.* [36] considered that vimentin could be a marker for Cajal-like cells (in the absence of a positive reaction for c-kit).

IF double-labeling of CD117/c-kit and caveolin-1 and caveolin-2 in human fallopian tube primary cultures showed both types of caveolar proteins expressed by t-ICC (superimpose Fig. 24A,B on Fig. 26). Cho and Daniel [78] reported coexpression of caveolin-1 and c-kit in ICC and intestinal smooth muscle, but our data add some detail on caveolin-1 and caveolin-2 cellular distribution: caveolae were more abundant at the level of cell processes of t-ICC, as seen in both TEM (*e.g.* Fig. 17A) and fluorescence microscopy.

IHC with antibodies against some additional antigens showed negative immunostaining for CD1a (Fig.42A), CD62P (Fig. 42B), CD68 (Fig.

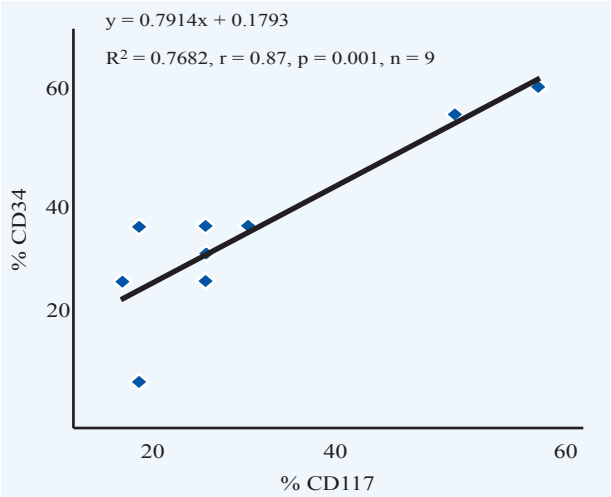

Fig. 31 Correlation between CD117/c-kit and CD34 expression on t-ICC. Serial fallopian tube sections were assessed for either CD34 or CD117/c-kit expression by IHC. Positive cells within lamina propria and muscularis were counted and results expressed as percentage of the total number of cells with t-ICC morphology.

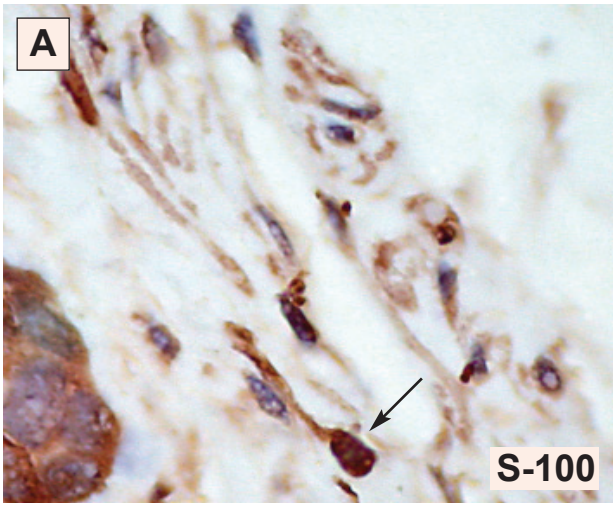

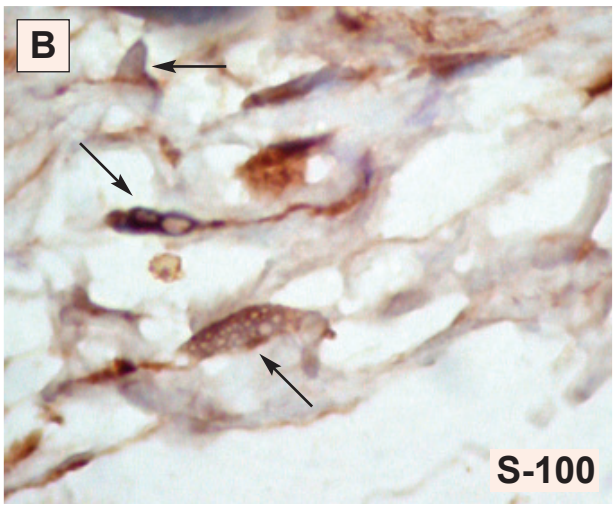

Fig. 32 A, B Human fallopian tube. Some t-ICC are S-100 immunoreactive (arrows). DAB (brown) was used to visualise the immune reaction. Counterstaining with Mayer's hematoxylin. Original magnification, 100x.

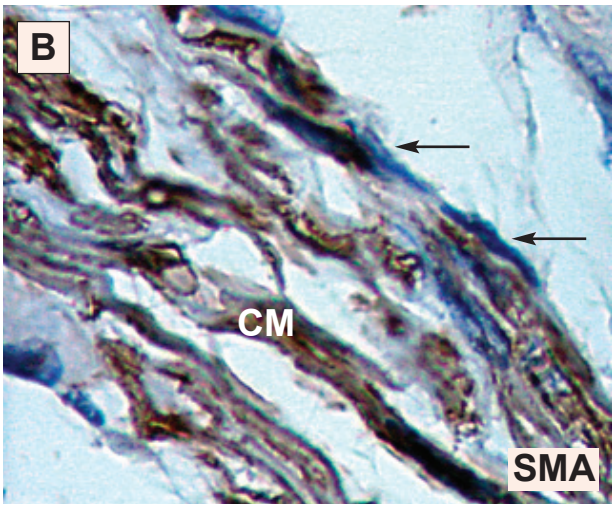

Fig. 33 A, B Human fallopian tube. **A**. α SMA immunostaining shows non-reactive t-ICC in the lamina propria (arrow). **B.** Note the two α SMA-negative spindle-shaped interstitial cells lining the circular muscle layer (CM) (arrows). Counterstaining with Mayer's hematoxylin. Original magnification, 100x.

43), GFAP (Fig. 44), NSE (Fig. 45), chromogranin A (Fig. 46A), PGP 9.5 (Fig. 47A). These results support distinction between t-ICC and other cell types (pericytes, macrophages, mast cells, smooth muscle fibers, neural cells, neuroendocrine cells, etc.) [84].

Collateral findings:

Neuroendocrine scattered cells ('JF')

We describe here cells located among smooth muscle cells, identified as positive for **chromogranin A** (Fig. 46B,C) or for **PGP9.5** (Fig. 47B). *In situ*, such cells have a different morphology than t-ICC. As expected, t-ICC were not immunoreactive for both chromogranin A and PGP9.5 (Figs. 46A and 47A).

Because of chromogranin A and PGP9.5 positivity, we suggest that these cells scattered among smooth muscle cells of fallopian tube wall could belong to a diffuse neuroendocrine system [85, 86]. We refer to these possible neuroendocrine cells as '*JF cells*'.

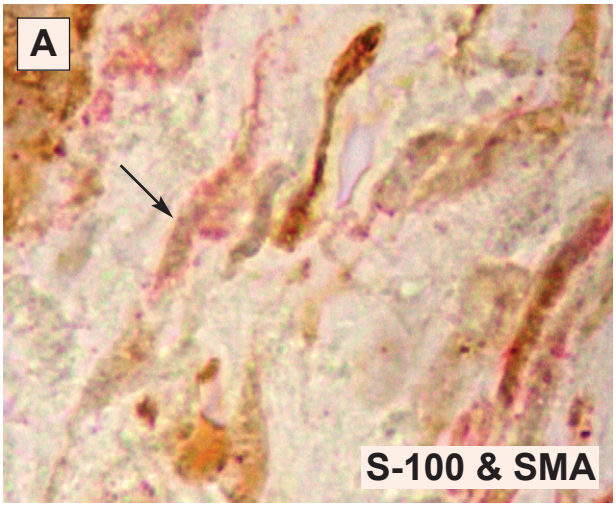

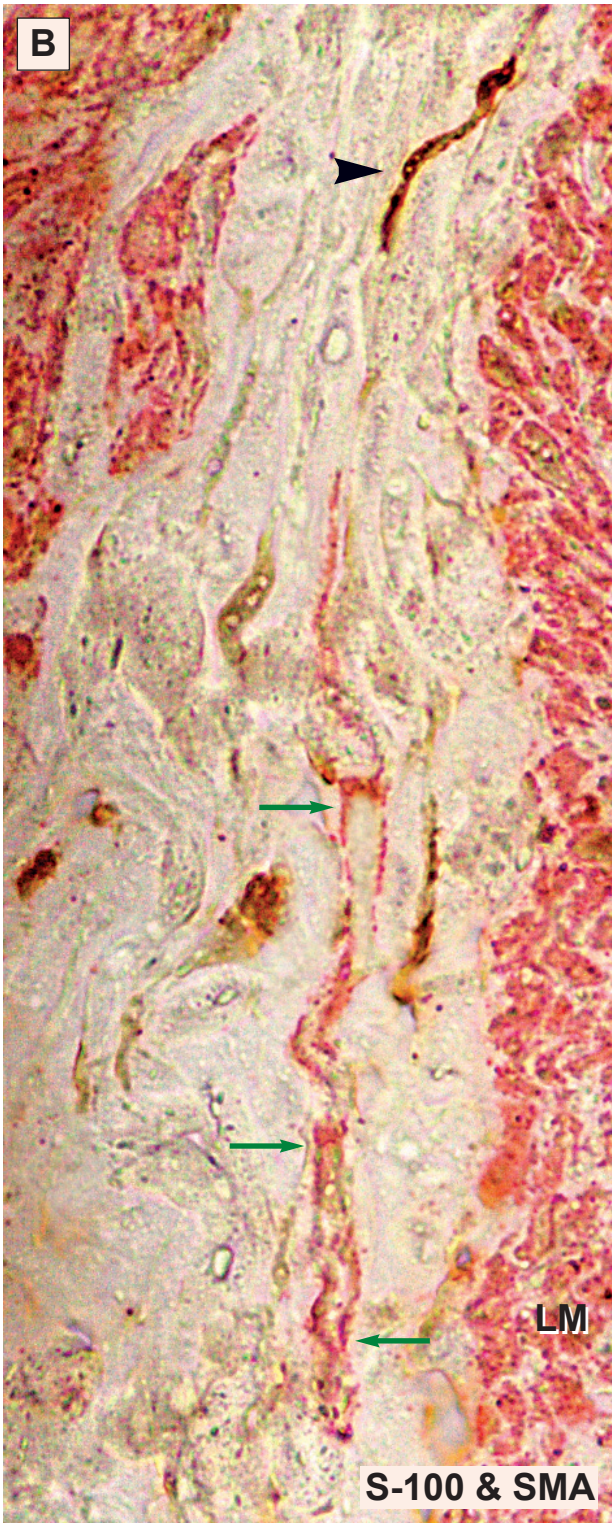

Fig. 34 A–C Dual immunohistochemical staining for S-100, brown (DAB) and SMA, red (Fast red) of the human fallopian tube lamina propria (A) and muscularis (B, C). Note the presence of t-ICC expressing both S-100 & SMA in lamina propria (black arrow), while muscularis t-ICC expressed either S-100 (black arrowheads) or SMA (green arrows). The longitudinal muscle layer (LM) stains for SMA. The image shown in B is a photographic reconstruction. Original magnification, 100x.

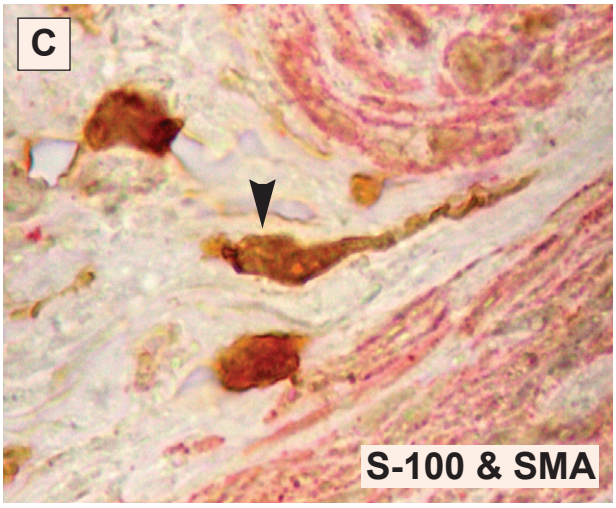

Very recently, Dursun *et al.* reported a case of primary neuroendocrine carcinoma of the human fallopian tube, apparently for the first time [87]. Although they noted Chromogranin A focally positive tumoral cells, by IHC, no explanation for the origin of this carcinoma was provided. We suggest that 'JF' neuroendocrine cells identified herein could represent the starting point for this tumor.

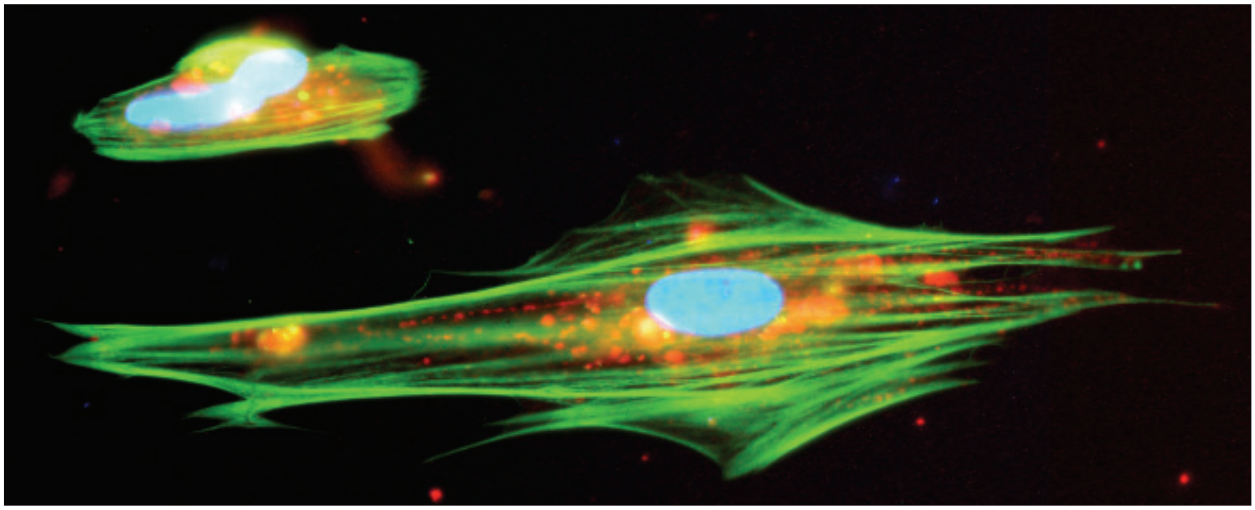

Fig. 35 Human fallopian tube; primary cultures (day 5). Double immunostaining for smooth muscle α-actin (green) and CD117/c-kit (red). The cell body of an ICC in the lower part of the image, shows SMA positivity, resembling stress fibers. The cell nucleus stains blue with Hoechst 33342. Original magnification, 60x.

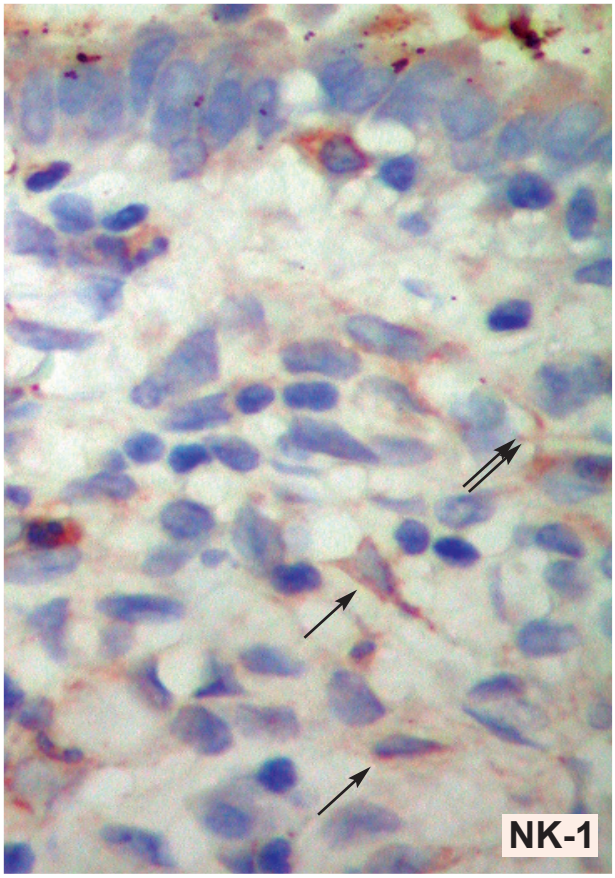

Fig. 36 NK-1 immunostaining of normal human fallopian tube. Arrows indicate triangular cells with thin processes, immunoreactive for NK-1; the double arrow points out long cell processes. Counterstaining with Mayer's hematoxylin. Original magnification, 100x.

Electrophysiology

The aim of the extracellular single unit recordings was to determine whether t-ICC in primary culture exhibit or not electrical activity. In our experiments, sustained spontaneous electrical activity was recorded in most of the investigated cells. Field potentials averaged 57.26 ± 6.56 mV in amplitude (n = 30), without showing a rhythmical pattern (Fig. 48). The potentials were rather short (0.98 ± 0.07 ms) when compared to the electrophysiological properties of smooth muscle cells [88]. These preliminary results show that t-ICC in subconfluent primary culture have spontaneous electrical activity. Since the single unit recording were done in primary cell cultures, derived from muscularis and lamina propria, it was not possible to establish the exact origin of the examined t-ICC.

Discussion

Identification of Cajal-like interstitial cells: methods and criteria

We report here the identification of a novel Cajal-like interstitial cell (t-ICC) in the non-epithelial space of human fallopian-tube wall (Fig. 49). These cells are similar to archetypal enteric cells of Cajal (ICC).

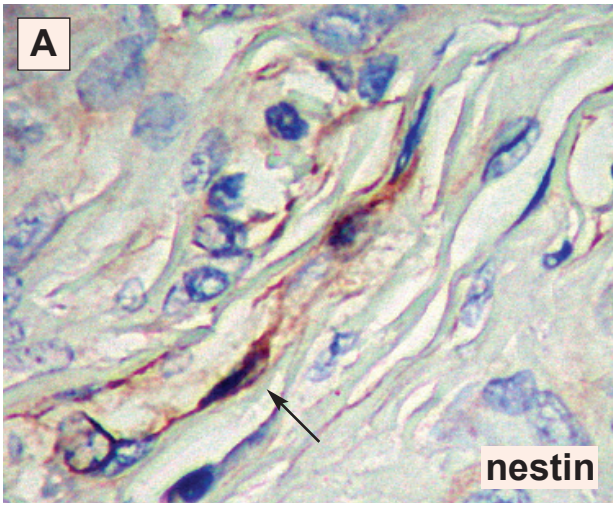

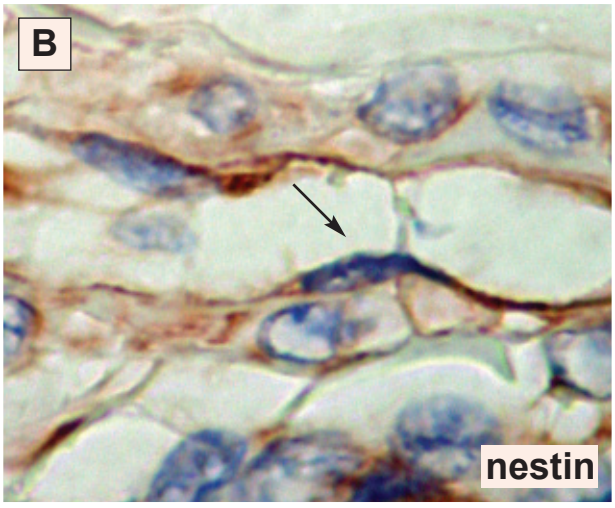

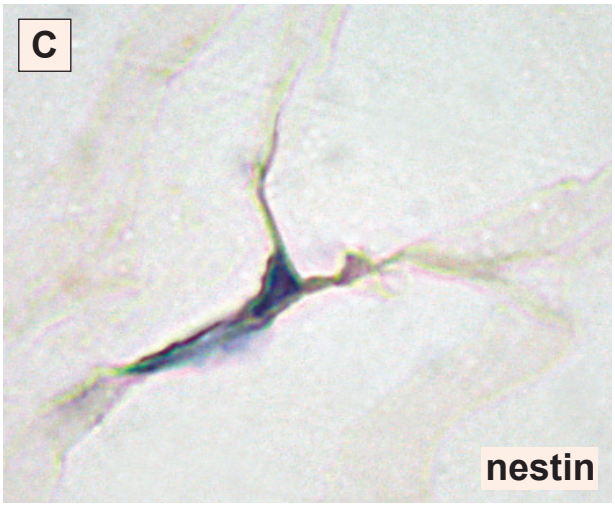

Fig. 37 A–C Human fallopian tube, immunostaining for nestin. **A, B.** In *lamina propria*, t-ICC show a cytoplasmic pattern of nestin expression (arrows). **C.** A t-ICC, located in the *loose connective tissue* underneath of serosa, exhibits long, nestin immunopositive processes. Original magnifications 40x (A) and 100x (B, C).

To establish the 'affiliation' to the (heterogenous) group of Cajal-like interstitial cells in a given tissue, we suggest the following algorithm:

I. Identification

A. Optical microscopy

a. (Supra)vital methylene-blue staining

b. Toluidine-blue staining of semi-thin sections of Epon-embedded tissue (after glutaraldehyde/osmium fixation) – NCLM

c. CD117/c-kit immunodetection – IHC and/or IF

B. Transmission electron microscopy (TEM).

II. Characterization

A. Cell cultures

B. Cellular electrophysiology

C. Biochemical and molecular analyses

A.a. The supravital methylene blue staining ('*en bloque*') and/or vital staining (cryosections) offer an **indication on the possible existence** of Cajal-like cells in the respective tissue. We have to remind here that, at the end of the 19th century, Ramon y Cajal described the cells which eventually received his name, right by using methylene-blue staining.

A.b. NCLM points out the topography, the relative density and the relationships of Cajal-like interstitial cells with other microscopic structures (*e.g.* Fig. 49). Moreover, NCLM discloses the limited diversity of cell-body shapes, and, especially, the morphology of the characteristic cytoplasmic processes. Briefly, NCLM gives **presumptive diagnosis**.

A.c. Positive IHC and/or IF for CD117/c-kit, together with the two above-criteria, give an **accurate diagnosis.**

B. TEM, when available, gives **certitude diagnosis**.

*

For the identification of Cajal-like interstitial cells we considered the following set of **criteria**, relying on topographical, morphological and antigenic attributes that exclude, quite accurately, other cell types:

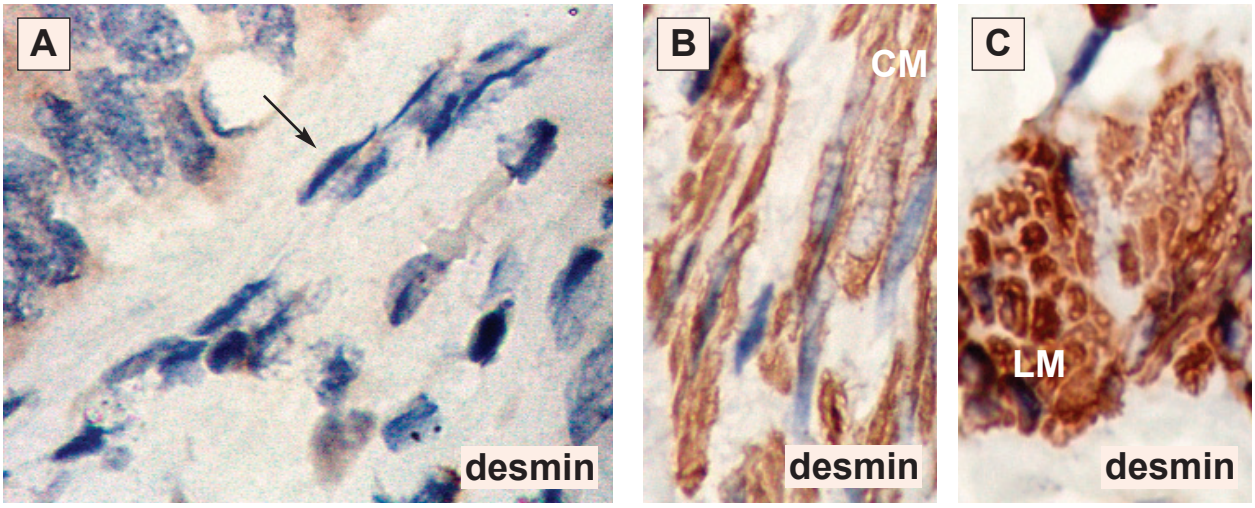

Fig. 38 A–C Human fallopian tube stained for desmin and counterstained with Mayer's hematoxylin (cross-sectioned). Putative t-ICC in lamina propria (**A**, arrow) lacks desmin expression, while smooth muscle cells in the circular (**B**) and longitudinal (**C**) muscle layers are desmin-immunoreactive. Original magnification 100x. CM = circular muscle layer; LM = longitudinal muscle layer.

- **Location** (Fig. 49) in interstitium (non-epithelial space); frequently join adjacent histologic structures (smooth muscle cells, nerves, small blood vessels or epithelia) *via* their
- **Characteristic processes**, and
- **CD117/c-kit positivity** (although we cannot exclude that sometimes Cajal and Cajal-like cells, that respect the first couple of criteria, might test negative for this marker).

Obviously, vital staining with **methylene blue** (relying on poorly understood molecular mechanisms) has more than historical significance, since, for instance, it reveals Cajal-like interstitial cells in myometrium [37] and mammary gland [45].

*

To facilitate the **certitude diagnosis** by **electron microscopy**, we propose the following set of ultrastructural criteria ('*platinum standard*') for Cajal-like interstitial cells:

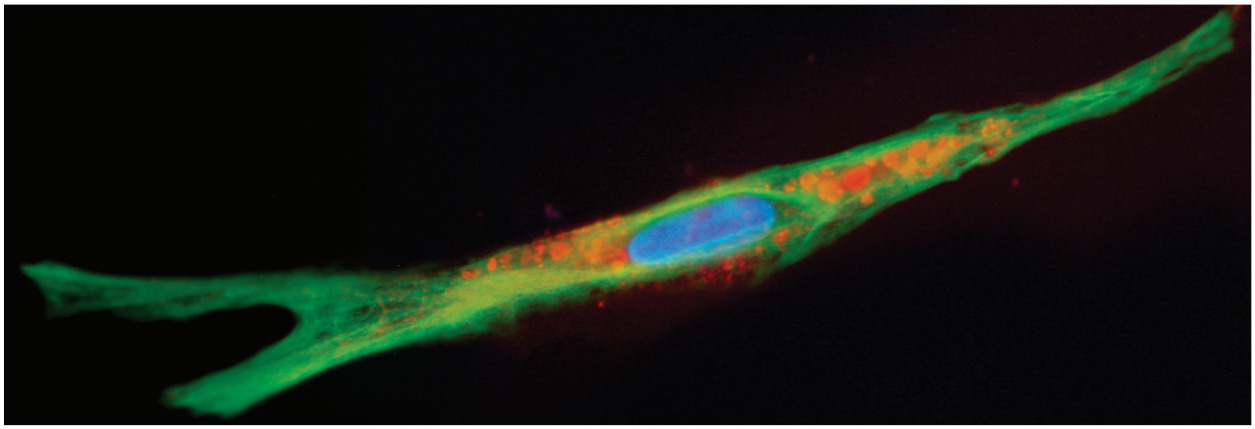

Fig. 39 Human fallopian tube; preconfluent t-ICC primary culture; immunostaining for desmin and CD 117/c-kit. The cell is positive for both desmin (green) and CD 117/c-kit (red). Nuclear counterstaining with Hoechst 33342 (blue), original magnification 60x. Compare with the same cell in Fig. 24 C.

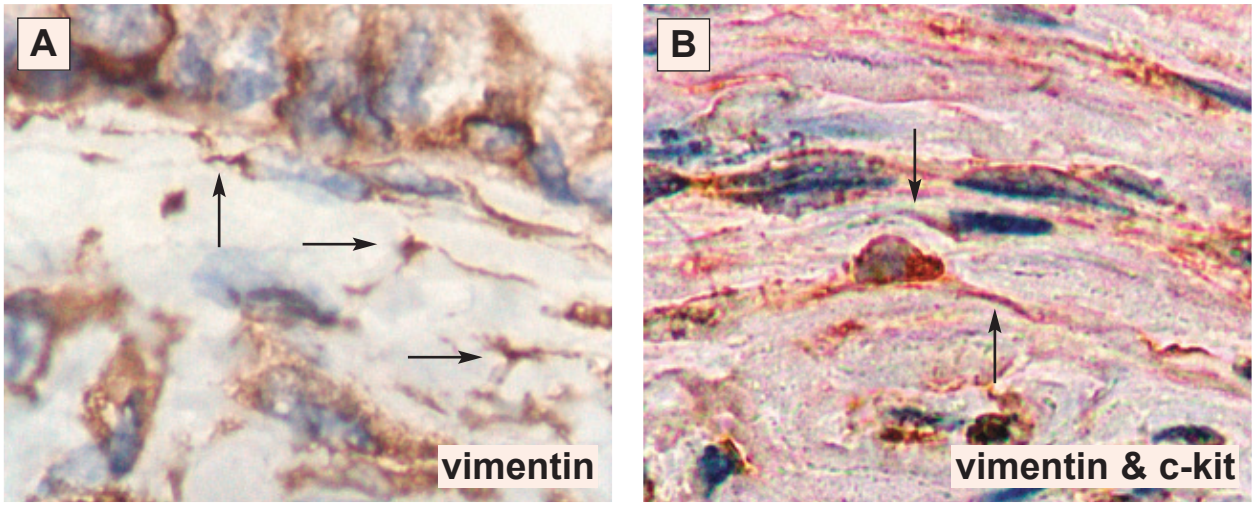

Fig. 40 A, B Human fallopian tube; IHC. Immunostaining for vimentin (**A**) and *double* immunostaining for vimentin plus CD117/c-kit (**B**). **A**. Note the vimentin immunoreactive t-ICC processes (arrows). **B.** Cells with morphology suggestive for t-ICC stain both for CD117/c-kit (brown - DAB) and vimentin (red - Fast red), mainly at the level of their long, moniliform processes (arrows). Counterstaining with Mayer's hematoxylin. Original magnification 100x.

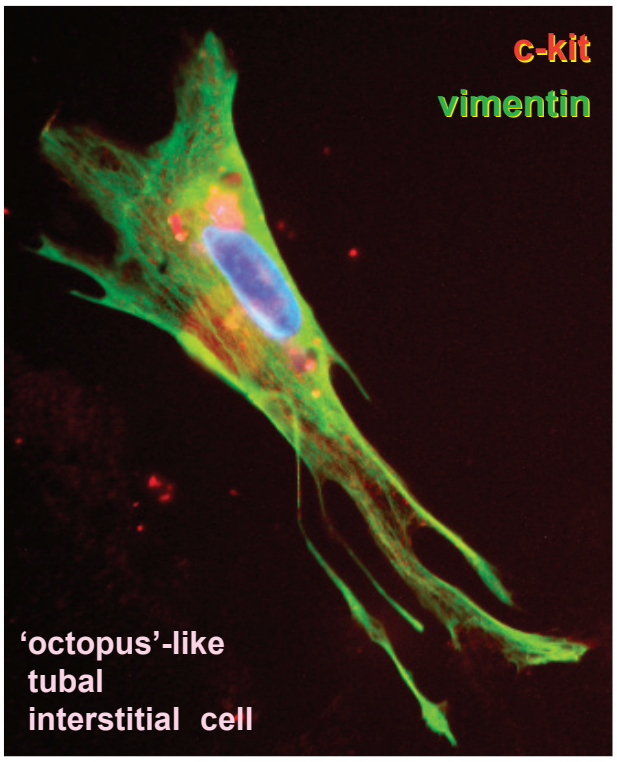

Fig. 41 Human fallopian tube; subconfluent primary culture. Double immunofluorescent labeling of an 'octopus'-like t-ICC: vimentin (green) and CD117/c-kit (red). Vimentin reactivity is mainly localized within the cell processes, and CD117/c-kit has a patchy pattern. Compare with Figs. 3C and 24D. The cell nucleus is shown in blue (Hoechst 33342); original magnification 60x.

1. **Location in the non-epithelial space**;
2. **Close contacts with targets**: nerve bundles, and/or epithelia, and/or smooth muscle cells, and/or capillaries;
3. **Characteristic cytoplasmic processes**:
   i. **Number** (1–5, frequently: 2–3);
   ii. **Length** (tens up to hundreds of μm);
   iii. **Thickness** (uneven caliber, ≤ 0.5 μm);
   iv. **Aspect**: *moniliform*, usually with mitochondria in dilations;
   v. **Presence of 'Ca^{2+} release units'**;
   vi. **Branching**: dichotomous pattern;
   vii. **Organization in network – labyrinthic system**: overlapping cytoplasmic processes;
4. **Gap junctions**: with smooth muscle cells or with each other;
5. **Basal lamina**: occasionally present;
6. **Caveolae**: 2-4% of cytoplasmic volume; ~0.5 caveolae / μm of cell membrane length;
7. **Mitochondria**: 5-10% of cytoplasmic volume;
8. **Endoplasmic reticulum**: about 1–2%, either smooth or rough;
9. **Cytoskeleton**: *intermediate* and *thin filaments*, as well as *microtubules*, present;
10. **Myosin thick filaments**: undetectable.

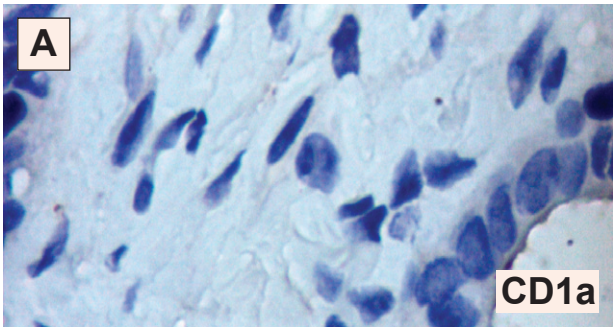

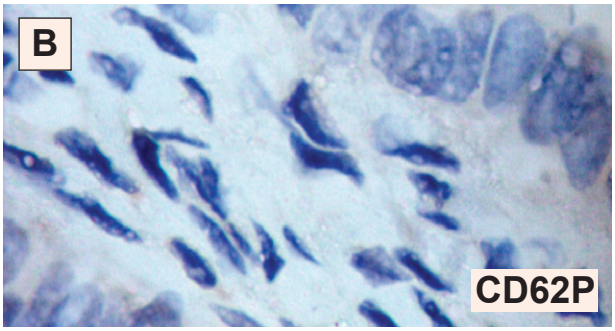

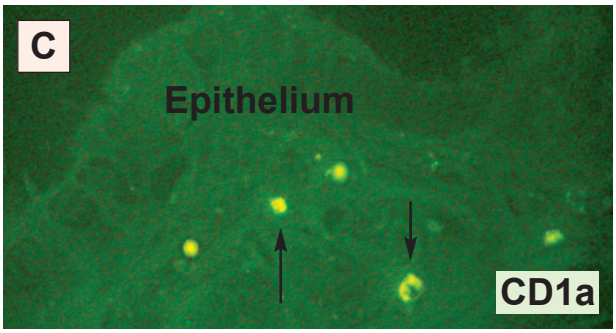

Fig. 42 A–C Human fallopian tube **A, B**. No positive immune reaction of cells in lamina propria for CD1a and CD62P**. C.** IF using FITC-conjugated anti-CD1a monoclonal antibodies. Arrows indicate cells CD1a-immunoreactive in the human fallopian tube lamina propria. However, the lack of processes and an overall round shape suggest a cell type different from t-ICC. Original magnification: 40x (A, B); 20x (C).

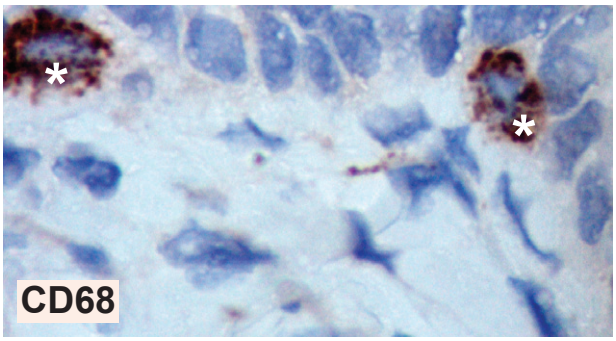

Fig. 43 IHC for CD68 distribution in human fallopian-tube *lamina propria*. The only immunoreactive cells (∗) are subepithelial macrophages (mast cells ?), while the recognizable t-ICC do not bind the antibody. Mayer's hematoxylin counterstaining; original magnification 100x.

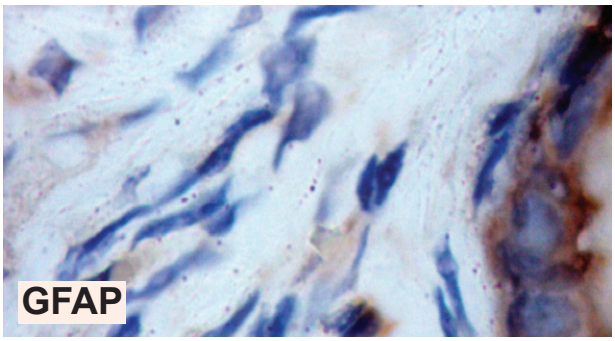

Fig. 44 Human fallopian tube lamina propria stained for GFAP. Cells with morphology suggestive for t-ICC are negative for GFAP. Mayer's hematoxylin counterstaining; original magnification 100x.

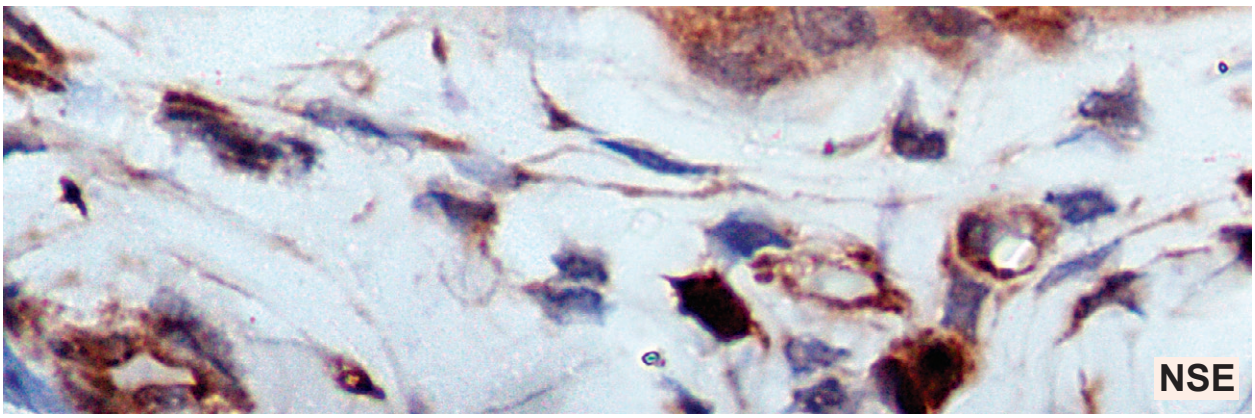

Fig. 45 Human fallopian tube labeled for NSE (photographic reconstruction). *Lamina propria* t-ICC lack NSE immunoreactivity. Original magnification 100x.

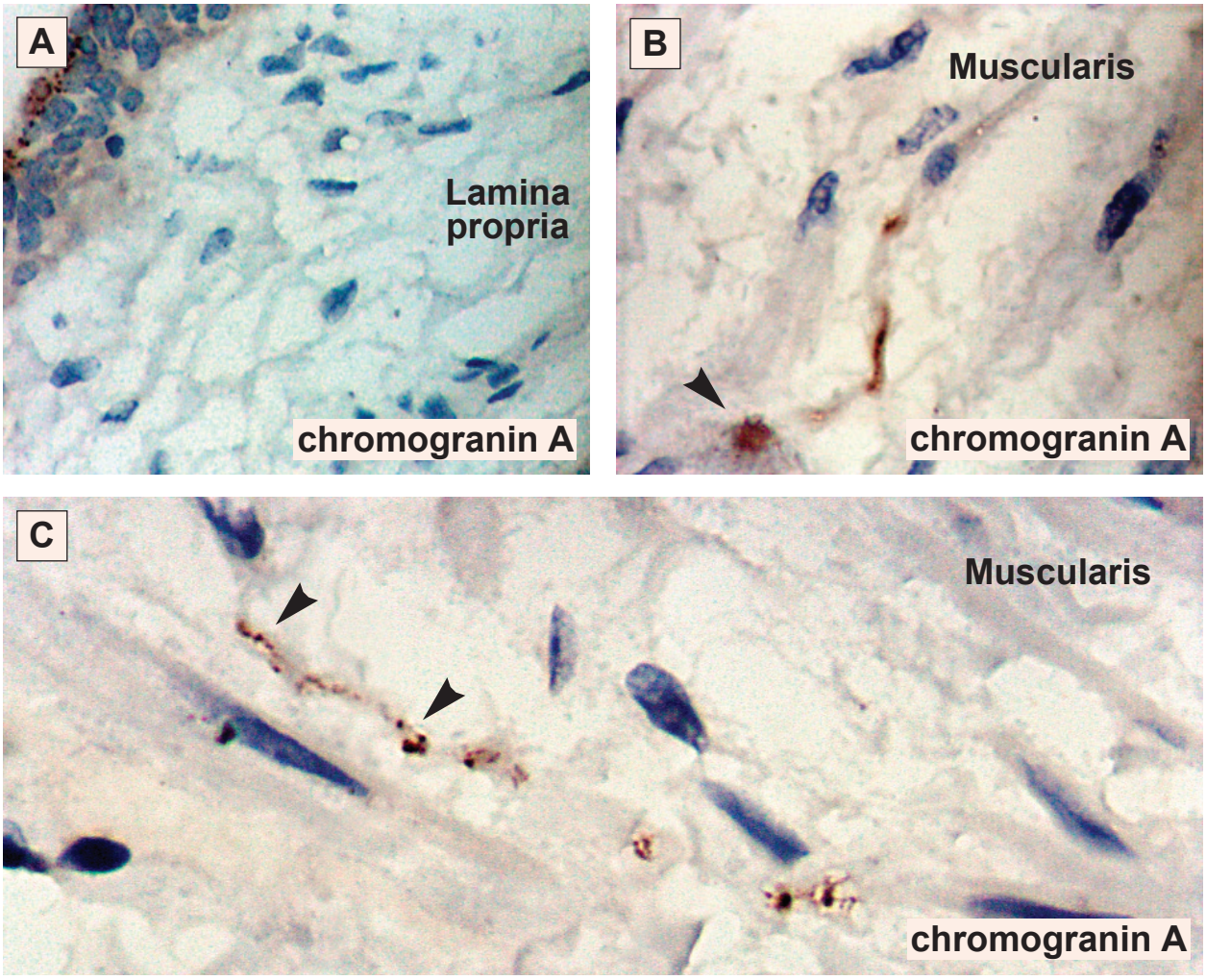

Fig. 46 A–C Human fallopian tube immunostained for chromogranin A. **A.** No chromogranin A positive cells are seen in *lamina propria*. **B, C.** Several chromogranin A-positive granules can be seen (arrowheads) in the muscular layer. Original magnification, 100x.

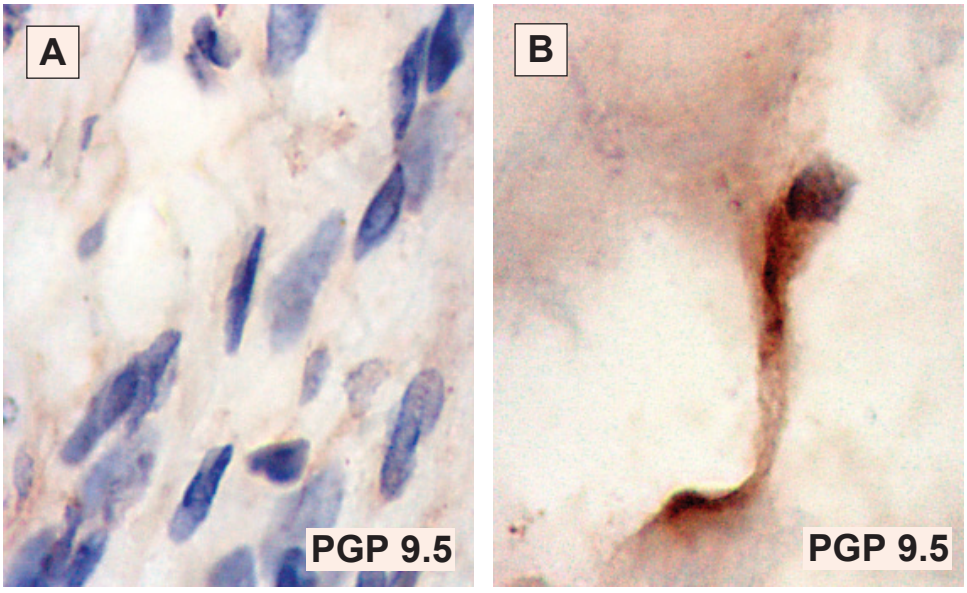

Fig. 47 A, B. Immunohistochemical detection of PGP9.5 in human fallopian tube. **A**. No staining is seen in the *lamina propria*. **B**. Immunoreactive cells are detected in the muscular layer, among the smooth muscle fibers. Original magnification 100x.

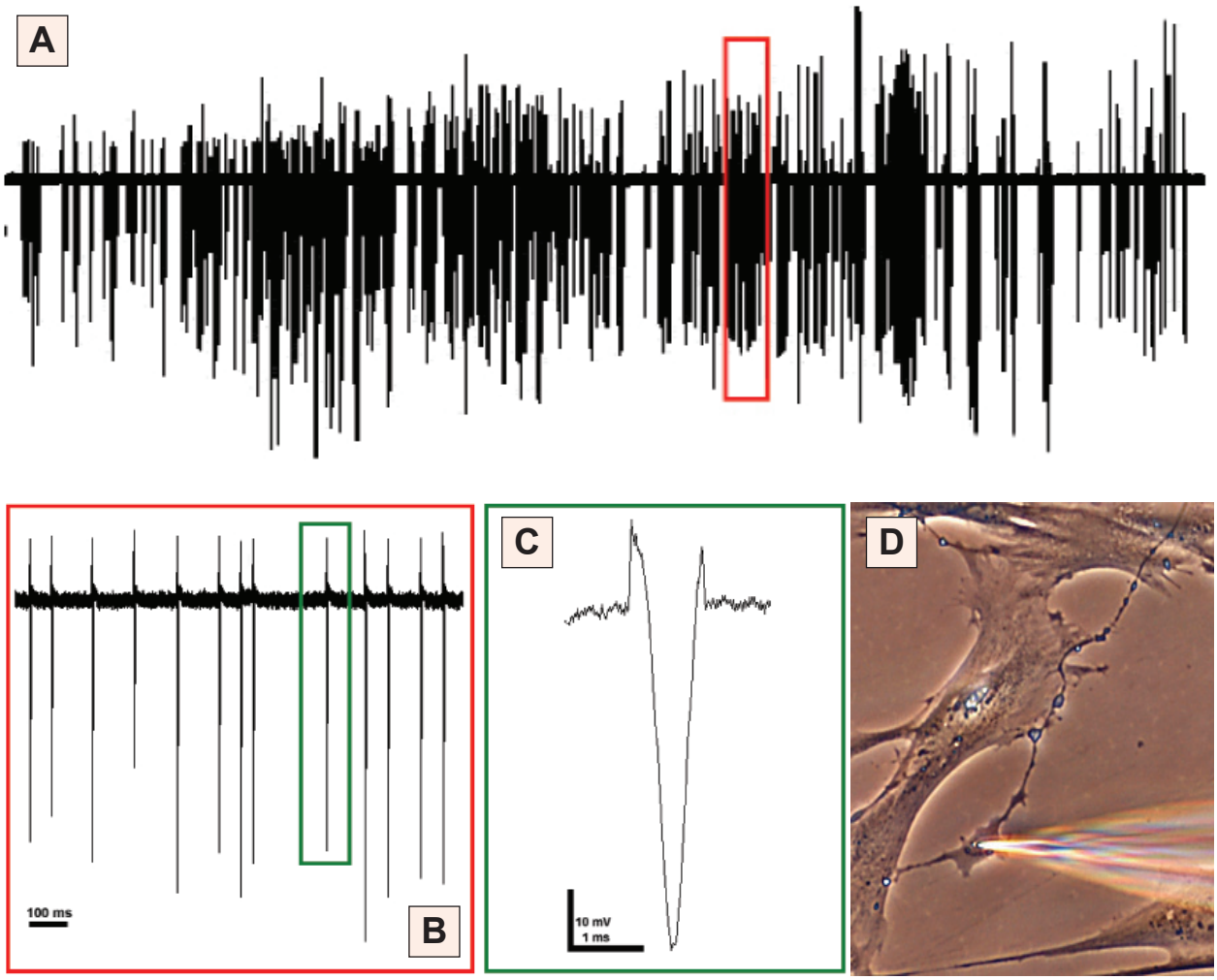

Fig. 48 A–D. **A, B.** Extracellular single unit recordings display sustained spontaneous electrical activity in t-ICC. **C.** Spontaneous field potential pattern. **D.** Phase contrast microscopy (40x) showing the recording glass electrode in the proximity of the t-ICC body.

In our opinion, *the first six criteria of the 'platinum standard' could be sufficient* to diagnose an interstitial (Cajal-like) cell.

t-ICC: Uncommitted (bipotential) progenitor cell

Markers traditionally assigned to somatic stem cells (hematopoietic, neural, etc) have been found in ICC subpopulations: CD117 [22, 23], CD34 [24], nestin [89], vimentin [90], the embryonic form of myosin heavy chain [91]. This could rise the question whether interstitial Cajal-like cells are terminally differentiated or not.

Cells retaining their self-renewal capacity and ability to give rise to specialized progeny within a specific tissue can be considered somatic stem cells [92]. Apparently, ICC and Cajal-like cells match this description.

It seems that ICC are (not post-) mitotic cells: *in vitro* studies showed that they undergo stem cell factor-dependent proliferation [93, 94]; preventing c-kit signaling leads to their depletion in experimental [95] and pathologic [96] circumstances; GIST are linked to monoclonal, abnormal ICC proliferation [97].

Cajal cells are able to switch phenotype, since they (trans?)differentiate into smooth muscle cells, when c-kit signaling is blocked [98]. Moreover, their malignant counterparts in GIST occasionally express either smooth muscle [99] or neuroendocrine [100] markers.

Canonical ICC and smooth muscle cells arise from a common c-kit-positive mesenchymal progenitor. The precursor cell expresses vimentin and shares ultrastructural features with the "adult" cell type [95,

98]. t-ICC described here might belong to two (possibly overlapping) subpopulations: one endowed with spontaneous electrical activity, closer to enteric ICC, and the other, less similar to archetypal ICC, closer to progenitor cells. It remains to be seen whether functionally dissimilar Cajal-like subpopulations have distinct locations. Moreover, no experimental evidence excluding the possibility that Cajal-like cells might become a typical ICC. From this point of view, *Cajal-like cells could mean more than simply ICC*.

To summarize, Cajal-like cells are an amazingly heterogenous population that could retain differentiation potential or, at least, be able to switch phenotype under normal or pathologic circumstances.

t-ICC: An immune surveillance role?

Yamazaki and Eyden described in human fallopian tube a network of CD34-positive interstitial cells with a putative immune surveillance role [101]. CD117/c-kit expression was not investigated, making it difficult to determine the relationship between the CD34-positive cell network and CD117 positive t-ICC.

One may expect a partial overlap of the two cell types, as some enteric ICC [102] and some Cajal-like cells [46, 90, 103] are positive for CD34 and, to a certain extent, look similar. However, it seems reasonable to assume important differences between the two cell types, as their proportions in the whole cell population are significantly dissimilar [101]. Differences can be also found when looking at the origins of these cells: CD34 positive fibroblasts might have a blood-borne precursor [104] that crosses endothelia, whereas ICC and Cajal-like cells are more likely to arise from tissue-resident mesenchymal progenitor cells [105].

Arguments that apparently favor a role for any of the two cell types in immune surveillance are the presence of close contacts that might play a role in transfering antigenic peptides to antigen presenting cells for cross-priming [106] (seen here in Fig. 22A), and the strategical location of t-ICC at the cross-roads of various histologic compartments, some in direct contact with the environment. Interactions between t-ICC and cells of the innate immune system (macrophages - Fig. 22A) could represent another indication of their involvment in organism defense.

On the other hand, the t-ICC lack of markers usually associated with immune functions (*e.g.* CD1a, CD62P, CD68), as well as the lack of structures that have a role in antigen processing and presentation, apparently question the immune surveillance viewpoint. Nevertheless, further studies are required to describe the cellular and molecular mechanisms that might be involved.

As shown in Fig. 49, the stroma of lamina propria in the human fallopian tube is mainly composed of a Cajal-like cell reticulum. A subepithelial meshwork of Cajal-like cells (c-kit positive, CD34 ?) and CD34-positive (c-kit ?) undifferentiated cells seems to mark the epithelial-stromal border. However, the sole presence of such a network do not ascribe it an immune surveillance role.

t-ICC: Networks for pacemaking

A pacemaker role is now generally accepted for enteric ICC, which generate electrical rhythmicity in the gastrointestinal tract [22, 23, 107]. Why should not t-ICC be responsible for the human fallopian tube peristalsis ? The more so as, Yoneda *et al.* [108] reported that, in mouse proximal colon, the submucosal c-kit-positive bipolar cells spontaneously generate plateau potentials with rhythms different from those generated by smooth muscle cells.

In terms of physiological evidence, our electrophysiological results suggest that t-ICC could possess electrical properties that do not rule out a presumptive pacemaker role. Two important prerequisites are fulfilled, as concerns t-ICC as pacemaking network: a) the existence of numerous gap junctions (cf. [109] and Figs. 19, 20 and 22B), and b) integrated Ca^{2+} handling by endoplasmic reticulum and mitochondria [107], in other words, the finding of 'Ca^{2+} release units' (Fig 23B,C), which include caveolae too. Thus, our data correlate well with recent studies, on intestinal smooth muscle, designed to examine the relationship between caveolin-1, Ca^{2+}-handling and ICC pacing [78]. Nevertheless, *in vitro* studies may not be exactly applicable to intact ICC networks [110].

t-ICC: Possible regulators of neurotransmission and intercellular signaling

By analogy with the role ascribed to enteric ICC [17, 20], there is no reason to overlook the possible participation of t-ICC in regulating neurotransmis-

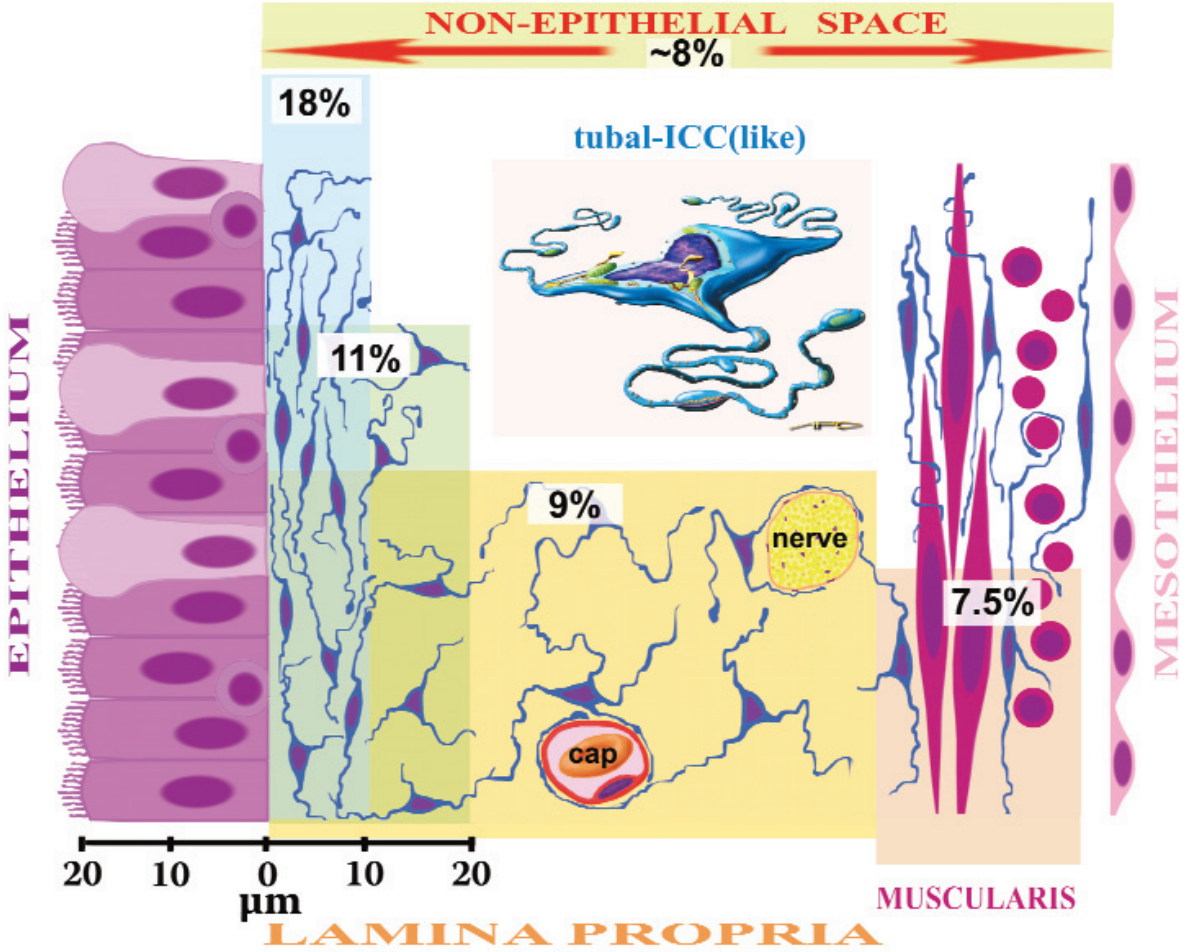

Fig. 49 Schematic drawing (not to scale): cross section of the human fallopian tube wall, ampular region. Numbers represent the *relative density of t-ICC* in a given area (percentage of t-ICC out of *all* cells seen in that area). Data were obtained mainly by NCLM (semi-thin sections stained with toluidine-blue): 4903 cells – from 82 photographs, randomly taken, were counted. t-ICC are located between the mucosal epithelium (left) and the serosal mesothelium (right). In fact, t-ICC are residents in *lamina propria* and in *muscularis* (circular myocytes are cut longitudinally and longitudinal myocytes are cut transversally). Note the *gradient of t-ICC relative density*: from ~18%, immediately underneath of mucosal epithelium, towards ~7.5% in muscularis. Close spatial relationships of t-ICC mesh with nerve bundles and/or capillaries are also depicted.

sion. At the level of human fallopian tube, besides the well-known contractile effect of acetylcholine [111], the possible modulation of adrenergic neurotransmission by endogenous purines was reported [112], and purinergic receptors described [113]. Moreover, the involvement of NO/cGMP pathway in control of human fallopian tube contractility was established [114, 115]. The strategical location of t-ICC, across the fallopian tube wall, shown in Fig. 49, suggests the speculation that *via* secretory mechanisms, these Cajal-like cells are players in a subtle and redundant game. t-ICC have at least three ways to regulate the activity of neighboring cells: auto-, juxta- and para-crine. Anyway, the juxtacrine mechanisms are supported by TEM findings (Figs. 19, 20 and 22).

In our opinion, a special place in fallopian tube physiology should be occupied by the close relationships between the subepithelial t-ICC network and the adjacent epithelium. Presumably, such relationships are established by secretory paracrine mechanisms, and we can imagine one-way or 'round trip' molecular traffic. The regulation of oviductin secretion [116] might be an example.

t-ICC:
Possible players in tissue remodeling

Extracellular matrix and certain cell types (*e.g.* myofibroblasts, 'distant relatives' of interstitial Cajal-like) are incriminated recently in tissue remodeling [117–119]. Moreover, vascular remodeling seems to be, at least in part, due to a phenotypic conversion, reminiscent of a fibroblast developmental program [120]). The novel type of Cajal-like cells described here might participate in remodeling human fallopian tube tissues, where inflammation or infection recurrently occur. One may speculate that the differential expression of certain antigens on t-ICC found in our study could be the result of such a phenotypic versatility.

Instead of conclusions

The gap between the clinical progress supporting reproductive technologies [121, 122] and the almost obsolete information available on molecular histology and physiology of human fallopian tube is surprising and challenging.

Acknowledgements

This study was partially supported by the grant VIASAN 0391/2004 from the National Ministry of Education and Research. The authors gratefully thank to the staff of Diagnostic Immunohistochemistry Unit, 'Victor Babes' National Institute of Pathology, Mrs. Maria Buzatu , Mrs. A. Bungardean, Mr. T. Regalia for expert technical assistance, Dr. A.C. Popescu for his help with Fig. 49, and Dr. Mircea Leabu, for useful suggestions and critical reading of the manuscript.

References

1. **Orci L, Pepper MS.** Microscopy: an art?. *Nat Rev Mol Cell Biol*. 2002; 3: 133-7.
2. **Cajal SR.** Sur les ganglions et plexus nerveux de l'intestin. *C.R. Soc Biol (Paris)*. 1893; 45: 217-23.
3. **Cajal SR.** Les nouvelles idées sur la structure du système nerveux chez l'homme et chez les vertébrés. Paris: C. Reinwald & C^{ie}; 1895.
4. **Min KW, Seo IS.** Interstitial cells of Cajal in the human small intestine: immunochemical and ultrastructural study. *Ultrastruct Pathol*. 2003; 27: 67-78.
5. **Thuneberg L.** One hundred years of interstitial cells of Cajal, *Microsc Res Tech*. 1999; 47: 223-38.
6. **Vajda J, Feher E.** Distribution and fine structure of the interstitial cells of Cajal. *Acta Morphol Acad Sci Hung*. 1980; 28: 251-8.
7. **Faussone Pellegrini MS, Cortesini C.** Ultrastructural features and localization of the interstitial cells of Cajal in the smooth muscle coat of human esophagus, *J Submicrosc Cytol*. 1985; 17: 187-97.
8. **Faussone-Pellegrini MS, Pantalone D, Cortesini C.** Smooth muscle cells, interstitial cells of Cajal and myenteric plexus interrelationships in the human colon. *Acta Anat (Basel)*. 1990; 139: 31-44.
9. **Rumessen JJ, Peters S, Thuneberg L.** Light- and electron microscopical studies of interstitial cells of Cajal (ICC) and muscle cells at the submucosal border of human colon. *Lab Invest*. 1993; 68: 481-95
10. **Rumessen JJ.** Identification of interstitial cells of Cajal. Significance for studies of human small intestine and colon. *Dan Med Bull*. 1994; 41: 275-93.
11. **Hagger R, Gharaie S, Finlayson C, Kumar D.** Distribution of the interstitial cells of Cajal in the human anorectum. *J Auton Nerv Syst*. 1998; 73: 75-9.
12. **Thuneberg L, Rumessen JJ, Mikkelsen HB, Peters S, Jessen H.** Structural aspects of interstital cells of Cajal as intestinal pacemaker cells, In: Huizinga JD, editor. Pacemaker activity and intercellular communication. Boca Raton: CRC Press; 1995. p. 193-222.
13. **Komuro T, Seki K, Horiguchi K.** Ultrastructural characterization of the interstitial cells of Cajal. *Arch Histol Cytol*. 1999; 62: 295-316.
14. **Faussone Pellegrini MS, Thuneberg L.** Guide to the identification of interstitial cells of Cajal. *Microsc Res Tech*. 1999; 47: 248-66.
15. **Huizinga JD, Thuneberg L, Vanderwinden JM, Rumessen JJ.** Interstitial cells of Cajal as targets for pharmacological intervention in gastrointestinal motor disorders. *Trends Pharmacol Sci*. 1997; 18: 393-403
16. **Daniel EE, Berezin I.** Interstitial cells of Cajal are they major player in control of gastrointestinal motility? *J Gastrointest Motil*. 1992; 4: 1-24.
17. **Sanders KM.** A case for interstitial cells of Cajal as pacemakers and mediators of neurotransmission in the gastrointestinal tract. *Gastroenterol*. 1996; 111: 492-515
18. **Koh SD, Sanders KM, Ward SM.** Spontaneous electrical rhythmicity in cultured interstitial cells of Cajal, isolated from the murine small intestine. *J Physiol (Lond)*. 1998; 513: 203-13.
19. **Thomsen L, Robinson TL, Lee JCF, Farraway LA, Hughes MJG, Andrews DW, Huizinga JD.** Interstitial cells of Cajal generate a rhythmic pacemaker current. *Nature Med*. 1998; 4: 848-51.
20. **Hirst GD, Ward SM.** Interstitial cells: involvement in rhythmicity and neural control of gut smooth muscle. *J Physiol*. 2003; 550: 337-46.
21. **Maeda H, Yamagata A, Nishikawa S, Yoshinaga K, Kobayashi S, Nishi K, Nishikawa SI.** Requirement of c-kit for development of intestinal pacemaker system. *Development*. 1992; 116: 369-75
22. **Ward SM, Burns AJ, Torihashi S, Sanders KM.** Mutation of the proto-oncogene c-kit blocks development of interstitial

cells and electrical rhythmicity in murine intestine. *J Physiol*. 1994; 480: 91-7.

23. **Huizinga JD, Thuneberg L, Kluppel M, Malysz J, Mickkelsen HB, Bernstein A.** W/kit gene required for interstitial cells of Cajal and for intestinal pacemaker activity. *Nature*. 1995; 373: 347-9.
24. **Hirota S, Isozaki K, Moriyama Y, Hashimoto K, Nishida T, Ishiguro S, Kawano K, Hanada N, Kurata A, Takeda M, Muhammad TG, Matsuzawa Y, Kanakura Y, Shinomura Y, Kitamura Y.** Gain-of-function mutations of c-kit in human gastrointestinal stromal tumors. *Science*. 1998; 279: 577-80
25. **Burton LD, Housley GD, Salih SG, Jaeenwood D.** P2X2receptor expression by interstitial cells of Cajal in vas deferens implicated in semen emission. *Auton Neurosci Basic Clin*. 2000; 84: 147-61.
26. **Sergeant GP, Hollywood MA, McCloskey KD, Thornbury KD, McHale NG.** Specialized pacemaking cells in the rabbit urethra. *J Physiol*. 2000; 526: 359-66.
27. **Sergeant GP, Hollywood MA, McCloskey KD, McHale NG, Thornbury KD.** Role of IP(3) in modulation of spontaneous activity in pacemaker cells of rabbit urethra. *Am J Physiol Cell Physiol*. 2001; 280: C1349-56.
28. **Johnston L, Sergeant GP, Hollywood MA, Thornbury KD, McHale NG.** Calcium oscillations in interstitial cells of the rabbit urethra. *J Physiol.* 2005; 565: 449-61.
29. **McCloskey KD, Gurney AM.** Kit positive cells in the guinea-pig bladder. *J Urol.* 2002; 168: 832-6.
30. **Blyweert W, Aa F, Ost D, Stagnaro M, Ridder D.** Interstitial cells of the bladder: the missing link? *BJOG*. 2004; 111: 57-60.
31. **Hashitani H, Yanai Y, Suzuki H.** Role of interstitial cells and gap junctions in the transmission of spontaneous Ca^{2+} signals in detrusor smooth muscles of the guinea-pig urinary bladder. *J Physiol*. 2004; 559: 567-81.
32. **Gillespie JI, Markerink-van Ittersum M, de Vente J.** cGMP-generating cells in the bladder wall: identification of distinct networks of interstitial cells. *BJU Int*. 2004; 94: 1114-24.
33. **Davidson RA, McCloskey KD.** Morphology and localization of interstitial cells in the guinea pig bladder: structural relationships with smooth muscle and neurons. *J Urol*. 2005; 173: 1385-90
34. **Pezzone MA, Watkins SC, Alber SM, King WE, de Groat CW, Chancellor MB, Fraser MO.** Identification of c-kit-positive cells in the mouse ureter: the interstitial cells of Cajal of the urinary tract. *Am J Physiol Renal Physiol*. 2003; 284: 925-9.
35. **Metzger R, Schuster T, Till H, Franke FE, Dietz HG.** Cajal-like cells in the upper urinary tract: comparative study in various species. *Pediatr Surg Int.* 2005; 21: 169-74
36. **Duquette RA, Shmygol A, Vaillant C, Mobasheri A, Pope M, Burdyga T, Wray S.** Vimentin-positive, c-KIT-negative interstitial cells in human and rat uterus: A role in pacemaking? *Biol Reprod*. 2005; 72: 276-83.
37. **Ciontea MS, Radu E, Regalia T, Ceafalan L, Cretoiu D, Gherghiceanu M, Braga RI, Malincenco M, Zagrean L, Hinescu ME, Popescu LM.** C-kit immunopositive interstitial cells (Cajal-type) in human myometrium. *J Cell Mol Med*. 2005; 9: 407-20.
38. **Pucovsky V, Moss RF, Bolton TB.** Non-contractile cells with thin processes resembling interstitial cells of Cajal found in the wall of guinea-pig mesenteric arteries. *J Physiol*. 2003; 552: 119-33.
39. **Harhun MI, Gordienko DV, Povstyan OV, Moss RF, Bolton TB.** Function of interstitial cells of Cajal in the rabbit portal vein. *Circ Res*. 2004; 95: 619-26.
40. **Harhun MI, Pucovsky V, Povstyan OV, Gordienko DV, Bolton TB**. Interstitial cells in the vasculature. *J Cell Mol Med*. 2005; 9: 232-43.
41. **McCloskey KD, Hollywood MA, Thornbury KD, Ward SM, McHale NG.** Kit-like immunopositive cells in sheep mesenteric lymphatic vessels. *Cell Tissue Res*. 2002; 310: 77-84.
42. **Exintaris B, Klemm MF, Lang RJ.** Spontaneous slow wave and contractile activity of the guinea pig prostate. *J Urol*. 2002; 168: 315-22.
43. **Van der Aa F, Roskams T, Blyweert W, De Ridder D.** Interstitial cells in the human prostate: a new therapeutic target? *Prostate*. 2003; 56: 250-5.
44. **Hashitani H, Suzuki H.** Identification of interstitial cells of Cajal in corporal tissues of the guinea-pig penis. *Br J Pharmacol*. 2004; 141: 199-204.
45. **Popescu LM, Andrei F, Hinescu ME.** Snapshots of mammary gland interstitial cells: methylene blue vital staining and c-kit immunopositivity. *J Cell Mol Med*. 2005; 9: 476-7.
46. **Popescu LM, Hinescu ME, Ionescu N, Ciontea MS, Cretoiu D, Ardeleanu C.** Interstitial cells of Cajal in pancreas. *J Cell Mol Med*. 2005; 9: 169-90.
47. **Hendrickson MR, Kempson RL.** Normal histology, of the uterus and fallopian tubes. In: Sternberg SS, editor. Histology for pathologists, 2nd edition. Philadelphia: Lippincott–Raven; 1997. p. 879-928.
48. **Hunt JL, Lynn AA.** Histologic features of surgically removed fallopian tubes. *Arch Pathol Lab Med*. 2002; 126: 951-5.
49. **Hunter RH.** Have the Fallopian tubes a vital role in promoting fertility? *Acta Obstet Gynecol Scand*. 1998; 77: 475-86.
50. **Leese HJ, Tay JI, Reischl J, Downing SJ.** Formation of Fallopian tubal fluid: role of a neglected epithelium. *Reproduction*. 2001; 121: 339-46.
51. **Arbab F, Goldsby J, Matijevic-Aleksic N, Huang G, Ruan KH, Huang JC.** Prostacyclin is an autocrine regulator in the contraction of oviductal smooth muscle. *Hum Reprod*. 2002; 17: 3053-9.
52. **Morimoto T, Head JR, MacDonald PC, Casey ML.** Thrombospondin-1 expression in human myometrium before and during pregnancy, before and during labor, and in human myometrial cells in culture. *Biol Reprod*. 1998; 59: 862-70.
53. **Niculescu I.** An atlas concerning morphological aspects of visceral nerve endings. 1st ed. Bucharest: Editura Medicala; 1958.
54. **Yack JE.** Janus Green B as a rapid, vital stain for pheripheral nerves and chordotonal organs in insects. *J Neurosci Methods.* 1993; 49: 17-22.
55. **Keij JF, Bell-Prince C, Steinkamp JA.** Staining of mitochondrial membranes with 10-nonyl acridine orange, MitoFluor Green, and MitoTracker Green is affected by mitochondrial membrane potential altering drugs. *Cytometry*. 2000; 39: 203-10.

56. **Vanden Berghe P, Hennig GW, Smith TK.** Characteristics of intermittent mitochondrial transport in guinea pig enteric nerve fibers. *Am J Physiol Gastrointest Liver Physiol.* 2004; 286: G671-82.
57. **Bancroft JD, Gamble M,** editors. Theory and practice of histological techniques. 5th ed. London: Churchill Livingstone; 2002.
58. **Weibel ER.** Practical methods for biological morphometry. Stereological methods. London: Academic Press; 1979.
59. **Hsu SM, Raine L, Fanger H.** Use of avidin-biotin-peroxidase complex (ABC) in immunoperoxidase techniques: a comparison between ABC and unlabeled antibody (PAP) procedures. *J Histochem Cytochem*. 1981; 29: 577-80.
60. **Bussolati G, Gugliotta P.** Nonspecific staining of mast cells by avidin-biotin-peroxidase complexes (ABC). *J Histochem Cytochem*. 1983; 31: 1419-21.
61. **Alberti E, Mikkelsen HB, Larsen JO, Jimenez M.** Motility patterns and distribution of interstitial cells of Cajal and nitrergic neurons in the proximal, mid- and distal-colon of the rat. *Neurogastroenterol Motil*. 2005; 17: 133-47.
62. **Lazarow A, Cooperstein SJ.** Studies on the enzymatic basis for the Janus green B staining reaction. *J Histochem Cytochem*. 1953; 1: 234-41.
63. **Rumessen JJ, Vanderwinden JM.** Interstitial cells in the musculature of the gastrointestinal tract: Cajal and beyond. *Int Rev Cytol*. 2003; 229: 115-208.
64. **Huizinga JD, Faussone-Pellegrini MS.** About the presence of interstitial cells of Cajal outside the musculature of the gastrointestinal tract. *J Cell Mol Med*. 2005; 9: 468-73.
65. **Popescu LM, Diculescu I, Zelck U, Ionescu N.** Ultrastructural distribution of calcium in smooth muscle cells of guinea-pig taenia coli. A correlated electron microscopic and quantitative study. *Cell Tissue Res.* 1974; 154: 357-78.
66. **Brinsfield TH, Fisher M, Hawk HW.** Ultrastructure of endometrial stromal cells in the ewe during the estrous cycle and early pregnancy. *J Anim Sci*. 1974; 39: 565-74.
67. **Popescu LM.** A conceptual model of the excitation-contraction coupling in smooth muscle: the possible role of the surface microvesicles. *Studia Biophys.* 1974; 44: 141-53.
68. **Moore ED, Voigt T, Kobayashi YM, Isenberg G, Fay FS, Gallitelli MF, Franzini-Armstrong C.** Organization of Ca^{2+} release units in excitable smooth muscle of the guinea-pig urinary bladder. *Biophys J.* 2004; 87: 1836-47.
69. **Schurch W, Seemayer TA, Gabbiani G.** Myofibroblast. In: Sternberg SS, editor. Histology for pathologists, 2nd edition. Philadelphia: Lippincott–Raven; 1997. p. 129-65.
70. **Wheaton K, Sampsel K, Boisvert FM, Davy A, Robbins S, Riabowol K.** Loss of functional caveolae during senescence of human fibroblasts. *J Cell Physiol*. 2001; 187: 226-35.
71. **Capozza F, Cohen AW, Cheung MW, Sotgia F, Schubert W, Battista M, Lee H, Frank PG, Lisanti MP.** Muscle-specific interaction of caveolin isoforms: differential complex formation between caveolins in fibroblastic vs. muscle cells. *Am J Physiol Cell Physiol*. 2005; 288: C677-91.
72. **Schurch W, Seemayer TA, Gabbiani G.** The myofibroblast: a quarter century after its discovery. *Am J Surg Pathol*. 1998; 22: 141-7.
73. **Eyden B.** The myofibroblast: an assessment of controversial issues and a definition useful in diagnosis and research. *Ultrastruct Pathol*. 2001; 25: 39-50.
74. **Powell DW, Mifflin RC, Valentich JD, Crowe SE, Saada JI, West AB.** Myofibroblasts. I. Paracrine cells important in health and disease. *Am J Physiol*. 1999; 277: C1-9.
75. **Walter I.** Myofibroblasts in the mucosal layer of the uterine tube. *Ital J Anat Embryol*. 1998; 103: 259-66.
76. **Lee H, Douglas-Jones AG, Morgan JM, Jasani B.** The effect of fixation and processing on the sensitivity of oestrogen receptor assay by immunohistochemistry in breast carcinoma. *J Clin Pathol*. 2002; 55: 236-8.
77. **Torihashi S, Horisawa M, Watanabe Y.** c-Kit immunoreactive interstitial cells in the human gastrointestinal tract. *J Auton Nerv Syst*. 1999; 75: 38-50.
78. **Cho WJ, Daniel EE.** Proteins of interstitial cells of Cajal and intestinal smooth muscle, colocalized with caveolin-1. *Am J Physiol Gastrointest Liver Physiol*. 2005; 288: G571-85.
79. **Puxeddu I, Piliponsky AM, Bachelet I, Levi-Schaffer F.** Mast cells in allergy and beyond. *Int J Biochem Cell Biol*. 2003; 35: 1601-7.
80. **Vanderwinden JM, Rumessen JJ, De Laet MH, Vanderhaeghen JJ, Schiffmann SN.** CD34+ cells in human intestine are fibroblasts adjacent to, but distinct from, interstitial cells of Cajal. *Lab Invest*. 1999; 79: 59-65.
81. **Fina L, Molgaard HV, Robertson D, Bradley NJ, Monaghan P, Delia D, Sutherland DR, Baker MA, Greaves MF.** Expression of the CD34 gene in vascular endothelial cells. *Blood*. 1990; 75: 2417-26.
82. **Tsujimura T, Makiishi-Shimobayashi C, Lundkvist J, Lendahl U, Nakasho K, Sugihara A, Iwasaki T, Mano M, Yamada N, Yamashita K, Toyosaka A, Terada N.** Expression of the intermediate filament nestin in gastrointestinal stromal tumors and interstitial cells of Cajal, *Am J Pathol.* 2001; 158: 817-23.
83. **Torihashi S, Ward SM, Sanders KM.** Development of c-Kit-positive cells and the onset of electrical rhythmicity in murine small intestine. *Gastroenterology*. 1997; 112: 144-55.
84. **Grider JR.** Focus on "molecular markers expressed in cultured and freshly isolated interstitial cells of Cajal". *Am J Physiol Cell Physiol.* 2000; 279: C284-5.
85. **Vento P, Soinila S.** Quantitative comparison of growth - associated protein GAP-43, neuron specific enolase and protein gene product 9.5 as neuronal markers in mature human intestine. *J Histochem Cytochem.* 1999; 47: 1405-15.
86. **An S, Zenisek D.** Regulation of exocytosis in neurons and neuroendocrine cells. *Curr Opin Neurobiol*. 2004; 14: 522-30.
87. **Dursun P, Salman MC, Taskiran C, Usubutun A, Ayhan A.** Primary neuroendocrine carcinoma of the fallopian tube: a case report. *Am J Obstet Gynecol*. 2004; 190: 568-71.
88. **Kuriyama H, Kitamura K, Itoh T, Inoue R.** Physiological features of visceral smooth muscle cells, with special reference to receptors and ion channels. *Physiol Rev.* 1998; 78: 811-920.
89. **Vanderwinden JM, Gillard K, De Laet MH, Messam CA, Schiffmann SN.** Distribution of the intermediate filament nestin in the muscularis propria of the human gastrointestinal tract. *Cell Tissue Res*. 2002; 309: 261-8.
90. **Ortiz-Hidalgo C, de Leon B, Albores-Saavedra J.** Stromal tumor of the gallbladder with phenotype of interstitial cells of Cajal: a previously unrecognized neoplasm. *Am J Surg. Pathol*, 2000; 24: 1420-3.

91. **Sakurai S, Fukasawa T, Chong JM, Tanaka A, Fukayama M.** Embryonic form of smooth muscle myosin heavy chain (SMemb/MHC-B) in gastrointestinal stromal tumor and interstitial cells of Cajal. *Am J Pathol*. 1999; 154: 23-8.
92. **Raff M.** Adult stem cell plasticity: fact or artifact? *Annu Rev Cell Dev Biol.* 2003; 19:1-22.
93. **Epperson A, Hatton WJ, Callaghan B, Doherty P, Walker RL, Sanders KM, Ward SM, Horowitz B.** Molecular markers expressed in cultured and freshly isolated interstitial cells of Cajal. *Am J Physiol Cell Physiol*. 2000; 279: C529-39.
94. **Li CX, Liu BH, Tong WD, Zhang LY, Jiang YP.** Dissociation, culture and morphologic changes of interstitial cells of Cajal *in vitro*, *World J Gastroenterol*. 2005; 11: 2838-40.
95. **Torihashi S, Ward SM, Nishikawa S, Nishi K, Kobayashi S, Sanders KM.** c-kit-dependent development of interstitial cells and electrical activity in the murine gastrointestinal tract. *Cell Tissue Res*. 1995; 280: 97-111.
96. **Tong WD, Liu BH, Zhang LY, Xiong RP, Liu P, Zhang SB.** Expression of c-kit messenger ribonucleic acid and c-kit protein in sigmoid colon of patients with slow transit constipation. *Int J Colorectal Dis*. 2005; 20: 363-7.
97. **Isozaki K, Terris B, Belghiti J, Schiffmann S, Hirota S, Vanderwinden JM.** Germline-activating mutation in the kinase domain of KIT gene in familial gastrointestinal stromal tumors. *Am J Pathol*. 2000; 157: 1581-5.
98. **Torihashi S, Nishi K, Tokutomi Y, Nishi T, Ward S, Sanders KM.** Blockade of kit signaling induces transdifferentiation of interstitial cells of Cajal to a smooth muscle phenotype. *Gastroenterology*. 1999; 117: 140-8.
99. **Sarlomo-Rikala M, Kovatich AJ, Barusevicius A, Miettinen M.** CD117: a sensitive marker for gastrointestinal stromal tumors that is more specific than CD34. *Mod. Pathol*. 1998, 11: 728-34.
100. **Dhimes P, Lopez-Carreira M, Ortega-Serrano MP, Garcia-Munoz H, Martinez-Gonzalez MA, Ballestin C.** Gastrointestinal autonomic nerve tumours and their separation from other gastrointestinal stromal tumours: an ultrastructural and immunohistochemical study of seven cases. *Virchows Arch*. 1995; 426: 27-35.
101. **Yamazaki K, Eyden BP.** Ultrastructural and immunohistochemical studies of stromal cells in lamina propria of human fallopian tube ampullar mucosa: the recognition of 'CD34 positive reticular network' and its putative function for immune surveillance. *J Submicrosc Cytol Pathol*. 1995; 28: 325-37.
102. **Sircar K, Hewlett BR, Huizinga JD, Chorneyko K, Berezin I, Riddell RH.** Interstitial cells of Cajal as precursors of gastrointestinal stromal tumors. *Am J Surg Pathol*. 1999; 23: 377-89.
103. **Piaseczna PA, Rolle U, Solari V, Puri P,** Interstitial cells of Cajal in the human normal urinary bladder and in the bladder of patients with megacystis-microcolon intestinal hypoperistalsis syndrome. *BJU Int.* 2004; 94: 143-6.
104. **Bucala R, Spiegel LA., Chesney J, Hogan M, Cerami A.** Circulating fibrocytes define a new leukocyte subpopulation that mediates tissue repair. *Mol Med.* 1994; 1: 71-81.
105. **Young HM.** Embryological origin of interstitial cells of Cajal. *Microsc Res Tech*. 1999; 47: 303-8.
106. **Neijssen J, Herberts C, Drijfhout JW, Reits E, Janssen L, Neefjes J.** Cross-presentation by intercellular peptide transfer through gap junctions. *Nature*. 2005, 434: 83-8.
107. **Ward SM, Ordog T, Koh SD, Baker SA, Jun JY, Amberg G, Monaghan K, Sanders KM.** Pacemaking in interstitial cells of Cajal depends upon calcium handling by endoplasmic reticulum and mitochondria. *J Physiol*. 2000; 525: 355-61.
108. **Yoneda S, Takano H, Takaki M, Suzuki H.** Properties of spontaneously active cells distributed in the submucosal layer of mouse proximal colon. *J Physiol*. 2002; 542: 887-97.
109. **Hanani M, Farrugia G, Komuro T.** Intercellular coupling of interstitial cells of Cajal in the digestive tract. *Int Rev Cytol*. 2005; 242: 249-82.
110. **Daniel EE, Willis A, Cho WJ, Boddy G.** Comparisons of neural and pacing activities in intestinal segments from W/W++ and W/W(V) mice. *Neurogastroenterol Motil*. 2005; 17: 355-65.
111. **Jankovic SM, Protic BA, Jankovic SV.** Contractile effect of acetylcholine on isolated ampullar segment of Fallopian tubes. *Pharmacol Res*. 2004; 49: 31-5.
112. **Samuelson UE, Wiklund NP, Gustafsson LE.** Endogenous purines may modulate adrenergic neurotransmission in the human fallopian tube. *Neurosci Lett*. 1988; 86: 51-5.
113. **Ziganshin AU, Vafina ZR, Fatkullin IF.** Pharmacological characterization of P2-receptors in human fallopian tubes. *Bull Exp Biol Med*. 2004; 137: 242-5.
114. **Ekerhovd E, Brannstrom M, Alexandersson M, Norstrom A.** Evidence for nitric oxide mediation of contractile activity in isolated strips of the human Fallopian tube. *Hum Reprod*. 1997; 12: 301-5.
115. **Ekerhovd E, Norstrom A.** Involvement of a nitric oxide-cyclic guanosine monophosphate pathway in control of fallopian tube contractility. *Gynecol Endocrinol*. 2004; 19: 239-46.
116. **Briton-Jones C, Hung Lok I, Yuen PM, Chiu TTY, Cheung LP, Haines C,** Regulation of human oviductin mRNA expression in vivo. *Fertil Steril*. 2001; 75: 942-6.
117. **Streuli C.** Extracellular matrix remodelling and cellular differentiation. *Curr Opin Cell Biol.* 1999, 11: 634-40.
118. **Tomasek JT, Gabbiani G, Hinz B, Chaponnier C, Brown RA.** Myofibroblasts and mechanoregulation of connective tissue remodelling. *Nat Rev Mol Cell Biol.* 2002; 3: 349-63.
119. **Demouillere A, Darby IA,Gabbiani G.** Normal and pathologic soft tissue remodeling: role of the myofibroblast, with special emphasis on liver and kidney fibrosis. *Lab Invest*. 2003; 83: 1689-707.
120. **Sartore S, Chiavegato A, Faggin E, Franch R, Puato M, Ausoni S, Pauletto P.** Contribution of adventitial fibroblasts to neointima formation and vascular remodeling. From innocent bystander to active participant. *Circ Res*. 2001; 89: 1111-21.
121. **Watrelot A, Hamilton J, Grudzinskas JG.** Advances in the assessment of the uterus and fallopian tube function. *Best Pract Res Clin Obst Gynaecol*. 2003; 17: 187-209.
122. **Talevi R, Gualtieri R.** *In vivo* versus *in vitro* fertilization, *Eur J Obst Gynecol Reprod Biol.* 2004; 115S: S68-S71.

ANDREAE VESALII

Invictissimi Caroli V. Imperatoris Medici

OPERA OMNIA

ANATOMICA

&

CHIRURGICA

Cura

HERMANNI BOERHAAVE

Medicinae, Botanices, Collegii Practici, & Chemiae in Academia Lugduno-Batava Professoris,

&

BERNHARDI SIEGFRIED ALBINI

Anatomes & Chirurgiae in eadem Academia Professoris.

TOMUS PRIMUS.

LUGDUNI BATAVORUM,

Apud { JOANNEM Du VIVIE, ET JOAN. & HERM. VERBEEK. } Bibliop.

MDCCXXV

1725

FREDERICI RUYSCHII,

Anatomes & Botanices Professoris, Academiae Caesareae Curiosorum Collegae, nec non Regiae Societatis Anglicanae & Parisinae Membri,

OPERA

OMNIA

ANATOMICO-MEDICO-

CHIRURGICA,

HUC USQUE EDITA.

Quorum

Elenchus pagina sequenti exhibetur,

CUM FIGURIS ÆNEIS.

AMSTELODAMI,

Apud JANSSONIO-WAESBERGIOS.

M. D. C. C. XXXVII.

1737

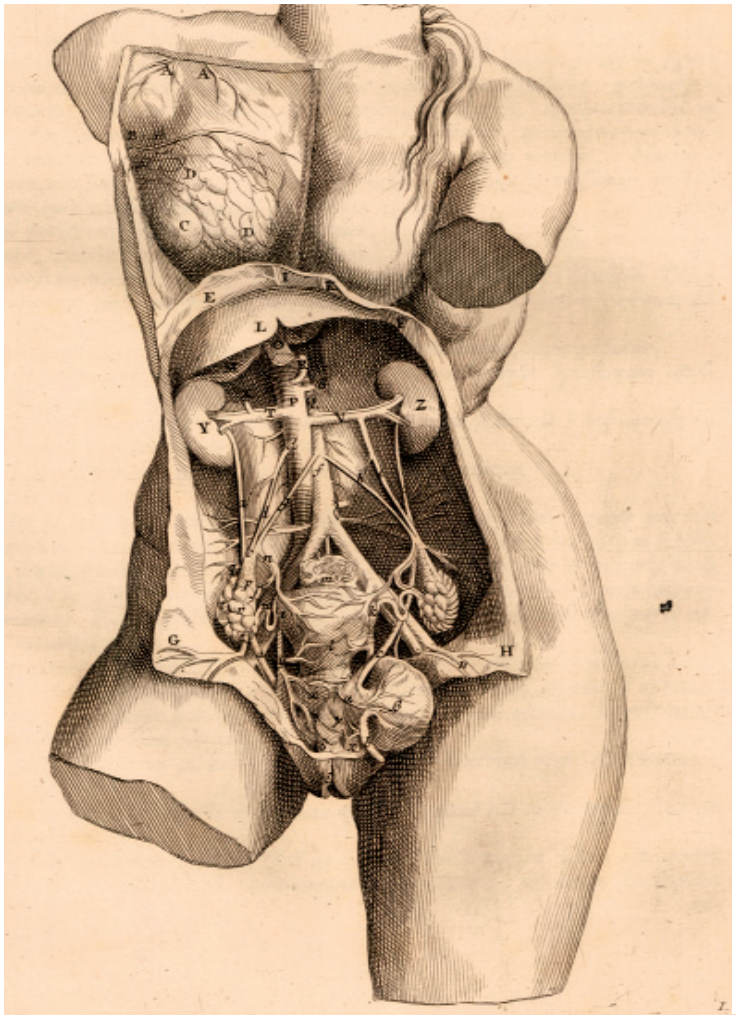

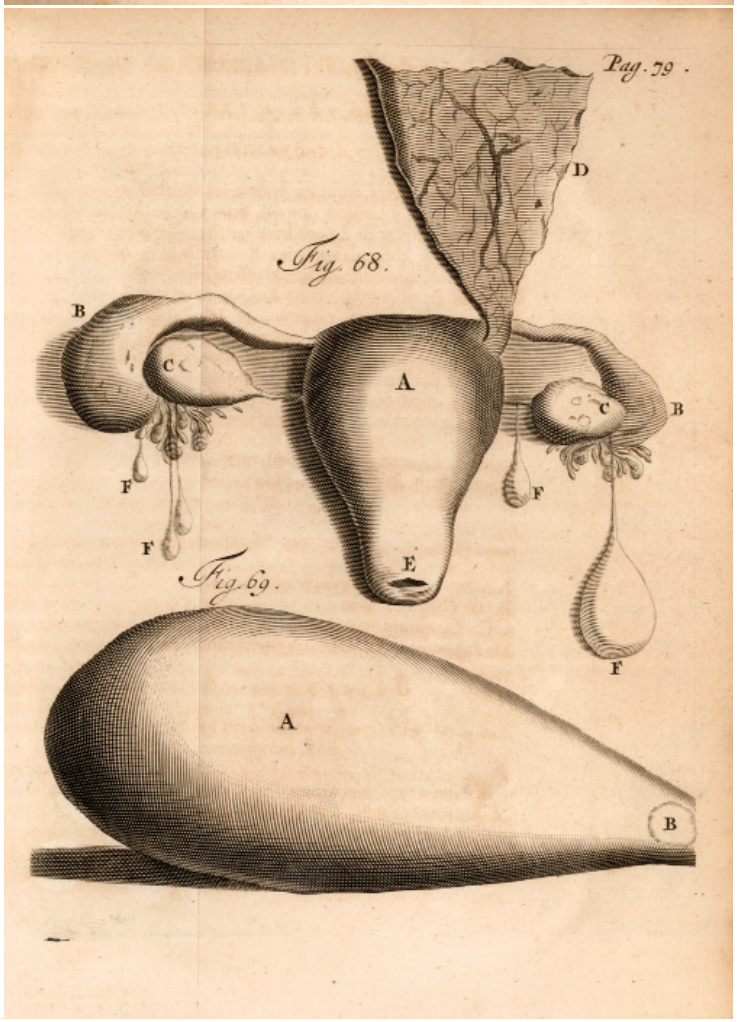

Fallopian tubes (oviducts) as seen by ancient anatomists.

Reproductions from **Andrea Vesalius**, *Opera omnia anatomica & chirurgica* (1725) and **Fredericus Ruysch**, *Opera omnia anatomico-medico-chirurgica* (1737). Courtesy of the Medical Library of the 'Carol Davila' University of Medicine and Pharmacy, Bucharest (library catalogue #CS XVIII V10 and #CS XVIII IV15).